THE EFFECTS OF RESPIRATORY MUSCLE TRAINING ON STRENGTH AND PERFORMANCE IN COLLEGIATE SWIMMERS

By

VIPA BERNHARDT

A DISSERTATION PRESENTED TO THE GRADUATE SCHOOL
OF THE UNIVERSITY OF FLORIDA IN PARTIAL FULFILLMENT
OF THE REQUIREMENTS FOR THE DEGREE OF
DOCTOR OF PHILOSOPHY

UNIVERSITY OF FLORIDA

Vipa Bernhardt

ACKNOWLEDGMENTS

First and foremost, I would like to thanks my parents, Chamaipon and Helge, for their endless support and for always being there for me, even though the Atlantic Ocean separates us. Skype has been one of the best technical advances for our widely spread-out family to be able to talk and see each other. To my brother, Jens, whose footsteps I followed and that led me to pursue a career in science.

Special thanks go to my graduate mentor, Dr. Paul Davenport, for his teaching, guidance, and encouragement. Thanks to my supervisory committee: Dr. David Fuller, Dr. Nancy Denslow, Dr. Danny Martin, Dr. Linda Hayward, and Dr. Roger Reep for the support and comments throughout my dissertation process.

I am grateful for having had the opportunity to share my experience with my fellow labmates, past and present: Drs. Pei-Ying Sarah Chan, Kate Pate, Karen Hegland, Andrea Vovk and soon-to-be Drs. Mark Hotchkiss, Irene Tsai, Poonam Jaiswal. As well as the other scientists in and around B3-16: Drs. Teresa Pitts, Barbara Smith, and soon-to-be Dr. Ana Bassit. I would like to thank Stacey Nedrud for her help and friendship in and out of the lab, Will Walters for critical comments, and Mandy Huff for continual moral support. I would also like to acknowledge Dr. Natalia Garcia-Reyero for her help with the microarrays.

Last but not least, I would like to thank the UF swim team: the coaches Gregg Troy, Martyn Wilby, and Pete Knox for their support to carry out my project and allowing me to interfere somewhat with swim practices and the swimmers who did the extra work for my research.

TABLE OF CONTENTS

page

ACKNOWLEDGMENTS 4

LIST OF TABLES 8

LIST OF FIGURES 9

ABSTRACT 11

CHAPTER

1 INTRODUCTION 13

Exercise and Respiration 13
Intermittent Transient Tracheal Occlusions (ITTO) in Rats as a Model for Respiratory Muscle Training 16
Respiratory Load Compensation Response 17
Sensory Gating 19
Specific Aims 22
Specific Aim 1: To Investigate the Effects of Expiratory Muscle Strength Training in Collegiate Swimmers 22
Specific Aim 2: To Investigate the Changes in the Gene Expression Profile of the Medial Thalamus following ITTO in Anesthetized Rats 23
Specific Aim 3: To Investigate the Changes in the Gene Expression Profile of the Medial Thalamus following 10 Days of Repeated ITTO in Conscious Rats 24

2 THE EFFECTS OF EXPIRATORY MUSCLE STRENGTH TRAINING IN COLLEGE SWIMMERS 28

Introduction 28
Materials and Methods 31
Subjects 31
Experimental Design 31
Procedures 32
Pulmonary function assessment 32
Maximum expiratory pressures 32
Expiratory muscle strength training (EMST) 32
Airflow training (AFT) 33
$\dot{V}O_2$max test on swim bench 33
Timed interval swim tests 34
Statistical Analysis 35
Results 35
Demographics 35
Pulmonary Functions and MEP 36

$\dot{V}O_2$ Test 36
Swimming Performance 37
Discussion 38
Pulmonary Functions and MEP 38
Oxygen Consumption ($\dot{V}O_2$) 39
Functional Significance of Improvements in Swim Performance Times 41
Properties of Respiratory Muscles 42
Pacing Strategies 46
Potential Mechanisms 47
Perception of Breathlessness 48
Conclusions 51

3 TRACHEAL OCCLUSION IN ANESTHETIZED RATS MODULATES GENE EXPRESSION PROFILE OF MEDIAL THALAMUS 63

Introduction 63
Materials and Methods 67
Animals 67
Surgical Procedures 67
Experimental Protocol 68
Physiological Data Analysis 69
Total RNA Isolation 70
RNA Amplification and Microarray Analysis 70
Gene Ontology and Pathway Analysis 71
Results 72
Physiological Responses to ITTO 72
Modulation of Gene Expression Profile Following ITTO 72
Discussion 73
Airway Occlusions Elicit the Load Compensation Response 73
Airway Obstruction in Disease and Association with Anxiety and Depression 74
Airway Occlusions Induce Serotonin Receptor HTR2A and Reduce Dopamine Receptor DRD1 75
Airway Occlusions Alter Genes Involved in Anti-Apoptosis 77
Functional Analysis 78
Conclusions 79

4 TRACHEAL OCCLUSION CONDITIONING IN CONSCIOUS RATS MODULATES GENE EXPRESSION PROFILE OF MEDIAL THALAMUS 88

Introduction 88
Materials and Methods 91
Animals 91
Surgical Procedures 91
Placement of tracheal occluder 91
Analgesia and postoperative care 92
Experimental Protocol 92
Microarray Analysis 93

Results 93
Modulation of Gene Expression Profile Following ITTO 93
Gene Ontology and Pathway Analysis 93
Discussion 95
Thalamic Firing Mode and Sensory Gating 95
Chronic Exposure to ITTO Modulates Genes Involved in Stress, Anxiety, and Depression 99
Chronic Exposure to ITTO Modulates SHOX2 101
Chronic Exposure to ITTO Modulates Pathways Involved in Learning and Memory, Cell Processes, and Cell Signaling 102
Conclusions 103

5 SUMMARIES AND CONCLUSIONS 110

Summary of Study Findings 110
Study #1 Summary 110
Study #2 Summary 111
Study #3 Summary 112
Discussion 113
The Role of Serotonin in Response to Respiratory Stimuli 113
The Effects of Respiratory Training 114
Methodological Considerations and Directions for Future Studies 115
Fatigue due to Regular Training 116
Respiratory Training Stress Stimulus 116
$\dot{V}O_2$max Testing 117
Prevalence of Respiratory Disease in Swimmers 118
Specificity of Medial Thalamic Nuclei 118
Genomics Versus Proteomics 119
Conclusions 119

APPENDIX

A RATING SCALES 121

B LIST OF MODULATED GENES FOLLOWING ACUTE ITTO 123

C LIST OF MODULATED GENES FOLLOWING REPEATED ITTO 138

D LIST OF MODULATED GENE ONTOLOGY BIOLOGICAL PROCESSES FOLLOWING REPEATED ITTO 157

LIST OF REFERENCES 160

BIOGRAPHICAL SKETCH 177

LIST OF TABLES

Table		page
1-1	Summary of EMST studies with reported MEP and functional changes.	26
2-1	Anthropometric data participants	53
2-2	Pulmonary function test data	53
2-3	Maximum expiratory pressure test data.	54
3-1	Control breath comparisons of breath timing, Pes, and ΔEMGdia between experimental and control animals	83
3-2	Comparisons between control, occlusion, and recovery breaths in the experimental animals	83
3-3	Comparisons between control, occlusion, and recovery breaths in the experimental animals with combined values from O1 and O2	83
3-4	Genes of interest that were significantly regulated following ITTO.	85
3-5	Highly regulated biological processes following ITTO were found with gene ontology analysis.	86
4-1	Candidate genes significantly differentially regulated following chronic ITTO.	106
4-2	Significantly modulated Gene Ontology Biological Processes.	106
B-1	List of modulated genes following acute ITTO	123
C-1	List of modulated genes following repeated ITTO	138
D-1	List of modulated GO groups following repeated ITTO	157

LIST OF FIGURES

Figure		page
1-1	Model of respiratory information processing including sensory signal transduction, subcortical, cortical, and perceptual processing	27
2-1	Components of the training devices for A) EMST, B) AFT.	52
2-2	Percent change in MEP for each individual	54
2-3	The EMST group significantly increased MEP post-training compared to pre-training.	54
2-4	Pre- and post-performance times for 6 x 100 m freestyle test for both EMST and AFT groups	55
2-5	Percent change in 100 m time for each individual.	56
2-6	Percent change of mean swim time during the 6 x 100 m freestyle test for EMST and AFT groups.	56
2-7	Correlation of % time change during 6 x 100 m test and change in MEP pre- to post-training for each individual.	57
2-8	Percent time change of the first 100 m interval	58
2-9	Percent time change of the last 100 m interval	58
2-10	Heart rate before and during the 6x100 m freestyle test.	59
2-11	Changes in Ratings of Breathlessness between first and last rating within one 6x100 m test	60
2-12	Changes in Ratings of Perceived Exertion between first and last rating within one 6x100 m test	60
2-13	Functional significance of % improvements in swim time pre- and post-training compared to the 2008 Olympic Games Men's 100 m freestyle preliminary races	61
2-14	Possible mechanisms leading to the sensation of breathlessness.	62
3-1	Diagram of surgical preparation including placement of tracheal occluder, esophageal pressure tube, and diaphragm electrodes.	80
3-2	Location of collected thalamic tissue sample	81
3-3	Physiological changes as a result of ITTO	82

3-4 Comparisons between control, occlusion, and recovery breaths in the experimental animals. A) Ti, B) Te, C) Ttot, D) P_{es}, E) EMG_{dia} 84

3-5 Interaction between dopamine (DRD1) and serotonin receptors (HTR2A) under the control of MAPK1 87

4-1 Schematic of the experimental protocol for repeated ITTO. 104

4-2 Representative plethysmograph pressure traces for one occlusion trial on day 10 105

4-3 Pathway analysis of transcripts ($p < 0.05$) involved in the biological processes of learning and/or memory. 107

4-4 Pathway analysis of transcripts ($p < 0.05$) involved in cell processes. 108

4-5 Pathway analysis of transcripts ($p < 0.05$) involved in cell signaling. 109

5-1 Model for possible effects of respiratory muscle training on perception. 120

Abstract of Dissertation Presented to the Graduate School
of the University of Florida in Partial Fulfillment of the
Requirements for the Degree of Doctor of Philosophy

THE EFFECTS OF RESPIRATORY MUSCLE TRAINING ON STRENGTH AND PERFORMANCE IN COLLEGIATE SWIMMERS AND ON THALAMIC GENE EXPRESSION IN A RAT MODEL

By

Vipa Bernhardt

December 2010

Chair: Paul W. Davenport
Major: Medical Sciences

Exercise performance in highly trained athletes may be limited by the respiratory system, possibly due to respiratory muscle fatigue and/or feeling of breathlessness. The feeling of breathlessness may be mediated by the medial thalamus, the proposed region responsible for gating of respiratory sensory feedback to reach consciousness. The present studies were undertaken to evaluate the effects of an expiratory muscle strength training (EMST) in collegiate swimmers and to determine the role of the medial thalamus in a rat model of intrinsic, transient tracheal occlusions (ITTO).

Study #1 tested the hypothesis that EMST could increase the maximum expiratory pressure (MEP)-generating capacity, decrease the perception of effort and breathlessness, and improve swimming performance in highly trained swimmers. The results demonstrated that EMST significantly increased MEP. Swimming performance, as measured by a 6 x 100 m freestyle test, showed a trend for improvement in swim time, however, the change was not statistically significant. Ratings of breathlessness and effort, which were assessed during the swim test, were also not statistically

significant but showed a trend for improvement. The results suggest that EMST could be used as an adjunct for swimmers' athletic conditioning.

Study #2 tested the hypothesis that ITTO in anesthetized animals would induce immediate gene expression changes in the medial thalamus. Analysis showed an up-regulation of genes involved in the stress response. Results from this study supported the role of the medial thalamus as a component in the gating of respiratory stimuli, specifically the stressful stimuli of tracheal occlusions.

Study #3 tested the hypothesis that 10 days of repeated exposure to ITTO in conscious animals would induce gene expression state changes in the medial thalamus. Results from this study demonstrated that repeated ITTO elicited state changes in the expression of genes involved in neuronal firing mode, suggesting a modulation of gating of respiratory information.

Together, these three experiments suggest that EMST could be beneficial in highly trained swimmers and that this positive effect may be due to an increase in expiratory muscle strength and a change in gating of respiratory feedback through the medial thalamus, which could delay the feelings of breathlessness.

CHAPTER 1
INTRODUCTION

Exercise and Respiration

Historically, exercise training has primarily focused on improving the cardiovascular system and strengthening the locomotor musculature. Very little attention has been given to the respiratory system because it was thought this system was "over-built" compared to the rest of the oxygen transport system, because the capacity of the pulmonary system is usually much greater than the demand placed on it during exercise in the healthy, young adult (Dempsey et al., 1990). It was not until the 1980's that this view was challenged by studies performed by Dempsey and colleagues (Dempsey, 1986). Dempsey hypothesized that in highly trained athletes the respiratory system might become the limiting factor during exercise, ultimately causing the individual to terminate the exercise. This hypothesis was based on the idea that with training, the capabilities of the cardiovascular and musculo-skeletal systems exceed that of the respiratory system. Indeed, a number of studies since then have demonstrated that the respiratory system does not adapt to the same extent as the cardiovascular system and the locomotor muscles in response to whole body training (Dempsey, 2006), rendering it the weak link in the oxygen transport chain. Specifically, the lung's diffusion capacity and pulmonary capillary blood volume does not change in the highly trained, while maximum pulmonary blood flow increases linearly with the enhanced maximal oxygen consumption ($\dot{V}_{O_2}max$) (Dempsey et al., 1990). Also, although ventilatory demands increase markedly, the capability of the airways to produce higher flow rates or of the lung parenchyma to stretch to higher tidal volumes remains unaltered.

The cascade of events leading to exercise termination, as proposed by Dempsey, includes physiological factors such as respiratory muscle fatigue, as well as neural factors such as the metaboreflex and the sensation of breathlessness (Dempsey et al., 2008). Early work by Loke et al. (Loke et al., 1982) showed that maximal inspiratory and expiratory pressures (MIP and MEP, respectively) measured after a marathon was significantly lower than pre-marathon values, suggesting potential global respiratory muscle fatigue following exercise. Studies using a more direct technique of transcutaneous bilateral phrenic nerve stimulation have demonstrated inspiratory muscle (diaphragm) fatigue during heavy endurance exercise (Babcock et al., 1995; Johnson et al., 1993; Mador et al., 1993). Expiratory (abdominal) muscle fatigue following exercise has been demonstrated using surface electromyography (Fuller et al., 1996) and magnetic stimulation of the nerve roots supplying the abdominal muscles (Taylor et al., 2006; Verges et al., 2006). Both inspiratory (Mador and Acevedo, 1991) and expiratory (Taylor and Romer, 2008; Verges et al., 2007) muscle fatigue impairs exercise performance. The metaboreflex is activated when blood flow and oxygen delivery to contracting muscles is insufficient for the rate of metabolism, so that chemical products of muscle metabolism accumulate within the muscle. This accumulation would stimulate group III and IV afferents which, in turn, elicit a reflex increase in sympathetic activity to the heart and vasculature which increases heart rate and blood pressure (Mitchell, 1990). Simultaneously, the increased sympathetic outflow causes vasoconstriction and thus reduced oxygen transport to the exercising limb muscles, possibly leading to peripheral limb fatigue (Dempsey et al., 2006). The most recent evidence for the existence of a respiratory muscle metaboreflex comes from a

study using inspiratory pressure threshold loading in rowers, in which a load of 60% MIP elicited a sustained increase in heart rate, mean arterial pressure, diastolic and systolic blood pressure (McConnell and Griffiths, 2010). Increased respiratory and peripheral locomotor muscle fatigue is thought to activate higher brain centers for the conscious awareness of breathlessness and exertion (Dempsey et al., 2008). Thus, the extremely uncomfortable sensation of breathlessness may be the deciding factor for exercise termination.

Since respiratory muscle fatigue is one of the first steps in the cascade, interventions using respiratory muscle strength training (RMST) could potentially delay or eliminate fatigue during high-intensity exercise. RMST was first performed, and is still being used in the clinical setting to improve cough and swallow function, and alleviate dyspnea in pathological conditions such as Chronic Obstructive Pulmonary Disease (COPD) (Harver et al., 1989; Lisboa et al., 1997; Weiner et al., 2003a), Multiple Sclerosis (MS) (Chiara et al., 2006), and Parkinson's Disease (PD) (Pitts et al., 2008). Exercise physiologists soon followed to examine the potential ergogenic effects of RMST in the athletic population. Most studies have focused on training the inspiratory muscles, while only very few studies have examined the effects of expiratory muscle training on exercise performance in athletes. Table 1-1 summarizes the studies using expiratory muscle strength training including protocols and results. Comparisons between previous studies of RMST are difficult because of the implementation of diverse implementation of training regimens, different laboratory tests of exercise performance, and the diverse subject population ranging from athletes to lung disease patients. Limitations of many of these studies include the lack of control or sham

groups. Chapter 1 examines the effects of a specific expiratory muscle strength training (EMST) protocol on maximal expiratory pressure generating capacity and exercise performance in highly trained collegiate swimmers by comparing an EMST group with a placebo air-flow training (AFT) group.

Intermittent Transient Tracheal Occlusions (ITTO) in Rats as a Model for Respiratory Muscle Training

Respiratory muscle training in humans is a voluntary process that requires the participant's motivation, attention, and ability to follow directions; qualities that animals do not fulfill. One way to elicit respiratory muscle training in animals is to perform tracheal occlusions. Our laboratory has developed a rat model of ITTO that promotes a better understanding of the effects of training on muscle tissue, neural activation and changes in gene expression profiles via invasive techniques. In our model of ITTO, occlusions are administered by inflating a rubber cuff that is secured around the extrathoracic trachea. Inflating the cuff closes off the lumen of the trachea. An occlusion of a complete breath (during one inspiration and expiration cycle) represents an infinite inspiratory and expiratory resistive load. In order to maintain alveolar ventilation during resistive loading, an animal's respiratory muscles must work harder. The first experiments were carried out while the animals were under urethane anesthesia, allowing for the examination of the respiratory load compensation reflex and the immediate effects of ITTO on the respiratory neural network (Chapter 3). Anesthesia suppresses breathing and the modulatory involvement of higher brain centers. Thus, the next experiments focused on ITTO in conscious, behaving rats. In these studies the animals were presented with repeated ITTO for 10 days to allow for conditioning and learning effects (Chapter 4).

Using the ITTO model, remodeling of diaphragm and intercostal muscles has been found in the form of significant increases in cross-sectional areas of fast-twitch type IIx/b fibers, suggesting respiratory muscle hypertrophy (Smith et al., 2010). Experiments using c-Fos, an indirect protein marker of neuronal activity that is expressed when neurons fire action potentials (Bullitt, 1990), and cytochrome oxidase, a mitochondrial enzyme marker for neuronal functional activity, have shown extensive modulation of the neural network including brainstem respiratory nuclei as well as supra-pontine nuclei involved in discriminative and affective neural pathways (Pate et al., 2008; Pate et al., 2010). Of particular interest was the finding of a significant increase in c-Fos activation in the medial thalamus following tracheal occlusions (Vovk et al., 2006), because it is thought that the thalamus acts as a gatekeeper for sensory information to higher brain centers. In addition, ITTO conditioning has been shown to produce anxiety-like behaviors (Pate et al., 2010).

These experiments clearly demonstrated that tracheal occlusions modulate the respiratory neural network, not just in the brainstem where the subconscious respiratory rhythm is generated, but also in higher brain centers involved in the perception and sensation of breathing. The ITTO model could thus be used to examine the molecular changes that occur with this type of respiratory muscle training and could potentially elucidate the role of the perception of breathlessness on limiting exercise performance.

Respiratory Load Compensation Response

The respiratory system is continually active, and any prolonged interruption is a threat to an animal's survival. Thus, it is of critical importance to maintain ventilation in the face of a variety of stimuli by adjusting the breathing pattern. Breathing frequency (f_b) and tidal volume (V_t) are the two components contributing to ventilation ($\dot{V}_E = V_t * f_b$).

Clark and von Euler (Clark and von Euler, 1972) described the relationship between volume and timing in anesthetized cats. They demonstrated that inspiratory time (Ti) depends on inspiratory volume and that the subsequent expiratory time (Te) depends on the preceding Ti. This volume-timing relationship was abolished after vagotomy, indicating that intact vagi were required to evoke the volume-timing response. A similar volume-timing relationship was found when a mechanical stimulus in the form of an external resistive load was applied. Loading of the inspiratory (Zechman et al., 1976) or expiratory (Koehler and Bishop, 1979) phase caused a decrease in volume and an increase in the duration of the respective loaded breath phase. The response to the added loads was called the respiratory load compensation reflex. Load compensation is a sensory-motor response utilized to maintain appropriate alveolar ventilation. Vagotomy prevents afferent feedback and leads to prolonged breath phases that are terminated by an inherent brainstem pattern generator (Zechman et al., 1976). As with vagotomy, complete tracheal occlusions prevent changes in lung volume, decreasing vagal afferent activity. The increased breath durations seen in response to occlusion approach values similar to those seen with vagotomy, confirming that vagal feedback from the respiratory pump is an important component in activating the load compensation response (Phillipson, 1974; Zechman et al., 1976).

A respiratory load of sufficient magnitude can be consciously perceived by the human and elicit uncomfortable sensations proportional to the size of the load (Killian et al., 1981). The reflexive load compensation response is activated by resistive loads and occlusions, but breathing is also behaviorally modulated in conscious animals and humans (Davenport and Vovk, 2009).

Sensory Gating

Gating of incoming sensory information is a way to control what and how much information will be received by higher brain centers. Gating is thought to be a protective mechanism for humans and animals to prevent the conscious perception of unnecessary stimuli and instead attend only to the meaningful ones. Sensory information from the periphery travels via spinal afferents to subcortical structures, where the stimuli are filtered and selected to either be relayed on to the cognitive centers or discarded. One of the proposed brain areas functioning as a gate for respiratory stimuli is the thalamus (Chan and Davenport, 2008). Malfunction of the thalamic gate or any interference with neurotransmitter modulatory systems have been associated with states of psychosis and delirium (Gaudreau and Gagnon, 2005) and disorders such as schizophrenia, post traumatic stress disorder, psychotic mania, and obsessive compulsive disorder (Javanbakht, 2006). Specifically, modulations to the serotonergic and dopaminergic systems appear to be important in gating processes. Activation of the serotonin receptor subtype 2A (HTR2A) reduces sensory gating so that more sensory information reaches cortical areas and thus consciousness, which in turn can lead to the pathology of anxiety disorders (Javanbakht, 2006). In addition, Carlsson and colleagues (Carlsson et al., 1999) have postulated that hyperactivity of dopamine reduces the protective influence of the inhibitory action of striatothalamic GABAergic neurons onto thalamocortical glutamatergic neurons, which can then lead to sensory overload and hyperarousal, confusion, or psychosis. Indeed, it has been shown that neuroleptic drugs that block receptors in the brain's dopaminergic pathways improve sensory functioning and gating in schizophrenic patients (Freedman et al., 1987).

Gating of respiratory activity is important for an animal's well-being. Eupneic breathing is usually not consciously perceived, meaning that respiratory afferents during normal breathing are gated out and do not reach higher brain centers. However, if ventilation changes sufficiently or breathing is attended to, the sensation is gated in and the animal becomes aware of its breathing (Chan and Davenport, 2008). This awareness is usually associated with distressing emotion (O'Donnell et al., 2007). Figure 1-1 shows the proposed schematic model of respiratory somatosensation and gating. The respiratory control center located in the brainstem provides ventilatory motor drive via descending bulbospinal projections that synapse with anterior horn cells in the cervical and thoracic spinal cord which in turn project to the respiratory muscles (Guz, 1997). Voluntary control of respiration is processed from the motor cortex through corticospinal connections to the respiratory muscles. Ventilation, including changes in volume, pressure, oxygen (O_2), and carbon dioxide (CO_2), is monitored by sensory feedback receptors positioned in the respiratory muscles, airways, lung, and chemoreception centers. These afferents connect back to the brainstem respiratory control center for automatic, subconscious control of breathing. In addition, respiratory afferents have been shown to reach the cerebral cortex. Specifically, electrical stimulation of the phrenic nerve resulted in the activation of neurons in the primary somatosensory cortex in the cat (Davenport et al., 2010). Breathing occurs mostly without conscious awareness, suggesting that a gate probably exists between the brainstem respiratory centers and higher brain regions.

The thalamus may be involved in respiratory gating based on evidence from several studies. Chen et al. (Chen et al., 1992) showed that when respiratory drive was

stimulated as measured by increased phrenic nerve activity, previously tonically active thalamic single units switched to rhythmic increases in firing that was associated with each respiration. Retrograde tracing experiments in cats indicated that phrenic afferents activate thalamocortical projections (Yates et al., 1994). Also, Zhang and Davenport (Zhang and Davenport, 2003) showed that inspiratory occlusions activated thalamic neurons in cats and rats. Positron emission tomography (PET) studies in humans exposed to hypercapnia identified neuronal activation extending from the upper brainstem, up through the midbrain, hypothalamus, and thalamus (Corfield et al., 1995). Other PET and functional magnetic resonance imaging studies in humans have shown that voluntary hyperpnea, or the behavioral modulation of breathing, activates distinct cortical (primary sensorimotor cortices, supplementary motor, and premotor cortex) as well as subcortical (thalamus, globus pallidum, caudate, and cerebellum) structures (McKay et al., 2003).

Respiratory information relayed through the thalamus reaches cortical areas for recognition and discrimination, as well as the limbic system for emotional processing (Figure 1-1) (Davenport and Vovk, 2009). It is the interplay between these brain areas that are responsible for the generation of the perception of breathlessness. This feeling of breathlessness, known clinically as the symptom dyspnea, is an aversive sensation. Animals and humans alike modify their behavior to avoid feeling breathless, such as terminating exercise as soon as the sensation becomes overwhelmingly uncomfortable. This situation is especially detrimental for respiratory disease patients who avoid exercise and maintain an inactive lifestyle, creating other serious impacts on health.

Perception of breathlessness also negatively affects the competitive athlete and it could be the limiting factor of performance.

Specific Aims

Specific Aim 1: To Investigate the Effects of Expiratory Muscle Strength Training in Collegiate Swimmers

Rationale: The hydrostatic pressure of water challenges the body's respiratory and cardiovascular systems. An early study of the mechanics of respiration during submersion in water found that vital capacity and expiratory reserve volume decreased and the total work of breathing increased significantly (Hong et al., 1969). Competitive swimmers are unique in that ventilation is limited to their stroke cycle; inspiration occurring only when the swimmer's face is out of the water, and expiration taking place under water (exception: backstroke). Thus while under water, the swimmer has to exhale against the pressure of the water, essentially inducing expiratory flow limitation (EFL). EFL during cycling exercise has been shown to limit exercise performance to about 65% of the individuals maximal work rate (Iandelli et al., 2002). A significant decrease in quadriceps muscle blood flow and increase in intercostals muscle blood flow suggest a redistribution of the cardiac output away from the locomotor and toward the respiratory muscles (Athanasopoulos et al., 2010). Furthermore, perception of dyspnea and leg muscle fatigue was significantly greater with EFL compared to unloaded exercise (Athanasopoulos et al., 2010; Iandelli et al., 2002; Kayser et al., 1997).

The respiratory muscles are skeletal muscles and thus adapt to a training stimulus in the same way as other skeletal muscles. In limb muscles, increases in strength have been shown to occur very rapidly in the early phase of a training protocol

(Hakkinen and Komi, 1983; Moritani and deVries, 1979). Recent studies in normal healthy people and respiratory disease patients have shown that expiratory muscle strength training (EMST) can specifically strengthen the muscles involved in expiratory air movement to generate higher positive pressures (Baker et al., 2005; Chiara et al., 2006; Gosselink et al., 2000; Griffiths and McConnell, 2007; Saleem et al., 2005; Sapienza et al., 2002; Sasaki et al., 2005; Smeltzer et al., 1996; Suzuki et al., 1995; Weiner et al., 2003b). However, there are only few and inconclusive studies on the effects of expiratory muscle training on performance in highly trained athletes such as college varsity swimmers. An increased ability to generate expiratory pressure could facilitate the swimmer's respiration. Presumably, the athlete will need to produce less effort during the breathing cycle and the feeling of breathlessness will be reduced. Conversely, for the same effort, the athlete can increase performance because respiration will become less of a limiting factor. A reduced perception of breathlessness, or a reduced work of breathing, would require a lower fraction of the cardiac output, so that more can be diverted to the locomotor muscles, thus decreasing the perception of exertion.

Hypotheses: Compared to air-flow training, four weeks of EMST will:

- Increase the maximum expiratory pressure generating capacity
- Decrease the perception of breathlessness and exertion
- Improve swim performance

Specific Aim 2: To Investigate the Changes in the Gene Expression Profile of the Medial Thalamus following ITTO in Anesthetized Rats

Rationale: Complete tracheal occlusion places an maximally obstructive load on the airway and should elicit a load compensation response, with modulation of breath timing and esophageal pressure. Airway occlusion is a stressful stimulus (Pate et al.,

2010). Respiratory diseases involving acute or chronic exposures to airway occlusion, such as asthma and chronic obstructive pulmonary disease (COPD) are associated with significantly higher rates of anxiety and depression compared to the general population (Moussas et al., 2008).

The thalamus is the proposed brain structure responsible for the gating of respiratory sensory information to the cortex. Information is continuously sent to this region from where it is either relayed to higher brain centers or suppressed. Thus, even in an anesthetized state, modulation of the gene expression profile of the thalamus can elucidate the immediate changes occurring with airway occlusion.

Hypotheses: ITTO in anesthetized rats will induce:

- A load compensation response with changes in breath timing and esophageal pressure
- Gene expression changes in the medial thalamus, specifically, modulation of neurotransmitter receptor genes involved in stress and anxiety pathways

Specific Aim 3: To Investigate the Changes in the Gene Expression Profile of the Medial Thalamus following 10 Days of Repeated ITTO in Conscious Rats

Rationale: Respiratory muscle weakness and fatigue have been implicated in an increased perception of breathlessness (1999; Gandevia et al., 1981; Kayser et al., 1997; Mador and Acevedo, 1991) and studies have shown that strength or endurance training of these muscles can improve this condition (Romer et al., 2002; Suzuki et al., 1995; Verges et al., 2008a; Verges et al., 2008b). However, the underlying mechanisms of the reduced perception following respiratory muscle training are not clear. Strength training causes adaptive changes within the nervous system that allow for full activation of a muscle in specific movements and better coordination of the activation of the relevant muscles, thereby effecting a greater net force (Sale, 1988). It is possible that

the increased capacity of the muscles leads to an increased threshold for load detection, potentially resulting in decreased feedback from the muscles. The reduced feedback could result in less activation of neurons in the thalamic gate, reducing the degree of information relayed to the cortex for load perception. Additionally, challenging the respiratory system with added external loads could change the threshold of the thalamic gate itself, such that an increase in sensory threshold would result in less gating-in of aversive respiratory feedback.

Since chronic airway obstructions in human patients are associated with increased risk of depression, repeated ITTO could trigger the molecular cascade leading to this detrimental condition.

Hypotheses: Repeated ITTO in conscious rats induce gene expression changes in the medial thalamus, specifically:

- Modulation of genes involved in sensory gating
- Modulation of genes involved in anxiety and depression

Table 1-1. Summary of EMST studies with reported MEP and functional changes.

Study	Participants	EMST protocol	MEP changes	Functional changes
(Suzuki et al., 1995)	Healthy	30% MEP, 15min, 2x/d, 4wk	EXP: ↑ 25.4%	Progressive treadmill exercise test: ↓ dyspnea
(Smeltzer et al., 1996)	MS	3x15reps, 2x/d, 7d/wk, 3mo	EXP: ↑ 36%, CONT: ↓ 1.9%	Not studied
(Gosselink et al., 2000)	Severe MS	60% MEP, 3x15reps, 2x/d, 3mo	↑ 35%, (N.S. compared to CONT)	Improved cough measures
(Hoffman-Ruddy, 2001)	Professional Singers	80% MEP, 4x6reps, 4 wk	EXP: ↑ 84%, CONT: ↑ 1.4%	EXP: ↓dyspnea during singing, ↑ relative energy, phase duration
(Sapienza et al., 2002)	High School Band Players	75% MEP, 4x6reps, 5d/wk, 2wk	↑ 48%	Not studied
(Weiner et al., 2003b)	COPD	15-60%, 30min/d, 6d/wk, 3mo	EXP: ↑ 21%	6min walk test: ↑ distance 19%, ↔ dyspnea daily activities
(Sasaki et al., 2005)	Healthy Women	30% MEP, 2x15min/d, 2wk	↑ 10.3%	Progressive walking treadmill test: ↓ $\dot{V}O_2$/kg and RPE
(Saleem et al., 2005)	1 PD Patient	75% MEP, 5x5reps	4wks: ↑ 55% 20wks: ↑158%	Improved UPDRS III scores
(Baker et al., 2005)	Healthy	75% MEP, 5x5reps, 5d/wk, 4 or 8 wk	4wks: ↑ 41%, 8wks: ↑ 51%	Not studied
(Chiara et al., 2006)	MS	40-80% MEP, 4x6reps, 8 wk	↑ both MS and CONT	Improved max voluntary cough values in mild MS
(Kim et al., 2009)	Sedentary Elderly	75% MEP, 5x5reps, 4 wk	↑ 44%	Improved cough measures
(Griffiths and McConnell, 2007)	Club Rowers	50% MEP, 30reps, 2x/d	4wks: ↑ 3.5% (N.S.) 6wks combined IMST/EMST: ↑31%	6 min all-out rowing test: N.S.
(Mota et al., 2007)	COPD	50% MEP, 30min/d, 3d/wk, 5 wk	EXP: ↑ 19%	6min walk test: ↑ distance 13%, Improved dyspnea at rest and QoL
(Kroff, 2008)	Women Field Hockey Players	Combined IMST/EMST, 30 breaths, 2x/d, 12 wk	EXP: ↑ 9% CONT: ↑ 4%	20 m shuttle run test: ↑ number of shuttles in EXP and CONT

Studies are listed in chronological order.

EXP = experimental group; CONT = control group; MS = Multiple Sclerosis; N.S. = not statistically significant ($p > 0.05$); COPD = Chronic Obstructive Pulmonary Disease; PD = Parkinson's Disease; $\dot{V}O_2$ = oxygen consumption; RPE = ratings of perceived exertion; UPDRS III = Unified Parkinson's Disease Rating Scale; QoL = Quality of Life.

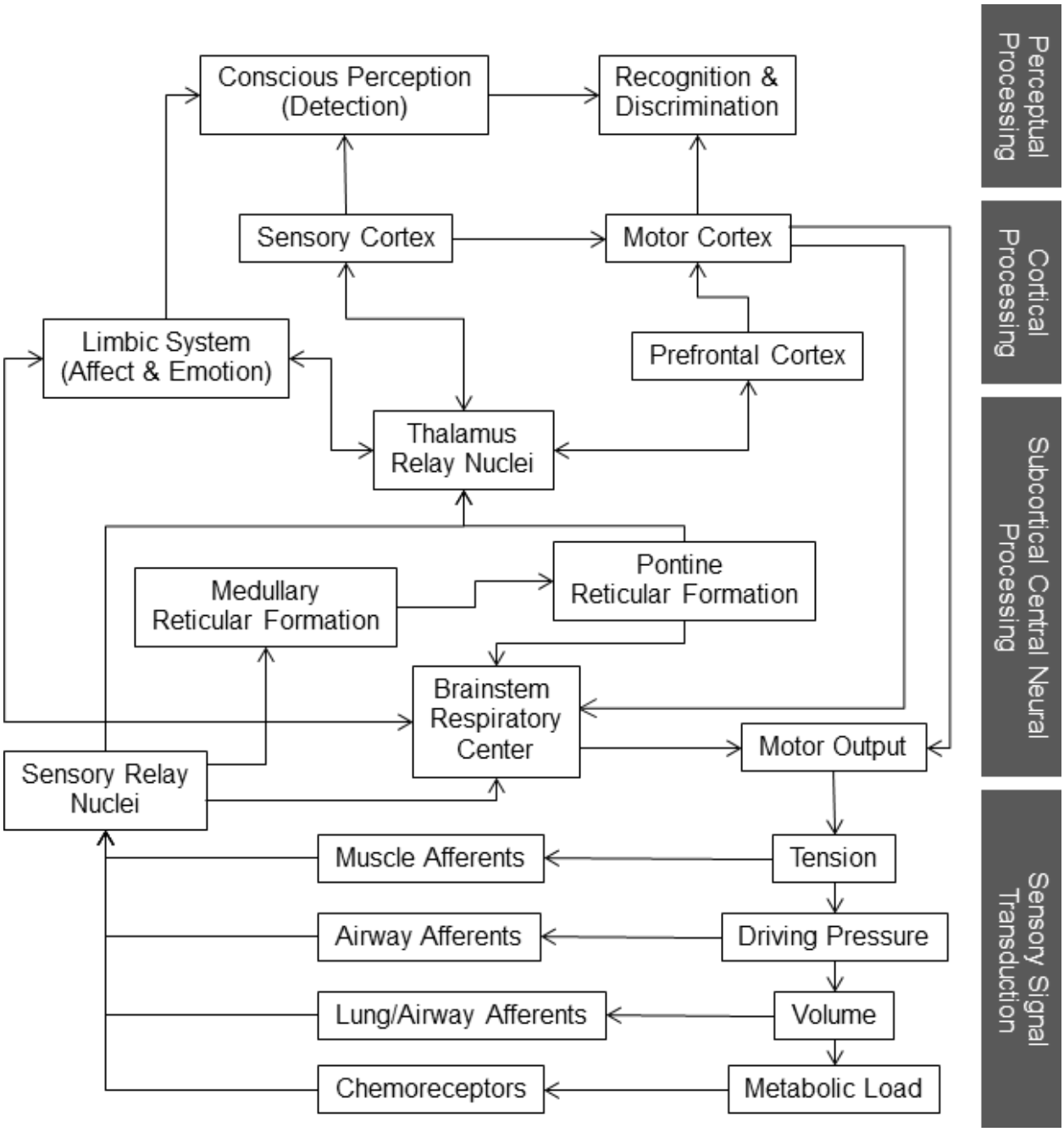

Figure 1-1. Model of respiratory information processing including sensory signal transduction, subcortical, cortical, and perceptual processing. In this model, the thalamus is acting as a gate for respiratory information to be relayed to the cortex and limbic system.

CHAPTER 2
THE EFFECTS OF EXPIRATORY MUSCLE STRENGTH TRAINING IN COLLEGE SWIMMERS

Introduction

Competitive swimmers control their breathing pattern to match the stroke cycle. In comparison to land-based sports, water exercise places additional challenges on the athlete's body due to the hydrostatic pressure of the aqueous environment, especially the respiratory system. During swimming, inspiration occurs only when the swimmer's face is out of the water, with expiration taking place under water. Thus, while under water, the swimmer has to exhale against the pressure column of the water which requires additional expiratory muscle force. Thus, swim performance may be directly affected by the strength of expiratory muscle pressure generating capacity.

Recent evidence has shown that expiratory muscle training can specifically strengthen the muscles involved in expiratory air movement to generate higher positive pressures (Baker et al., 2005; Chiara et al., 2006; Gosselink et al., 2000; Griffiths and McConnell, 2007; Saleem et al., 2005; Sapienza et al., 2002; Sasaki et al., 2005; Smeltzer et al., 1996; Suzuki et al., 1995; Weiner et al., 2003b). Expiratory muscle strength training (EMST) increases maximum expiratory pressures (MEP) in almost all study populations, from normal healthy individuals (Baker et al., 2005; Sapienza et al., 2002; Sasaki et al., 2005; Suzuki et al., 1995), to athletes (Amonette and Dupler, 2002; Griffiths and McConnell, 2007), to patients suffering from COPD (Weiner et al., 2003b), MS (Chiara et al., 2006; Gosselink et al., 2000; Smeltzer et al., 1996), or PD (Saleem et al., 2005). The highest increases in MEP could be seen with a strength training protocol of short expiratory burst of greater than 60% MEP. Sapienza and colleagues (Sapienza et al., 2002) trained high school band players at 75% MEP with 25 breaths per day for 5

days per week and found increases of 47 and 48% in MEP in boys and girls, respectively, after 4 weeks of training. Using the same protocol, in a case study of early idiomatic PD, Saleem et al. (Saleem et al., 2005) reported a 55% increase in MEP after 4 weeks and 158% after 20 weeks. Chiara et al. (Chiara et al., 2006) also found a significant increase in MEP in patients with MS.

Only a few studies have examined the effects of EMST on exercise performance. Suzuki et al. (Suzuki et al., 1995) trained healthy subjects at 30% MEP for 15 minutes twice daily for 4 weeks. During an incremental submaximal running test, the subjects exhibited increased tidal volume, and decreased minute ventilation, breathing frequency, and ratings of dyspnea. Sasaki (Sasaki et al., 2005), using the same training paradigm, showed that $\dot{V}_{O_2}$/kg body weight and ratings of dyspnea decreased. The only study that examined EMST on performance in athletes reported that training at 50% MEP for 4 weeks increased MEP, however, no significant difference in performance could be found during an incremental rowing test (Griffiths and McConnell, 2007).

Traditionally, the respiratory system, specifically, the lung, airways, and respiratory muscles, have been viewed as being structurally overbuilt and usually well adapted for normal every-day use and moderate exercise in healthy people with respect to maximum metabolic requirements for gas transport (Aliverti, 2008; Dempsey, 1986; Maglischo, 2003). The large diffusion surface area and the short distance between the alveolar membrane and capillary ensure that ventilation is usually not a limiting factor for exercise metabolism. However, studies have shown that in highly trained athletes, the respiratory system may in fact impose a limiting factor to exercise performance (Boutellier et al., 1992; Dempsey, 2006; Harms et al., 2000). Indeed, with the increased

aerobic capacity in these athletes, the lung diffusion surface, the airways, and also the respiratory muscles, do not adapt to the training stimulus as much as other links in the oxygen transport system. Thus, the respiratory system can limit exercise during conditions of extraordinarily high metabolic demands. In addition, the work of breathing during near-maximal exercise requires about 15% of the total $\dot{V}_{O_2}$, compared with about 10% in moderately fit subjects (Aaron et al., 1992). The ability of the lungs to move O_2 into the body during inspiration and CO_2 out of the body during expiration at fast rates during high intensity exercise is directly related to the strength of the inspiratory and expiratory muscles that inflate and deflate the lungs. Depletion of O_2 and build-up of CO_2 during exercise will limit the duration and intensity of the activity. Thus, during timed competitions, inspiratory and expiratory muscle activity in the athlete is critical to maintain adequate gas exchange and energy balance. Additionally, the high work of breathing renders the swimmer susceptible to the feeling of breathlessness and the perception of exertion. These subjective sensations are usually the factors that are responsible for an athlete's premature termination of the activity and thus limit optimal performance.

It was hypothesized that expiratory muscle strength training using a pressure-threshold training device could increase the maximum expiratory pressure generating capacity, decrease the perception of breathlessness and exertion, and improve performance in highly trained collegiate swimmers. Peak airflow meters were hypothesized to have negligible effects on expiratory muscle strength as it provides no resistance to airflow.

Materials and Methods

Subjects

Seventeen University of Florida (Division I) varsity swimmers (fifteen males, two females) participated in this study. All procedures were approved by the University of Florida Institutional Review Board. All participants were classified as normal on the basis of habitual good health and no evidence of respiratory restriction or obstruction. All participants consented to the study requirements in writing.

Inclusion criteria consisted of:

- Participation at every scheduled swim practice session
- No history of cardiorespiratory disease
- No history of smoking
- No evidence of current major or minor illness
- No prior participation in expiratory muscle strength training

Exclusion criteria consisted of:

- $FEV_{1.0}$ of less than 80% of predicted
- Regular episodes of bronchoconstriction
- Taking medication for respiratory disease
- Positive pregnancy test (females)

Experimental Design

The study followed a single-blind, placebo-controlled pre-training/post-training repeated measures design. Participants were randomly assigned to an EMST or an airflow training (AFT) group. Both groups performed training 5 times per week for 4 weeks. Pulmonary functions, MEP, $\dot{V}_{O_2}$ during an incremental upper body performance test, and performance measures during a 6 x 100 m freestyle swim test were assessed.

Procedures

Pulmonary function assessment

Lung functions for all subjects were determined before and after EMST or AFT training. Instructions for spirometry testing were based on the American Thoracic Society Standard (1995). Following a few normal breaths, the subject inhaled deeply and then provided a forced expiration. Forced expiratory volume in one second ($FEV_{1.0}$) and forced vital capacity (FVC) were recorded (Jaeger Toennies) and the ratio $FEV_{1.0}$/FVC calculated. Resting respiratory resistance was measured by the forced oscillation method (Jaeger Toennies).

Maximum expiratory pressures

MEP was measured before and after training. MEP was defined as the greatest positive pressure obtained at the mouth sustained for at least 1 s while performing a maximal expiratory effort from total lung capacity (TLC). MEP was assessed using a portable pressure manometer with a 16 gauge controlled leak in the exhaust port to prevent generation of high pressures by the buccal muscles and maintain an open glottis during the measurements. The participants stood upright with their nose closed by a nose-clip. They were instructed to make maximal forceful expiratory efforts. Repeated measurements were taken, with a 1 to 2 min rest between trials, until 3 measurements within 10% variability were obtained. The best MEP measurement was recorded for data analysis.

Expiratory muscle strength training (EMST)

Each participant in the EMST group was assigned an expiratory pressure-threshold trainer. Trainers were handed out before each training session and collected at the end to ensure compliance. The training device consisted of a mouthpiece and a

one-way spring-loaded valve (Figure 2-1A). The participants were instructed to take a deep breath in, put their mouth around the mouthpiece, and exhale as hard as possible. Expiratory airflow was blocked by the valve until a sufficient pressure was produced to overcome the spring force. The threshold load was set initially at 75-80% of the participants' pre-training MEP and increased weekly by 15%. EMST was performed at the same time of day, five days per week for four weeks. Each training session consisted of five sets of five-breath repetitions with 1-2 min rest between sets.

Airflow training (AFT)

AFT was used as a placebo control. AFT was conducted with peak airflow meters (Figure 2-1B). The participants were told that the purpose of the study was to compare the EMST with the AFT device. As with EMST, the training devices were handed out only for the training sessions. The participants of the AFT group were instructed to target a specific expiratory airflow rate that was 75-80% of the pre-training maximal peak expiratory airflow rate. The participants were instructed to take a deep breath in and then exhale with as much force as needed to reach the desired airflow rate. The participants were able to see their effort on the device and could adjust the airflow rate of their next breath. The targeted airflow rate was increased each week by 15%. As for the EMST group, training was performed at the same time of day, five days per week for four weeks. Each training session consisted of five sets of five-breath repetitions with 1-2 min rest between sets.

$\dot{V}O_2$max test on swim bench

$\dot{V}O_2$max tests were performed before and after the training period. All participants had prior experience with the Vasa Swim Ergometer (Vasa, Essex, Vermont). This ergometer featured a flywheel drive system with variable wind resistance depending on

the pulling power of the subject. Wind resistance was adjusted by changing the opening of the damper door. An attached electronic monitor measured time and stroke rate. The participants lay in a prone position on the bench of the ergometer. The bench distance to the flywheel was fixed and the legs were supported for comfort and to reduce lower body movement. The participant used the paddles of the ergometer and mimicked the upper body movement of the butterfly stroke. A complete test consisted of 10 levels of 90 s each. The resistance of the ergometer was incrementally increased by using the seven levels of the damper door with a constant stroke rate (35 strokes per min); during the last three levels the stroke was increased by 2 strokes per min each time. Stroke rate was maintained by using a metronome. The test was terminated when the participant voluntarily stopped or after the 10 levels were completed. Throughout the test the participants were verbally motivated. The participants breathed through a mouthpiece that was connected to a metabolic cart (ParvoMedics, Sandy, UT). A nose clip ensured that the participant only breathed through their mouth. The rate of oxygen uptake, $\dot{V}_{O_2}$, and the rate of carbon dioxide output, $\dot{V}_{CO_2}$, and minute ventilation ($\dot{V}_E$) were measured via a sampling tube connected to the mouthpiece. Ratings of breathlessness (RB) and perceived exertion (RPE) were collected alternately every 45 sec. A modified Borg category-ratio scale ranging from zero to ten was used to assess the participants' subjective ratings throughout the test (Appendix A) (Borg, 2008).

Timed interval swim tests

Participants performed a timed interval swim test during the weeks before and after EMST or AFT training. This test consisted of all-out 6 x 100 m freestyle on an

interval of 2:30 min. The test was conducted in a 50-m outdoor swimming pool at the same time of day during a regular swim training session. A standard warm-up of 2000 m preceded the test. Time and alternately RB and RPE (Appendix A) were collected after each 100 m interval. Heart rates were collected after warm-up immediately before the test start, after interval #1, and after interval #6. Heart rate was measured using a chest belt with a transmitter that measures the electrocardiogram and sends the heart rate information to a wrist watch monitor (Polar Electro Inc., Lake Success, NY).

Statistical Analysis

All values were reported as mean ± SD unless stated otherwise. Baseline differences in anthropometrical data between subjects were compared using an independent Student's t-test. For pulmonary function ($FEV_{1.0}$, FVC, and $FEV_{1.0}$/FVC), pre- and post-training comparisons were analyzed using one-way ANOVA with repeated measures. MEP values, as well as average time, times of first and last 100 m during the 6 x 100 m swim test were compared using two-way repeated measures ANOVA (Subject, Factor 1 = Group EMST/AFT, Factor 2 = Time of measurements pre/post). Pearson's correlation was used to measure of dependence between changes in MEP and swim time.

Results

Demographics

Twenty-two swimmers originally volunteered and completed pre-testing. Five withdrew for reasons unrelated to this study. Seventeen (77%) underwent the complete training period and post-testing. Characteristics of these 17 are presented in Table 2-1. There were no significant differences in any of these data between the groups. Participants were randomly divided into either EMST or AFT groups. The EMST group

consisted of 3 sprint, 9 middle-distance swimmers; the AFT group included 3 sprint, 3 middle-distance, and 2 distance swimmers.

Pulmonary Functions and MEP

Pulmonary function values are shown in Table 2-2. PFT values in all subjects were greater than predicted ($FEV_{1.0}$: 113.67 ± 13.06% in EMST group and 118.63 ± 11.25% in AFT group; FVC: 118.67 ±12.97 in EMST group and 125.38 ± 12.08% in AFT group). There were no significant differences between groups and none of the values changed significantly with either EMST or AFT. $FEV_{1.0}$ and FVC values were greater than healthy non-athletes (% predicted) as well as land-based athletes and swimmers (Armour et al., 1993; Doherty and Dimitriou, 1997; Holmberg et al., 2007; Rong et al., 2008; Sonetti et al., 2001; Wells et al., 2005), and similar to national-level male swimmers (Armour et al., 1993).

All individuals in the EMST group showed significant increases in MEP, while those in the AFT exhibited non-significant small increases or decreases (Figure 2-2). There was a significant Time effect (pre/post) ($p = 0.001$) and interaction between Group and Time ($p = 0.049$). Post-hoc analysis showed that post-training values were significantly increased compared to the pre-training in the EMST group ($p = 0.004$), but not in the AFT group ($p = 0.236$) (Table 2-3 and Figure 2-3).

$\dot{V}O_2$ Test

Of the 17 participants, 2 did not perform the post-training $\dot{V}O_2$ test due to shoulder/wrist injuries unrelated to this study. The incremental swim ergometer $\dot{V}O_2$ test was a submaximal exercise for most swimmers. Of the 30 pre- and post-training tests, 23 were fully completed, while 7 were terminated by the participant either because of

maximum rating of breathlessness (2 individuals) or maximum rating of perceived exertion (5 individuals). The swim ergometer's computer reported the work expended for every stroke, which allowed for analysis of the correlation between the work rate and $\dot{V}O_2$. Both of these values increased throughout the test, consistent with the incrementally increasing resistance of the test protocol. There was no significant difference between the EMST and the AFT group, and neither pre- and post-training. There were no significant differences in minute ventilation, breathing frequency, and respiratory exchange ratio. Ratings of perceived exertion and breathlessness increased in all participants with no significant differences between groups or pre- and post-training.

Swimming Performance

Average swim time in the 6 x 100 m freestyle test decreased post-training by -1.0 ± 1.7 sec ($p = 0.084$) in the EMST group and -0.2 ± 1.6 sec in the AFT group ($p = 0.378$) (Figure 2-4). Post-hoc analysis revealed a significant difference between groups ($p = 0.036$) that was not dependent on pre- or post-values. Expressed in percent the improvement in time was -1.44 ± 2.73% in the EMST group and -0.29 ± 2.66% in the AFT (Figure 2-5). There was no significant difference in the time change between the groups ($p = 0.204$). There was no significant correlation between the individual changes in MEP and swimming performance between pre- and post-training ($r = 0.382$, $p = 0.160$) (Figure 2-6).

The first 100 m interval of the pre- and post- 6 x 100 m test was non-significantly slower in both groups (EMST: 1.21% ± 1.14, AFT: 1.53% ± 1.59) and the last 100 m

interval of each test was non-significantly faster in both groups (EMST: 1.56% ± 2.01, AFT: 0.6% ± 1.25) (Figures 2-7 and 2-8).

Heart rates increased significantly ($p < 0.001$) in all participants throughout the test compared to baseline. There was no significant difference between groups or pre- and post-training (Figure 2-9).

Ratings of perceived exertion and breathlessness increased significantly ($p < 0.001$) in all participants throughout the test. There were no significant differences between groups or pre- and post-training (Figures 2-9 and 2-10).

Discussion

Pulmonary Functions and MEP

Intensive swim training leads to increases in pulmonary functions (Clanton et al., 1987). In the present study we show that high level competitive swimmers exhibit larger than predicted FVC and $FEV_{1.0}$ values, consistent with previous studies (Doherty and Dimitriou, 1997; Stuart and Collings, 1959). Other studies have also demonstrated above average vital capacities, residual lung volumes, functional residual capacities, and total lung capacities in swimmers compared to non-water athletes and non-athletes (Cordain et al., 1990; Magel and Faulkner, 1967; McKay et al., 1983). The respiratory training in our study did not further increase lung function, suggesting that no structural changes in the anatomy of the respiratory system occurred with training.

MEP increased significantly in the EMST group, but not the AFT group. Since there was no change in pulmonary functions, the change in MEP cannot be explained based on lung mechanics. The ability to generate higher expiratory pressures is directly related to the strength of the expiratory muscles. Increased expiratory pressure generating capacity is particularly important during swimming since exhalation occurs

when the head is under water with a water pressure of at least 20 cmH_2O. AFT was not effective in increasing MEP; thus pressure-threshold strength training is a better method to increase expiratory muscle pressure generating capacity. Pre-training MEP values were similar to healthy non-athletes (Baker et al., 2005; Sapienza et al., 2002) and club-level rowers (Griffiths and McConnell, 2007), suggesting that the overall fitness and highly conditioned abdominal muscles of swimmers does not correlate with a higher expiratory pressure-generating capacity. The increase in MEP with EMST shows that respiratory training can be aimed specifically at targeted expiratory muscles.

Oxygen Consumption ($\dot{V}O_2$)

Exercise performance heavily depends on the interplay between the respiratory and cardiovascular systems. There are several steps in the oxygen consumption chain including cardiac output, inspired fraction of oxygen (FIO_2), alveolar ventilation, lung and muscle diffusion capacities, hemoglobin concentration, and mitochondrial rate of O_2 consumption (Wagner, 1996). It is believed that maximal O_2 transport from the lungs to the working locomotor muscles and diffusion from the muscle capillaries to the mitochondria are the major determinants of $\dot{V}O_2max$ (Saltin and Calbet, 2006; Wagner, 2006). $\dot{V}O_2max$ is defined as the maximum amount of oxygen a person can take up during one minute of exercise and is directly related to a person's ability to supply energy for muscular contraction through aerobic metabolism.

Traditionally, $\dot{V}O_2max$ tests are administered on a treadmill or stationary bicycle ergometer. However, specificity of the test in terms of the muscles used and the movements during the particular sport is critical to ensure that the measured $\dot{V}O_2$ relates to the actual $\dot{V}O_2$ the athlete experiences during training or competition. A trained

swimmer's body reacts very differently than that of a runner during various exercise tests (Armstrong and Davies, 1981; Corry and Powers, 1982; Holmer et al., 1974; Magel and Faulkner, 1967). Corry and Powers (Corry and Powers, 1982) showed that runners could reach only 53% of their running $\dot{V}O_2$max in an arm cranking exercise, while swimmers reached 79%. Other studies also have illustrated that elite swimmers had lower $\dot{V}O_2$max, heart rate, $\dot{V}E$, and ventilatory coefficient during maximum swimming than during maximum running or cycling (Holmer, 1972; Holmer et al., 1974; Magel and Faulkner, 1967). The swim ergometer used in the present study exhibits several advantages over other ergometers when measuring the respiratory responses of swimmers. First, the test was performed in a prone position imitating the swimmer's horizontal body position. Body position plays an important role in cardiopulmonary control due to gravity (Rowland et al., 2008). During heavy exercise, $\dot{V}O_2$ kinetics is slower in a horizontal than in an upright position (Koga et al., 1999) and venous return is greater reducing blood hydrostatic pressure in the legs (Holmer et al., 1974). Second, the swim ergometer simulates closely the actual stroke pattern of movement used by the swimmer in the water. Third, the flywheel drive system of the ergometer, which is the same as used in rowing ergometers, offers variable wind resistance depending on the pulling power of the test participant. This simulates the resistance of water in that the harder the participant pulls, the more resistance the flywheel provides. To our knowledge, our study is the first to use this particular swim ergometer to measure the respiratory responses of swimmers during an incremental exercise test. Other incremental $\dot{V}O_2$max studies have been conducted using a variety of models and

protocols (Armstrong and Davies, 1981; Konstantaki et al., 1998; Potts et al., 2002; Rowland et al., 2008; Swaine and Zanker, 1996).

The effects of respiratory muscle training on oxygen consumption are unclear, some studies showing improvements in $\dot{V}O_2$ (Holm et al., 2004; Sasaki et al., 2005), while others report no changes (Downey et al., 2007; Fairbarn et al., 1991; Gething et al., 2004; Romer et al., 2002; Sonetti et al., 2001; Sperlich et al., 2009). In the present study, there were no significant changes in $\dot{V}O_2$ or other measurements during the incremental exercise test after respiratory training. There is a limit on the $\dot{V}O_2$max an athlete can achieve that is set by genetic factors. Training can only improve $\dot{V}O_2$max until that limit is reached. Thus, the lack of improvement could be due to the already maxed out oxygen consumption chain in these athletes.

Functional Significance of Improvements in Swim Performance Times

Small, but noteworthy changes were detected in swimming performance. The observed 1.15% time difference between the two groups post-training represents the difference between first and twelfth place at the 2008 Olympic Games Men's 100 m freestyle preliminary races (Figure 2-11).

A recent study found remarkably similar swim performance time improvements after inspiratory muscle training (IMT) (Kilding et al., 2010). The IMT group performed 30 inspiratory efforts at 50% maximal inspiratory pressure (MIP) twice daily for six weeks, while the control group did a sham training consisting of 60 breaths at 15% MIP once daily. Swim performance was measured in time trials pre- and post-training. Significant improvements were found during a 100 m (-1.7 ± 1.4%) and 200 m (-1.5 ± 1.0%), but not a 400 m (0.6 ± 1.2%) time trial. The training paradigm in the present

study differed in that it was a lower-repetition, higher-intensity expiratory muscle strength training for a shorter period of time (four weeks). The swim performance test used here was an endurance sprint test rather than a time trial. The average 100 m freestyle times during the 6 x 100 m test achieved by the collegiate swimmers in our study were almost identical to the 1 x 100 m time trial in Kilding et al.'s study, indicating that our athletes performed at a higher level. The higher the level of performance is, the smaller and rarer the improvements are. Thus, an improvement of 1.15% can prove to be very beneficial for high-level athletes.

Properties of Respiratory Muscles

The respiratory system consists of inspiratory, expiratory, and accessory muscles, which may either separately, or in concert, limit exercise performance. Differences between the inspiratory and expiratory muscles include (a) muscle activity, (b) muscle fiber type, and (c) predisposition to fatigue. The muscle activity pattern differs greatly between inspiratory and expiratory muscles. The diaphragm, the most important inspiratory muscle, is continuously engaged in rhythmic activity to create a sub-atmospheric pressure driving air into the lungs. This muscle cannot pause to rest under any circumstance, so it must be very resistant to fatigue. Indeed, Johnson and colleagues (Johnson et al., 1993) have shown that the diaphragm only fatigues with prolonged constant-load exercise of high intensity levels greater than 85% of $\dot{V}O_2$max. Diaphragm fatigue did not occur following a maximal incremental exercise cycling performance in moderately fit subjects (Romer et al., 2007). However, Lomax and McConnell (Lomax and McConnell, 2003) measured maximal inspiratory pressures (MIP) before and after a single 200 m freestyle swim at 90-95% of race pace in

competitive swimmers. After the swim the average MIP decreased from ~112 to ~80 cm H_2O, suggesting that inspiratory muscle fatigue could be induced in this population in less than 2.7 min. In contrast to inspiration, expiration is usually a passive process during normal breathing due to the elastic recoil of the respiratory system that pushes air out without the need to contract the expiratory muscles. However, during exercise, the elastic recoil pressure of the lungs is not sufficient to keep up with the increased demand, so the expiratory muscles actively contract to force air out of the lungs. As ventilatory demand increases during constant work heavy exercise expiratory muscle pressures increase more than inspiratory muscle pressures so that the expiratory muscles take on a greater proportion of the total respiratory muscle work (Krishnan et al., 2000), thus relieving the inspiratory muscles. Inspiratory muscle pressures plateau while expiratory muscle pressures continue to increase throughout heavy exercise (Kearon et al., 1991). Expiratory muscles may facilitate inspiration by lowering the end-expiratory lung volume, thus providing passive elastic recoil of the inspiratory muscles during the initial portion of inspiration (Henke et al., 1988).

Muscle fiber morphology also varies between inspiratory and expiratory muscles. Histochemical profiling of human respiratory muscles have shown a fiber type distribution of about 50% slow twitch, 25% fast twitch (FTa) and 25% FTb fibers in the costal diaphragm, 62/20/18% in inspiratory intercostals, and 64/35/1% in expiratory intercostals (Mizuno, 1991). The cross-sectional area of the expiratory intercostals was found to be ~50% larger than inspiratory intercostals (Mizuno and Secher, 1989). The larger the muscle fiber, the stronger its contractile properties, and the faster its fatigue characteristics (Sieck and Prakash, 1997). According to these characteristics, the

expiratory muscles are able to contract with great force early on but are unable to sustain the high intensity so that force production decreases quickly. Furthermore, the high amount of large capillary-rich FTa and the lack of FTb fibers in the expiratory intercostals suggest that these muscles are used during repeated dynamic ventilatory actions requiring relatively large force (Mizuno and Secher, 1989). Our respiratory training in rats using tracheal occlusions showed significant increases in cross-sectional area of the fast twitch type IIx/b fibers in the diaphragm and intercostals muscles (Smith et al., 2010).

It has been shown that expiratory loading imposes a much higher oxygen consumption than inspiratory loading, suggesting that the efficiency of the expiratory muscles to overcome respiratory loads is much lower than that of the inspiratory muscles (Dodd et al., 1988). The larger fiber size of the expiratory muscles combined with their sporadic activation with increasing work of breathing renders them especially susceptible to fatigue. High-intensity, exhaustive exercise leads to a decline in expiratory muscle endurance (Fuller et al., 1996). Taylor et al. (Taylor et al., 2006) and Verges et al. (Verges et al., 2006) have shown that cycling exercise elicits abdominal muscle fatigue, as measured by magnetic stimulation. Cycling is traditionally viewed as a lower limb muscle exercise, yet these results show that the expiratory muscles perform a considerable amount of work as well. The observation that the abdominal muscles fatigued in this experimental setting argues that during swimming these muscles may fatigue even quicker because they play a dual role in stabilizing and rotating the body in the water. In these two studies the researchers recruited healthy male subjects of a broad range of fitness levels and demonstrated that there was no

significant correlation between the subjects' $\dot{V}O_2max$ and their abdominal muscle contractility (Taylor et al., 2006; Verges et al., 2006). This suggests that even highly trained athletes are not immune to respiratory muscle fatigue. Furthermore, Kyroussis et al. (Kyroussis et al., 1996) reported that the abdominal muscles fatigued after only two minutes of maximal isocapnic ventilation, as measured by twitch gastric pressure elicited by magnetic stimulation. Resistive loads added to inspiration or expiration induces muscle fatigue, which can be attributed directly to the high work of breathing against the load (Suzuki et al., 1991). Expiratory muscle fatigue can significantly impair exercise performance (Mador and Acevedo, 1991; Verges et al., 2006). Prior induction of expiratory muscle fatigue by resistive breathing resulted in a significant decrease in performance as measured by distance covered and speed during a 12 min running test, (Verges et al., 2007) as well as exercise time to exhaustion in a cycle ergometer test at 90% of peak power (Taylor and Romer, 2008).

The structural and functional properties of the respiratory muscle fibers can be modified in response to physiological and pathological conditions, such as training, aging, and respiratory diseases (Polla et al., 2004). Volianitis et al. (Volianitis et al., 2001) have shown that respiratory muscle fatigue in male rowers can be alleviated with respiratory muscle training. Thus strengthening the expiratory muscles could lead to a higher resistance to fatigue and in turn improve performance.

Interestingly, concurrent inspiratory and expiratory muscle training had little effect on performance parameters. Amonette and Dupler (Amonette and Dupler, 2002) reported that maximal $\dot{V}_E$ increased but $\dot{V}O_2max$ did not change in trained triathletes after 4 weeks of combined IMT/EMT of 30 breaths twice daily. The same training device

was employed by Wells et al. (Wells et al., 2005) in adolescent swimmers. Twelve weeks of concurrent IMT/EMT with increasing resistance (50-80% MIP/MEP) resulted in significant increases in all pulmonary function and respiratory muscle strength parameters. However, peak velocity during a swim test did not change and critical speed tended to improve but was not significant at 12 weeks. As Wylegala et al. (Wylegala et al., 2007) pointed out, the high intensities of training in the later weeks could have led to chronic respiratory muscle fatigue and may have blunted potential performance improvements especially if the recovery time was not sufficient before testing. Griffiths and McConnell (Griffiths and McConnell, 2007) trained two groups of competitive rowers for 4 weeks on either inspiratory or expiratory trainers at 50% MIP or MEP and then combined the groups for another 6 weeks of concurrent IMT/EMT training. During the last 6 weeks, MEP only increased significantly in the group that performed EMT in the first 4 weeks (31%). However, there were no significant changes in this group in the rowing test. All of these studies used a training protocol of 30 breaths at a relatively low intensity. Thus, this endurance training may not be as effective as a strength training protocol with high-intensity loading.

Pacing Strategies

The finding of increased time of the first 100 m interval and the decreased time of the last 100 m interval during the 6 x 100 m swim test can be attributed to the use of different pacing strategies by the swimmers. Pacing and the perception of effort are closely intertwined. When the perception of effort becomes too large, pace will decline. It has been suggested that a brain area exists that controls pace by incorporating knowledge of the endpoint, memory of prior events of similar distance or duration, and knowledge of external and internal conditions (St Clair Gibson et al., 2006). In the

present study, probably the most important factor that changed was the memory of the pre-training test. Before the tests, the swimmers were told to give maximal effort on all six intervals. During the post-training test, the swimmers remembered the previous test and the associated high perception of effort. This memory most likely resulted in a slow-start pacing strategy (St Clair Gibson et al., 2006), which is characterized by a submaximal pace at the beginning, in order to minimize possible system failure.

Potential Mechanisms

One potential mechanism by which the respiratory system influences exercise performance has been brought forth by Dempsey (Dempsey et al., 2008; Dempsey et al., 2006). According to this hypothesis the increased respiratory muscle work during heavy exercise leads to respiratory and limb muscle fatigue and, in turn, reduced exercise performance. In detail, Aaron et al. (Aaron et al., 1992) estimated that the respiratory muscles require 10-16% of total $\dot{V}_{O_2}$ and cardiac output due to hyperventilation during heavy exercise. This competition for cardiac output between the respiratory muscles and the exercising limb muscles would lead to respiratory muscle fatigue. Diaphragm fatigue has been shown to induce a metaboreflex via small diameter group IV fibers (Hill, 2000) causing increased sympathetic activation of vasoconstriction and decreased oxygen transport to limb musculature. The decreased cardiac output to the limb muscles could result in peripheral muscle fatigue and increased perception of effort, eventually leading to decreased exercise performance. Evidence that respiratory muscle work affects peripheral fatigue comes from a study by Romer et al. (Romer et al., 2006), which demonstrated that unloading of the respiratory muscles using a

proportional assist ventilator decreased exercise-induced peripheral muscle fatigue by 30-35%.

Strengthening of the respiratory muscles makes them more resistant to fatigue. A delay in respiratory muscle fatigue attenuates the metaboreflex vasoconstriction of limb muscles. In addition, more efficient respiratory muscles require less of the cardiac output. These two factors could result in delayed limb muscle fatigue, decreased perception of effort and breathlessness, and ultimately, increase exercise tolerance.

Perception of Breathlessness

The final factor limiting exercise is exercise related perception which is sensory and behavioral in nature (Killian and Campbell, 1995). These sensations include perception of general exertion, effort, and the feeling of breathlessness. When the discomfort associated with any of these factors becomes intolerable the subject will slow down or terminate the exercise. During a maximal effort exercise, the subject is aware of both the increasing central motor command and the decline in power output (Killian and Gandevia, 1996); the awareness of these two factors gives rise to the sensation of fatigue (Jones and Killian, 2000). Breathlessness, either in combination with peripheral muscle fatigue or by itself, is the most common factor limiting performance (Killian and Campbell, 1995). The sensation of breathing likely depends on several different mechanisms that are involved in the regulation of breathing including feed-forward and feedback mechanisms (Figure 2-12) (Chonan et al., 1990b). Perception of exertion and breathlessness develops when there is a mismatch between the central respiratory motor command and afferent information. When exercise intensity increases, the central motor command increases. Corollary discharges from descending motor commands to the sensory cortex increases and thus perception of

exertion and breathlessness increases. Also, when exercise intensity increases, increased inputs from a variety of receptors send their feedback to the sensory cortex, including receptors in the respiratory muscles, the chest walls, the lungs, the lower and upper airways, as well as chemoreceptors (Killian and Gandevia, 1996). Furthermore, with increasing muscle fatigue or weakness, the respiratory motor drive increases to achieve a given muscle tension, which in turn will increase the sense of effort (Homma and Masaoka, 1999). Subjects with weakened (Gandevia et al., 1981) or partially paralyzed (curarized) inspiratory muscles (Campbell et al., 1980) show higher magnitude estimations of respiratory loads and inspiratory muscle training significantly decreased this perception for small loads (Kellerman et al., 2000). Inspiratory muscle training could have decreased the motor drive in proportion to the increased respiratory muscle capacity or the decrease in muscle work for the task might have reduced the activation of mecahnoreceptors, thus decreasing sensory feedback (Kellerman et al., 2000)

The sensation of breathlessness is further augmented by increases in expiratory motor output induced by external resistive loads (Chonan et al., 1990a). With EFL during exercise in normal subjects, end-expiratory lung volume could not be reduced, so that end-inspiration occurred at an ever higher lung volume, leading to dynamic hyperinflation (Kayser et al., 1997). The work of the inspiratory muscles increased because of the increased elastic loads and the evermore disadvantageous part of the length-tension relationship. Severe dyspnea in the flow-limited subjects resulted in termination of the exercise (Kayser et al., 1997). Iandelli et al. (Iandelli et al., 2002) also demonstrated that performance during airflow-limited exercise was seriously impaired

mainly because of increased pressures developed by the expiratory muscles. In this study the control subjects rated their breathing sensation during the exercise a value of 4 on the Borg scale (0-10) at the maximum power output (W_{max}), while airflow-limited subjects defined their dyspnea rankings as 9.3 and they were only able to exercise to 65% of control W_{max}. Because expiration in swimming occurs under water, expiratory airflow is restricted by the pressure column of the water. This water column is a function of the depth of the swimmer's mouth from the surface of the water, about 20 cm H_2O. Thus, with the expiratory effort to overcome the water column pressure threshold load, swimmers may experience feelings of breathlessness sooner than non-water athletes, hence pressure threshold expiratory muscle strength training may be especially effective in compensating for the under-water exhalation load and reducing breathlessness. In the present study, there was a trend toward increased ratings of breathlessness post-training in the AFT group, while the perception in the EMST group did not change. Ratings of perceived exertion followed a similar trend in that the AFT group rated higher post-training and the EMST group lower. Pressure-threshold training has the potential to positively influence the conscious sensations of breathlessness and exertion as perceived through ventilatory factors, while air flow training did not. These observations are even more interesting given that the EMST group improved in swimming time more than the AFT group. It is possible that the lower perception of breathlessness and exertion in the EMST group caused the improvements in swim performance, which is consistent with the hypothesis of a complex brain control model of fatigue (Edwards and Walker, 2009).

Conclusions

Four weeks of a high-intensity, low-repetition expiratory muscle strength training paradigm significantly increased the maximal expiratory pressure generating capacity in highly trained collegiate swimmers compared to a non-resistance peak airflow training. Swim performance times tended to improve (not statistically significant) and there was a trend towards lower ratings of breathlessness and perceived exertion. These promising results merit further investigations into the ergogenic effects of EMST in athletes. EMST could be used as an adjunct for athletic performance to improve expiratory muscle strength.

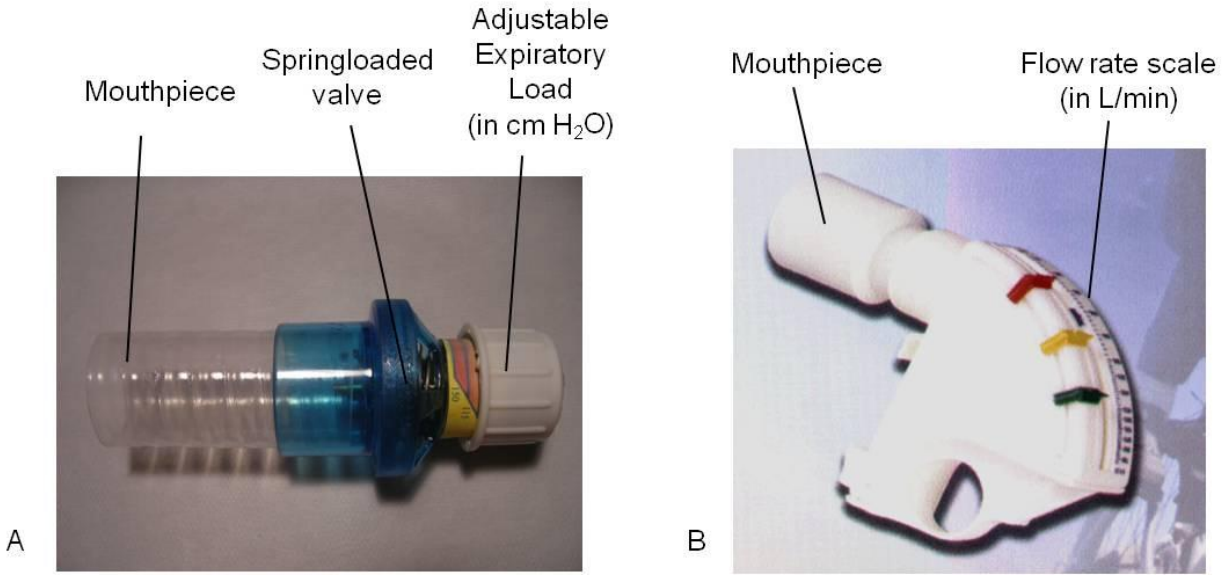

Figure 2-1. Components of the training devices for A) EMST, B) AFT.

Table 2-1. Anthropometric data participants. Values are presented as mean ± SD.

	EMST (n=9)	AFT (n=8)	p-value
Age (years)	19.6 ± 1.1	19.1 ± 1.0	0.420
Height (cm)	185.9 ± 9.8	182.9 ± 5.5	0.454
Body mass (kg)	82.4 ± 9.6	77.0 ± 4.7	0.169
Competitive training history (years)	10.6 ± 4.8	10.5 ± 4.6	0.981

Table 2-2. Pulmonary function test data. Values are presented as mean ± SD.

	Pre-Training		Post-Training		% Δ	p-value
	Value	% predicted	Value	% predicted		
EMST						
$FEV_{1.0}$ (L)	5.23 ± 1.04	113.67 ± 13.06	5.17 ± 1.14	112.44 ±16.82	-1.15	0.508
FVC (L)	6.48 ± 1.14	118.67 ± 12.97	6.47 ± 1.22	118.33 ± 15.91	-0.19	0.508
$FEV_{1.0}$/FVC	80.65 ± 7.48		79.69 ± 7.74		-1.18	0.156
AFT						
$FEV_{1.0}$ (L)	5.46 ± 0.58	118.63 ± 11.25	5.32 ± 0.62	115.63 ± 12.51	-2.54	0.113
FVC (L)	6.90 ± 0.75	125.38 ± 12.08	6.83 ± 0.71	118.29 ± 9.92	-0.92	0.523
$FEV_{1.0}$/FVC	79.56 ± 8.24		78.16 ± 8.30		-1.77	0.202

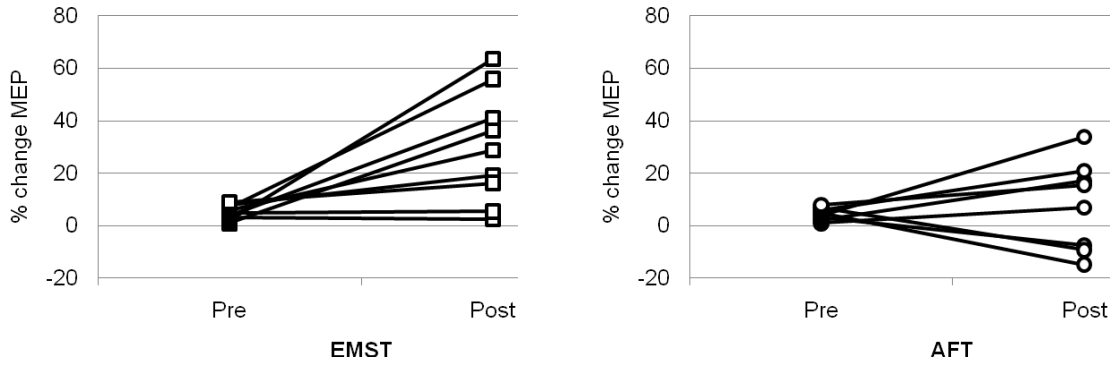

Figure 2-2. Percent change in MEP for each individual. All participants in the EMST group increased their maximal expiratory pressure generating capacity, while individuals in the AFT group showed only modest increases or decreases in MEP.

Table 2-3. Maximum expiratory pressure test data. Values are presented as mean ± SD.

	Pre-Training (in cmH_2O)	Post-Training (in cmH_2O)	% Δ	p-value
EMST	122.11 ± 21.22	157.67 ± 23.63	29.86	<0.0001
AFT	131.50 ± 30.42	142.00 ± 39.62	7.85	0.236

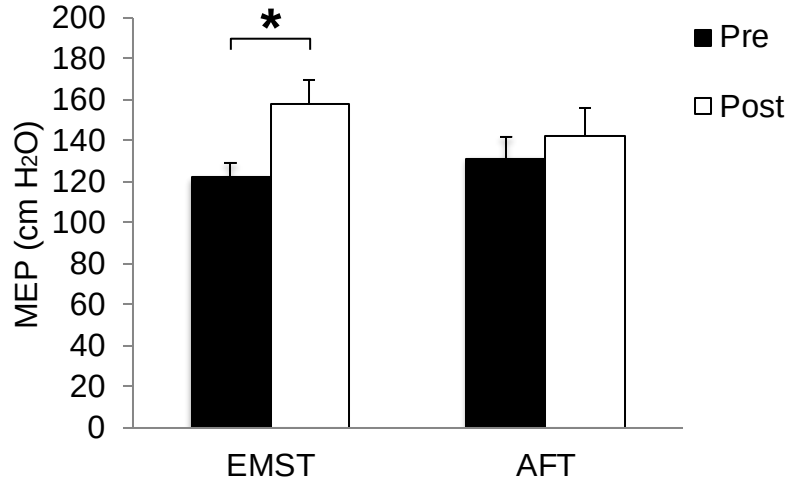

Figure 2-3. The EMST group significantly increased MEP post-training compared to pre-training. MEP changes in EMST group were significantly greater than in AFT group. Values expressed as mean ± SEM. * $p < 0.0001$.

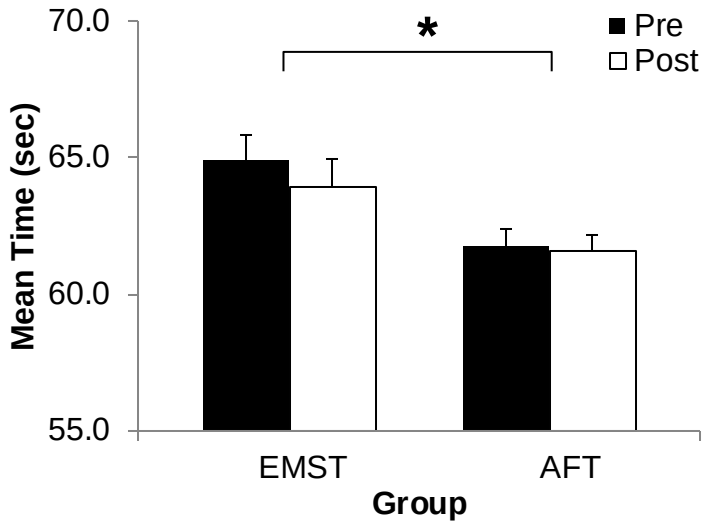

Figure 2-4. Pre- and post-performance times for 6 x 100 m freestyle test for both EMST and AFT groups. Values are mean ± SEM. * $p < 0.05$.

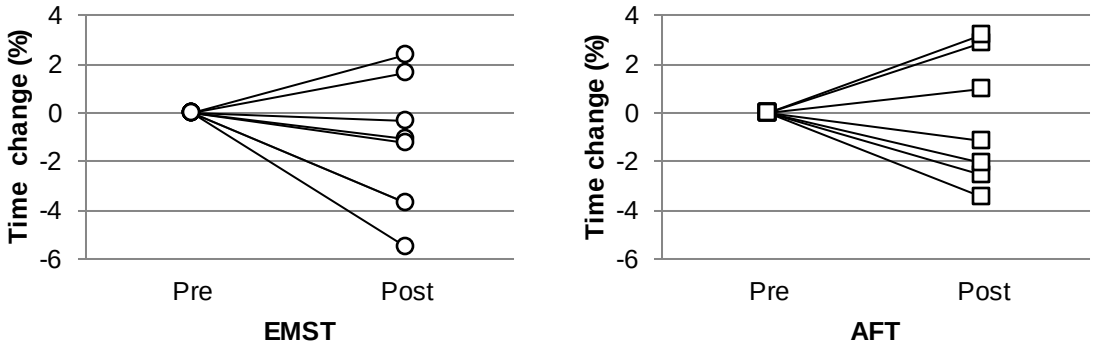

Figure 2-5. Percent change in 100 m time for each individual.

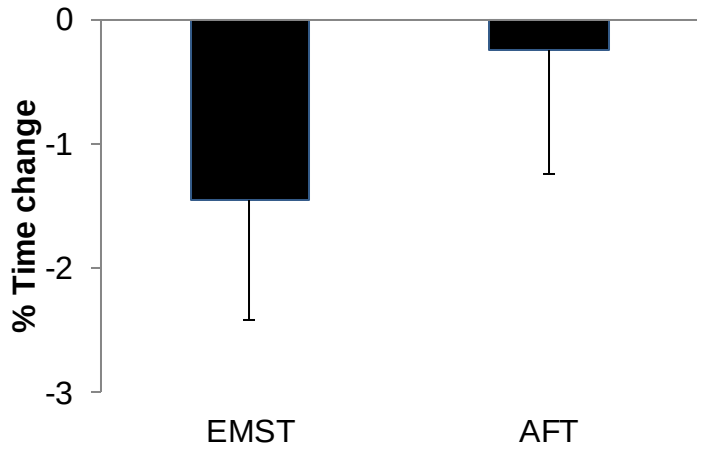

Figure 2-6 . Percent change of mean swim time during the 6 x 100 m freestyle test for EMST and AFT groups. Values are mean ± SEM.

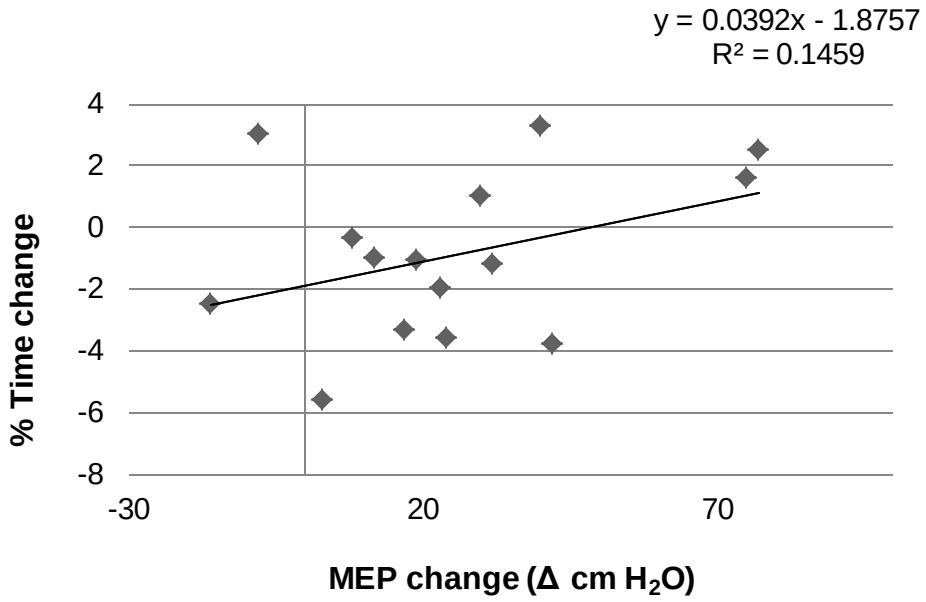

Figure 2-7. Correlation of % time change during 6 x 100 m test and change in MEP pre- to post-training for each individual.

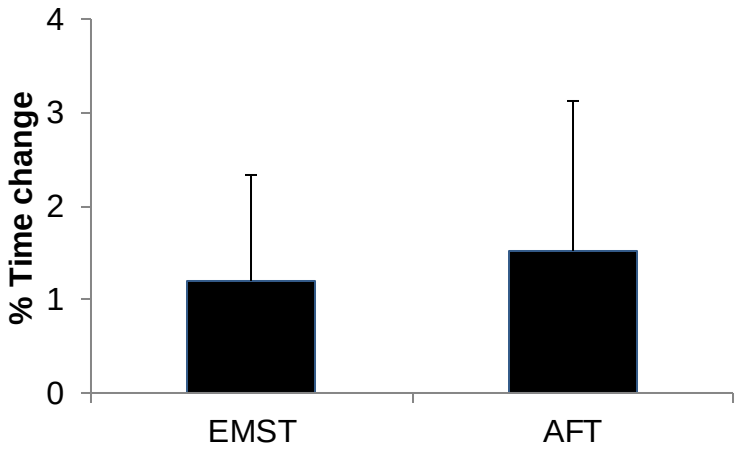

Figure 2-8. Percent time change of the first 100 m interval. Values are mean ± SEM.

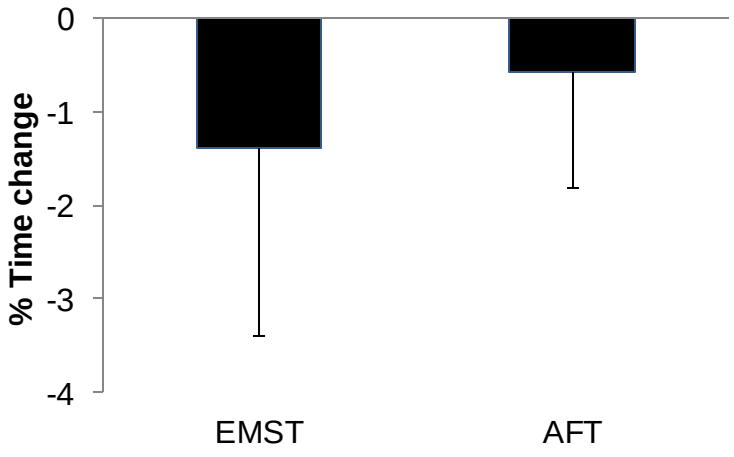

Figure 2-9. Percent time change of the last 100 m interval. Values are mean ± SEM.

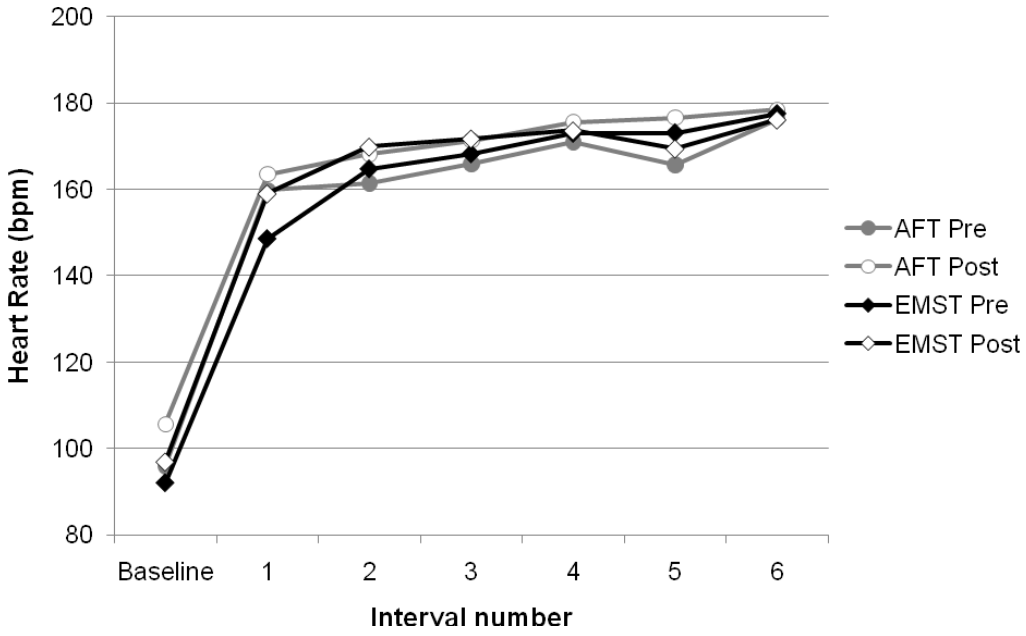

Figure 2-10. Heart rate before and during the 6x100 m freestyle test.

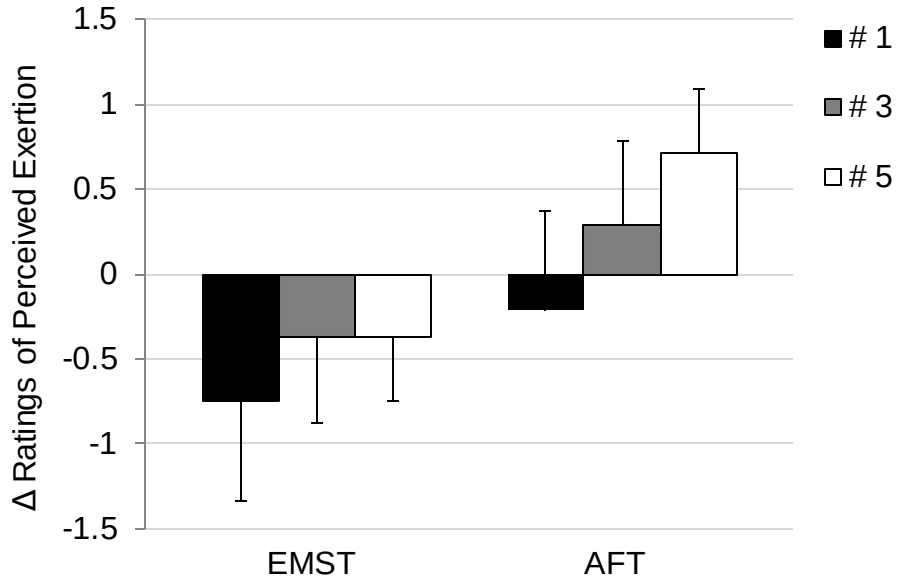

Figure 2-11. Changes in Ratings of Breathlessness between first and last rating within one 6x100 m test. Values are mean ± SEM.

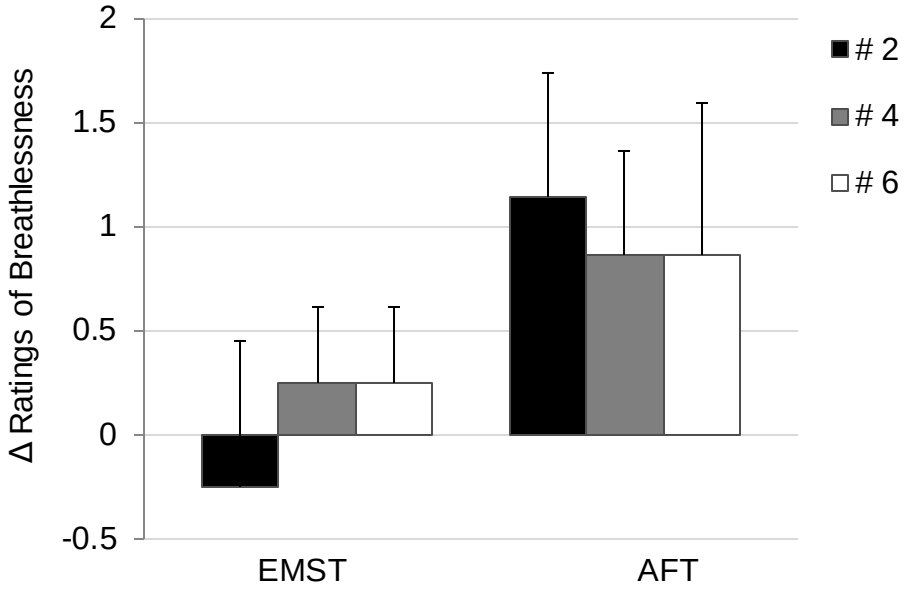

Figure 2-12. Changes in Ratings of Perceived Exertion between first and last rating within one 6x100 m test. Values are mean ± SEM.

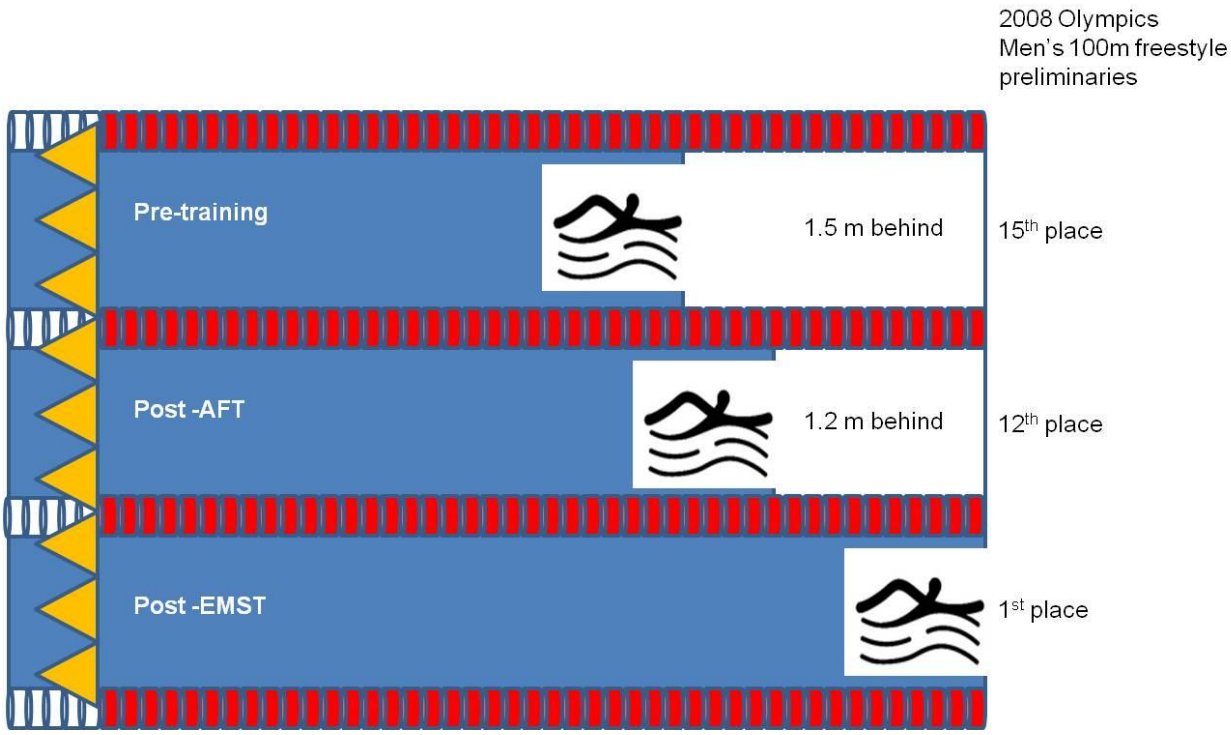

Figure 2-13. Functional significance of % improvements in swim time pre- and post-training compared to the 2008 Olympic Games Men's 100 m freestyle preliminary races.

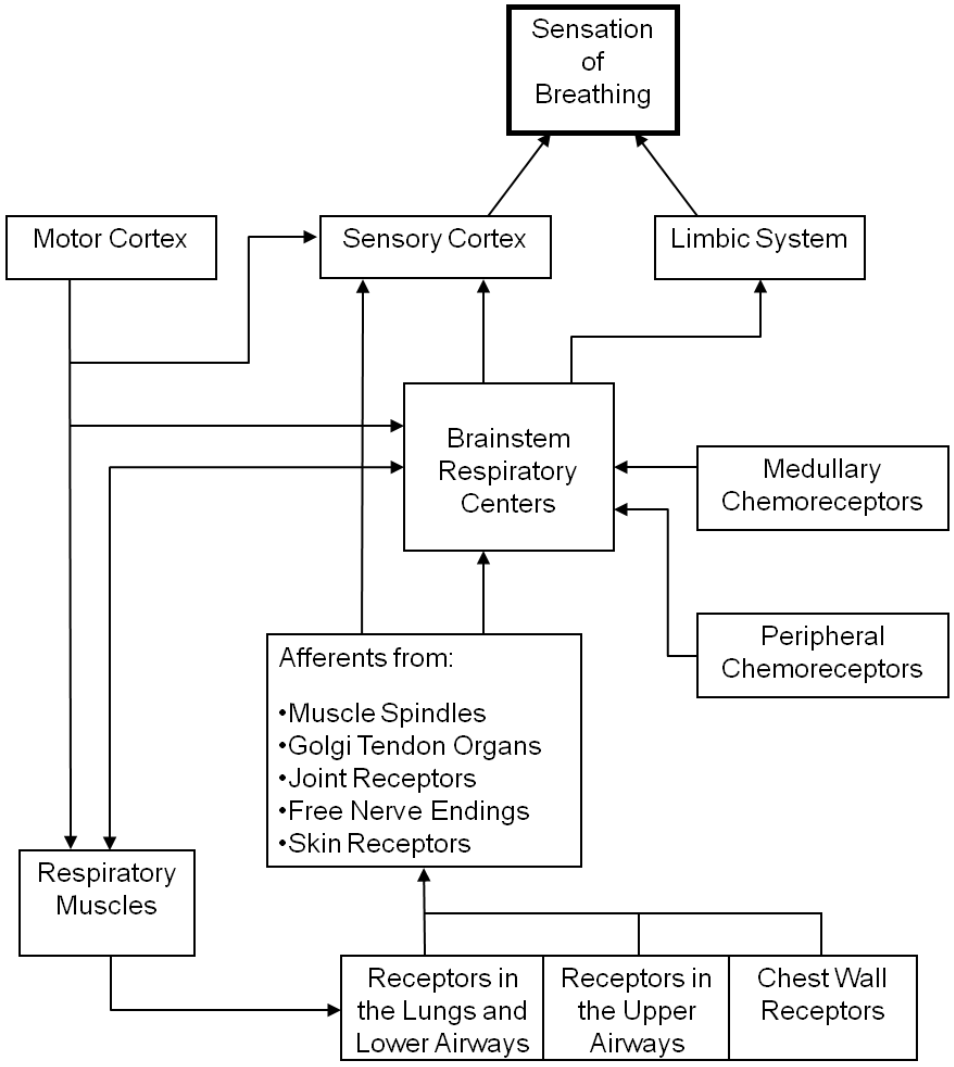

Figure 2-14. Possible mechanisms leading to the sensation of breathlessness.

CHAPTER 3
TRACHEAL OCCLUSION IN ANESTHETIZED RATS MODULATES GENE EXPRESSION PROFILE OF MEDIAL THALAMUS

Introduction

The sensation of dyspnea, or breathlessness, is one of the primary symptoms in pulmonary and cardiovascular diseases (Manning and Schwartzstein, 1995; O'Donnell et al., 2007). It is one of the symptoms that most limits patients with obstructive pulmonary diseases, and it can also be considered one of the most important factors in determining the severity of the disease and the health-related quality of life (Carvalho et al., 2007). Sensory information is continuously sent to the respiratory centers in the brainstem; minor changes in breathing are controlled by these centers without the activation of higher brain centers. When changes in respiratory information reach a certain threshold, then a gating-in process occurs resulting in the cognitive awareness of breathing (1999; O'Donnell et al., 2007). The conscious awareness of breathing as in dyspnea requires the activation of higher brain centers (O'Donnell et al., 2007).

The neural control pathway to the higher centers is thought to be a gated process (Chan and Davenport, 2008). Only information that is selectively attended to or is above a certain threshold would be able to pass through to the cortex. The brain structure involved in the gating of various sensory afferents, such as somatosensory, auditory, and visual information to the cortex is the thalamus (Kimble & Kaufman, 2004). Furthermore, our laboratory has found increased c-Fos expression in response to tracheal occlusions in the medial thalamus, indicating activity of neurons in this brain area (Pate et al., 2008; Vovk et al., 2006). Thus, it was hypothesized that respiratory sensory information may also be processed and relayed to higher brain centers through the thalamus.

The thalamus is the largest structure in the diencephalon, located centrally in the brain. It is ideally situated in a position to receive incoming sensory information and send nerve fibers out to the cerebral cortex in several directions. Functionally, the thalamus is believed to serve as the processing and relay station that most sensory information (one known exception is olfaction) must pass before reaching the cortex (Kimble and Kaufman, 2004; McCormick and Bal, 1994; Sherman and Guillery, 2002). For the well-studied visual, auditory, and somatosensory systems, different thalamic relay neurons are responsible for relaying specific information. Visual stimuli pass through the lateral geniculate nucleus, auditory information through the medial geniculate body, and somatosensory stimuli are processed by the ventrobasal complex (Alitto and Usrey, 2003). In the present study, it was hypothesized that respiratory afferents carry lung and airway information to the thalamus, specifically the medial thalamus as based on the c-Fos data, where it is processed and potentially relayed to the cortex.

Midline thalamic nuclei receive projections from areas such as the periaqueductal gray (Krout and Loewy, 2000b), the parabrachial nucleus (Krout and Loewy, 2000a), the superior colliculus (Krout et al., 2001), and the brainstem (Krout et al., 2002). The thalamus integrates many bidirectional connections with several regions of the cortex, most importantly the recurrent loop to and from various cortical areas, but also to the amygdala (possibly for emotional processing), the hippocampus (for learning and memory), and the limbic system (Newman, 1995, Kimble & Kaufman, 2004). A single thalamic nucleus can send afferents to multiple cortical areas (Herrero et al., 2002). Intralaminar thalamic nuclei have diffuse projections to the cerebral cortex (Jones and

Leavitt, 1974). Reciprocal corticothalamic neurons connect back to the thalamic relay and interneurons (McCormick and Bal, 1994). Anatomical studies have shown that about 50% of thalamic connections are coming from the cortex. It is believed that this corticothalamic feedback functions in “egocentric selection”, which refers to the ability of cortical neurons to analyze thalamic input, select certain sensory features, and then amplify the transmission of these features by feedback to the thalamus (Suga et al., 2002). This suggests that cortical areas can either enhance or suppress particular information. Other top-down connections such as from the cingulated gyrus and prefrontal cortex feeding back onto the thalamic neurons help in selecting stimuli that are relevant, salient, and novel (Kimble and Kaufman, 2004). In some instances, the thalamus may impair rather than facilitate the processing of environmental stimuli, such as during trauma (Kimble and Kaufman, 2004).

Thalamic relay neurons receive both excitatory (glutamatergic) and inhibitory (GABAergic) transmission and the balance/ratio between these signals is what eventually determines the response (McCormick and Bal, 1994). Other neurotransmitters and neuromodulators also influence thalamic neurons, most notably serotonin from the raphe nucleus (McCormick and Bal, 1994). Modulations of any component in the neural transmission pathway (such as transmitters, receptors, transporters) alter the signal processing of the thalamic relay neurons and thus change sensory information gating.

Genomic high-throughput technologies, such as DNA microarrays, serve as a powerful tool for identifying gene expression profiles in response to a specific stimulus. The development of microarrays has provided the opportunity to compare and analyze

gene expression differences of thousands of genes simultaneously, and characterize the biological processes occurring as a result of the impact. Oligonucleotide microarrays, as used in this study, are systematically prepared based on known gene sequence information. Probes on the arrays are 60 nucleotide in length, which has shown higher specificity and sensitivity compared to shorter oligos (Hughes et al., 2001). In this experiment a reference design was used. The reference sample was prepared by combining small amounts of RNA of all samples collected. This sample was then labeled with one color, while all target samples were labeled with another color. In the hybridization reaction for one microarray, the two differently labeled preparations (reference sample and one target sample) were then combined and simultaneously hybridized to the arrayed probes. Binding to the probes depends on the relative concentrations of mRNA transcript contained in the two samples. Hybridization was carried out on a rotational device in a hybridization chamber with the help of a gasket slide that enables active mixing and increases the chance for the target to come into contact with each probe. Scanning of the microarrays records and quantifies the amount of emitted light that was collected by exciting the fluorescent molecules conjugated to the hybridized targets. The ratio between signal intensities of the two fluorescent signals serves as an indicator of which genes were differentially modulated.

In the present study, comparative microarray analysis was performed to examine the molecular changes that occur immediately after ITTO. It was hypothesized that ITTO would induce short-latency (< 10 min) gene expression changes in the medial thalamus. RNA samples from the medial thalamic regions of two groups of rats were

used; one group receiving ITTO and one group of control animals not receiving occlusions.

Materials and Methods

Animals

Eight male Sprague-Dawley rats (276.8 ± 47.5 g) were housed two per cage in a temperature-controlled room (72°F) on a 12:12 light:dark cycle, and with free access to food and water. All animal experiments were approved by the Institutional Animal Care and Use Committee of the University of Florida.

Surgical Procedures

Animals were anesthetized by intraperitoneal injection of urethane (1.3-1.5 g/kg) and anesthesia was supplemented as needed (20 mg/ml). Anesthetic depth was verified by the absence of a withdrawal reflex to a rear paw pinch. Body temperature was measured using a rectal probe and maintained at 38°C with a heating pad. Animals were spontaneously breathing room air.

Figure 3-1 shows the surgical setup for recording of esophageal pressure (P_{es}) and diaphragm electromyography (EMG_{dia}). One end of a saline-filled tube was inserted through the mouth into the esophagus to measure P_{es}. The other end of the tube was connected to a polygraph system (Model 7400, Grass Instruments) via a pressure transducer and the analog output was amplified, digitized at 1kHz (CED Model 1401, Cambridge Electronics Design) and computer processed (Spike2, Cambridge Electronics Design). Pleural pressure changes were inferred from relative changes in P_{es}.

Diaphragm electromyographic (EMG_{dia}) electrodes were prepared from Teflon-coated wire. The ends of the wires were bared, bent and hooked into the costal

diaphragm through a small incision in the abdominal skin. Two electrodes were inserted for bipolar EMG_{dia} recordings. The electrode wires were connected to a high-impedance probe. The signal was amplified (P511, Grass instruments) and band-pass filtered (30-300 Hz). The analog outputs were digitized and processed as described above.

The trachea was exposed through a ventral incision via blunt dissection of surrounding tissue. An expandable cuff was sutured around the trachea, two cartilage rings caudal to the larynx. The cuff was connected to an air-filled syringe via a thin rubber tube. The syringe was used to inflate and deflate the cuff bladder. Prior to the experiments the inflation pressure needed to completely compress the trachea was determined using an excised trachea. A complete compression occluded the airway during both inspiration and expiration. Deflation restored the trachea back to its original condition to allow unobstructed breathing.

Experimental Protocol

The experimental group (n=4) was allowed to breathe unobstructed for 60 min following surgical preparations. Then the cuff was inflated to occlude the trachea for 2-4 breaths, followed by deflation of the cuff for a minimum of 15 breaths. The occlusions were repeated for a total of 10 min. P_{es} and EMG_{dia} were monitored continuously throughout the experiment to verify onset and removal of tracheal occlusions. The control animals (n=4) underwent the same surgical procedure, 70 min of unobstructed breathing, but did not receive tracheal occlusions. Immediately after completion of the 70 min post-surgical period, the animals were decapitated and their brains removed. The medial thalamus was located (Figure 3-2), excised, frozen in liquid nitrogen, and stored at -80°C until further use.

Physiological Data Analysis

Data were analyzed offline using analysis software Spike 2 (Cambridge Electronics Design). The EMG_{dia} was rectified and integrated (time constant = 50 ms), and inspiratory time (Ti), expiratory time (Te), and total time (Ttot) for each breath were calculated from the integrated EMG_{dia} signals. Ti was measured from the onset of the inspiration-associated increase in EMG_{dia} activity to the point at which EMG_{dia} peak activity began to decline (Figure 3-3). Te was measured from the end of Ti to the onset of the following inspiration (Figure 3-3). Baseline EMG_{dia} was defined as the minimum value of the EMG_{dia} during expiration. The EMG_{dia} amplitude (ΔEMG_{dia}) was calculated as the difference between baseline and peak EMG_{dia}. P_{es} amplitude was calculated as the difference between baseline and peak P_{es}. For the experimental group, within each occlusion presentation the control breath (C) was defined as the complete breath immediately prior to occlusion (O) application and the recovery breath (R) was defined as the first complete breath immediately after termination of occlusion. For the 10 min occlusion trial, one control breath, two occluded breaths (O1 and O2), and one recovery breath were measured for each occlusion presentation. Data from at least 28 occlusion trials for each experimental animal were used for analysis. For the control group, breathing pattern of control breaths was measured at matched time points.

SigmaStat for Windows Version 3.5 (Systat Software, Inc, Germany) was used for all statistical analyses of physiological data. All values are reported as mean ± SD. Ti, Te, Ttot, P_{es}, and ΔEMG_{dia} for control breaths (C) were compared between experimental and control animals using one-way ANOVA. Comparisons between C, O, and R breaths in the experimental animals were analyzed using one-way repeated measures ANOVA.

Total RNA Isolation

Total RNA was isolated from medial thalamic tissue with *RNA Stat-60* (Tel-test, Friendswood, TX). 10-20 mg of the frozen tissue was homogenized in *Stat-60* and chloroform added. The mixture was vortexed for 15 s and centrifuged at 12,000 g for 15 min at 4°C. The upper aqueous phase containing the RNA was carefully extracted. The extraction step was repeated and the RNA precipitated with isopropanol. Following another centrifugation at 12,000 g for 40 min at 4°C, the pellet was washed twice with 80% ethanol and air dried. To inactivate RNases, the pellet was resuspended in 40 µl *RNA secure* (Ambion, Austin, TX) following the manufacturer's protocol. Quantity and quality of total RNA was determined by spectrophotometry (260/280 ratios ≈ 2.0), and by electrophoresis through a 1% formaldehyde agarose gel stained with ethidium bromide.

RNA Amplification and Microarray Analysis

Array hybridizations were performed using a reference design. The reference material consisted of equal amounts of RNA from all eight thalamic samples. The cDNA synthesis, cRNA labeling and hybridization were performed following the manufacturer's kits and protocols (Agilent Low RNA Input Fluorescent Linear Amplification Kit and Agilent 60-mer oligo microarray processing protocol; Agilent, Palo Alto, CA). The thalamic samples were labeled with Cy5, while the reference sample was labeled with Cy3. The cRNA was amplified and purified using the QIAGEN RNeasy Kit (Qiagen Inc.). Dye incorporation was determined by using Nanodrop (>13 pmol/µg RNA). For the 4 x 44,000 rat genome DNA oligo microarray (Agilent Technologies Inc., Amadid: 014879), 825 ng of sample and 825 ng of reference was used for each array. Hybridization was carried out in a microarray hybridization chamber at 65°C for 17 hours. The glass slides

were then washed and scanned with a laser-based detection system (Agilent, Palo Alto, CA). A $\log_2$ transformed signal ratio between the experimental channel and the reference channel was calculated for each spot.

One-way ANOVA was performed on normalized $\log_2$-transformed signal ratios of each probe individually, followed by Tukey's honestly significant differences pair-wise comparisons to determine genes whose expression was significantly regulated by the tracheal occlusions compared to control. Genes were considered differentially expressed if the p-value was ≤ 0.05 and the $\log_2$ fold change was ≥ 0.4.

Gene Ontology and Pathway Analysis

Gene ontology annotations were derived from similarity searches of the NCBI Gene database. A *blastn* search for each of the 44,000 probes was performed to retrieve the gene ontology (GO) annotation. Once the GO annotations were retrieved, a GO tree was built following the hierarchical structure for the whole array. Then, another GO tree for the significant regulated genes was built. The two trees were compared at each node by running a Fisher's Exact Test ($p \leq 0.05$) when traversing the tree branches. Significantly over-represented GO categories were identified by the Fisher's p-value and the false discovery rate was determined.

Some of the genes that showed significant modulation were scanned against the Pathway Studio ResNet database (Ariadne Genomics, Rockville, MD). This database uses published information and catalogs the relationships between biological entities. Pathway Studio® (Ariadne Genomics) was used to identify and graphically display the functional interactions between the selected genes (Nikitin et al., 2003).

Results

Physiological Responses to ITTO

Breath timing and Pes response to ITTO are shown in Figure 3-3. Breathing frequency slowed due to an increase in Te. The P_{es} was more negative during occlusion and returned to baseline immediately after termination of occlusion. Comparisons of control breaths between experimental and control animals demonstrated no significant differences in Ti, Te, Ttot, P_{es}, or EMG_{dia} (Table 3-1).

Comparisons between C, O, and R breaths within each experimental animal revealed (Tables 3-2 and 3-3, and Figure 3-4) Te, Ttot, and P_{es} were significantly different between C and O, and between O and R, but not C and R. There was a trend toward significance in Ti. EMG_{dia} showed no significant differences. This shows that ITTO resulted in an increase in expiratory timing and thus total breath time.

Modulation of Gene Expression Profile Following ITTO

Statistical analysis of the microarray data showed that a total of 588 genes were altered ($p < 0.05$, $\log_2$ fold change ≥ 0.4) following the occlusion protocol, with 327 down-regulated and 261 genes up-regulated (Appendix Table B). Some candidate genes of interest included genes involved in stress-related pathways (Table 3-4).

Table 3-5 shows the GO categories for biological processes that were over-represented among the regulated genes ($p < 0.05$, FDR < 0.1). The most significantly regulated GO categories were “anti-apoptosis”, “response to stress”, “regulation of enzyme activity”, and “MAPKKK cascade”.

Discussion

Airway Occlusions Elicit the Load Compensation Response

When an animal is challenged with an increase in respiratory mechanical load, the respiratory control system elicits the load compensation reflex. This ventilatory load compensation response has been observed in anesthetized animals using external resistive loads to breathing and is characterized by the recruitment of respiratory muscle activity, an increase in breath duration and a decrease in tidal volume (Bishop et al., 1981; Bradley, 1972; Clark and von Euler, 1972; Davenport et al., 1981; Davenport et al., 1984; Davenport and Wozniak, 1986; Zechman et al., 1976). Depending on the timing within the breath phase of the added resistive load (end-inspiratory *versus* end-expiratory), inspiratory or expiratory duration is increased. The load compensation reflex is also dependent on selective phase loading (inspiration only or expiration only) and loading that occurs throughout the entire breath. In this study we applied complete tracheal occlusions for multiple breaths so the load was applied on both the inspiratory and expiratory breath phases. Load compensation breathing pattern was achieved by a more negative P_{es} and an increase in Ttot, primarily due to an increase in Te, while Ti increased non-significantly. The more negative P_{es} peak during occlusions demonstrates a larger inspiratory effort exerted by the animal to inhale. However, diaphragm activity (EMG_{dia}) was not significantly modulated, so the more negative P_{es} could be due to the respiratory mechanical changes, such as increased resistance. Inspiratory duration did not change significantly which is in congruence with an unaltered EMG_{dia} signal. One of the causes for the unchanged Ti and EMG_{dia} may be due to the timing of the onset of occlusion (Zechman et al., 1976).

The load compensation response lasted as long as the trachea was occluded and breathing patterns returned to baseline levels immediately following withdrawal of occlusion demonstrating that tracheal occlusions using an inflatable cuff are reversible.

Airway Obstruction in Disease and Association with Anxiety and Depression

Asthma is a respiratory disease characterized by reversible airways obstruction, airway inflammation, and hyperreactive airways (Valenca et al., 2006). Our animal model of reversible tracheal obstructions thus mimics one component of asthma. It is well acknowledged that respiratory diseases, such as asthma and chronic obstructive pulmonary disease (COPD) are associated with significantly higher rates of anxiety and depression compared to the general population (Moussas et al., 2008). In the US general population, it has been found that significantly more individuals suffering from a respiratory or lung disease have panic disorder or major depression than individuals without such a diagnosis (Goodwin and Pine, 2002). In a sample of 189 patients from a Brazilian outpatient clinic for the treatment of asthma and COPD, Carvalho et al. (Carvalho et al., 2007) found that almost all patients with controlled and uncontrolled asthma exhibited moderate to severe anxiety as determined by the State-Trait Anxiety Inventory (CA 97.5%, UA 93%), and 74% of COPD patients. Depression scores, as measured by the Beck Depression Inventory, were less pronounced in these patients (CA 20%, UA 49%, COPD 29%) but nevertheless a cause for concern. In a similar study on 132 pulmonary disease patients in a Greek hospital, Moussas et al. (Moussas et al., 2008) found that a total of 49.2% showed moderate or severe depression, while 26.5% had anxiety. Fernandes et al. (Fernandes et al., 2010) demonstrated a positive association of higher degrees of asthma severity with increased anxiety. In this study, 70% of the patients had a clinical diagnosis of anxiety and anxiety was associated with

worse subjective asthma outcomes and increased use of medication and healthcare services. Of 62 asthmatic patients from an outpatient clinic in Brazil, 24.1% had major depression disorder and 33.8% had an anxiety disorder as diagnosed by the Mini-International Neuropsychiatric Interview (Valenca et al., 2006). However, there was no association between the severity of asthma and the prevalence of anxiety and depression (Valenca et al., 2006). In a study on Veteran's Affairs patients with chronic breathing disorders, 50.1% showed moderate to severe depression and 64.2% had moderate to severe anxiety symptoms (Kunik et al., 2005). In a 20-year longitudinal and cross-sectional study with 591 participants between the ages of 19 and 40, Hasler et al. (Hasler et al., 2005) found that asthma was strongly associated with panic disorder and that the presence of asthma predicted subsequent panic disorder. Patients with severe asthma and a comorbid psychiatric disorder had almost 11-fold increased risk for two or more asthma exacerbations and almost 5-fold increased risk for two or more hospitalizations during the past year as compared with patients with severe asthma without psychiatric disorder (ten Brinke et al., 2001). These results show that anxiety and depression are associated with respiratory diseases and that in some vulnerable individuals, an increase in anxiety may lead to panic disorders, possible through dyspnea-induced fear conditioning (Hasler et al., 2005).

Airway Occlusions Induce Serotonin Receptor HTR2A and Reduce Dopamine Receptor DRD1

Medial thalamic mRNA transcripts of the serotonin receptor HTR2A were up-regulated following tracheal occlusions. It is well known that the serotonin system plays an important role in a variety of human psychopathological conditions, particularly mood and anxiety disorders (Charney et al., 1987; Hensler, 2006). Antidepressant treatment

has focused on modulating serotonergic neurotransmission (Jones and Blackburn, 2002). One of the challenges of the serotonin system is the sheer complexity of the 14 known receptor varieties categorized into seven receptor subtypes (Hoyer et al., 2002). Specifically, the HTR2A receptor has been identified to be involved in anxiety disorders in dogs (Vermeire et al., 2009). Antagonists to this receptor may be useful therapeutic agents in the treatment of generalized anxiety disorder and psychosis (Javanbakht, 2006; Jones and Blackburn, 2002). Activation of HTR2A receptors weakens the sensory gating so that more sensory information is able to reach consciousness, which in turn can lead to the pathology of anxiety disorders (Javanbakht, 2006). Behavioral studies in HTR2A knockout mice have shown changes in anxiety-related but not depression-related paradigms (Weisstaub et al., 2006). The knockout mice exhibited greater exploratory and risk behavior in conflict paradigms, such as the open field, dark-light choice, elevated plus-maze, and novelty-suppressed feeding tests. In depression-related behaviors, as measured by the forced swim test and the tail suspension test, the mice did not differ significantly from wild-type (Weisstaub et al., 2006).

The dopaminergic system has been identified to be involved in a myriad of functions, such as motivation, reward, pain processing, learning, and memory (Arias-Carrion and Poppel, 2007; Shyu et al., 1992). Hyperfunction of this system has been hypothesized to be associated with schizophrenia and attention deficit hyperactivity disorder (Carlsson et al., 1999; Di Chiara and Bassareo, 2007; Heijtz et al., 2007). This hypothesis is based on the antagonistic interaction between dopamine and glutamate projecting on GABAergic striatal neurons that exert an inhibitory effect on thalamocortical glutamatergic neurons, thereby filtering out part of the sensory input to

the thalamus to protect the cortex from a sensory overload (Carlsson et al., 1999). Hyperactivity of dopamine or hypofunction of the corticostriatal glutamate pathway should reduce this protective influence and could thus lead to confusion or psychosis (Carlsson et al., 1999; Gaudreau and Gagnon, 2005). Neuroleptic drugs that block dopaminergic pathways improve sensory functioning and gating in schizophrenic patients (Freedman et al., 1987).

Interaction between serotonin and dopamine systems can have either potentiating or antagonizing effects (Lieberman et al., 1998)). HTR2A antagonists have shown to increase dopamine release in a variety of brain regions (Hertel et al., 1996).

Airway Occlusions Alter Genes Involved in Anti-Apoptosis

Gene ontology analysis identified anti-apoptosis, negative regulation of apoptosis, and negative regulation of programmed cell death as being affected by airway occlusions. These findings suggest that the medial thalamus may be increasing cell-protective mechanisms. A postmortem study examining anatomical abnormalities in the thalamus of patients diagnosed with major depressive disorder discovered that in these subjects the mediodorsal nucleus of the thalamus had a significantly increased total number of neurons compared to nonpsychiatric subjects (Young et al., 2004). Other studies have demonstrated volume reductions in prefrontal cortex (Botteron et al., 2002) and hippocampus (Bremner et al., 2000) as well as decreased number of glia in the cortex (Ongur et al., 1998). Young et al. (Young et al., 2004) suggested that the elevated number of neurons in the medial thalamus may have had this reducing effect due to its projections to these other brains areas because excessive glutamatergic thalamic neurons could lead to excitotoxicity. Alternatively, increased GABAergic neurons could result in decreased output to the cortex, thus reducing the need for glial

support. It is not known which neuron population (excitatory projection neuron or inhibitory interneuron) is elevated in major depressive disorder. The results of the present study showing modulated pathways involved in anti-apoptosis could suggest a first step in the development of depression after airway occlusions.

Functional Analysis

Pathway Studio was used to visualize changes of gene expression following ITTO. An interaction between the dopamine receptor DRD1 and the serotonin receptor HTR2A exists that is controlled by MAPK1 (Figure 3-5). MAPK1 positively regulates the NMDA receptor, which in turn inhibits DLG4 and acts on DRD1. At the same time, MAPK1 inhibits CAV1, which regulates HTR2A. Following tracheal occlusions, the down-regulated expression of MAPK1 could have led to a decreased stimulation of the NMDA receptor and a decreased inhibition of CAV1. Even though NMDA receptor and CAV1 did not show differential gene expression, MAPK1 could potentially regulate the function of these genes. The decreased function of NMDA receptor would lead to a decrease in DRD1; indeed, a significant decrease in DRD1 expression was found in the occlusion group. Decreased NMDA receptor function could also result in less inhibition of DLG4, which in turn could result in increased stimulation of HTR2A. Furthermore, decreased inhibition of CAV1 means increased function and increased stimulation of HTR2A. HTR2A gene expression was indeed up-regulated following occlusions. DRD1 and HTR2A control the activation and release of neurotransmitters and other small molecules. There was a reciprocal interaction between DRD1 and HTR2A that seems to be predominantly regulated by MAPK1.

Conclusions

A single trial of ITTO in anesthetized rats elicited a load compensation response characterized by an increase in Te and thus Ttot and a decrease in P_{es}. ITTO also induced a change in the gene expression profile of the medial thalamus including genes involved in the stress response and anti-apoptosis. The results suggest that the medial thalamus is a component of the respiratory neural network responding to respiratory load stimuli.

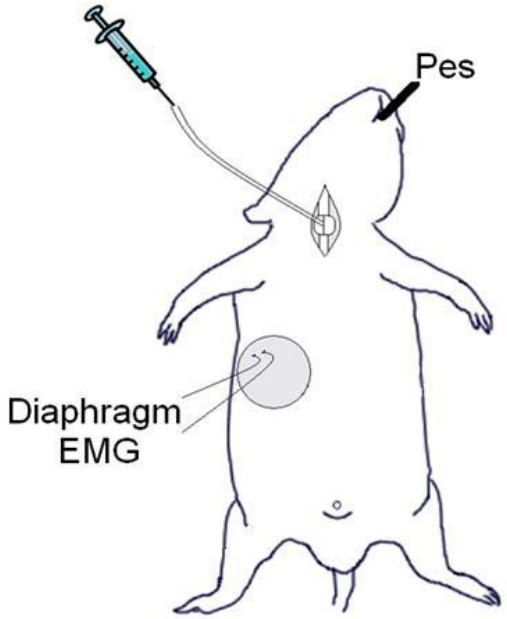

Figure 3-1. Diagram of surgical preparation including placement of tracheal occluder, esophageal pressure tube, and diaphragm electrodes.

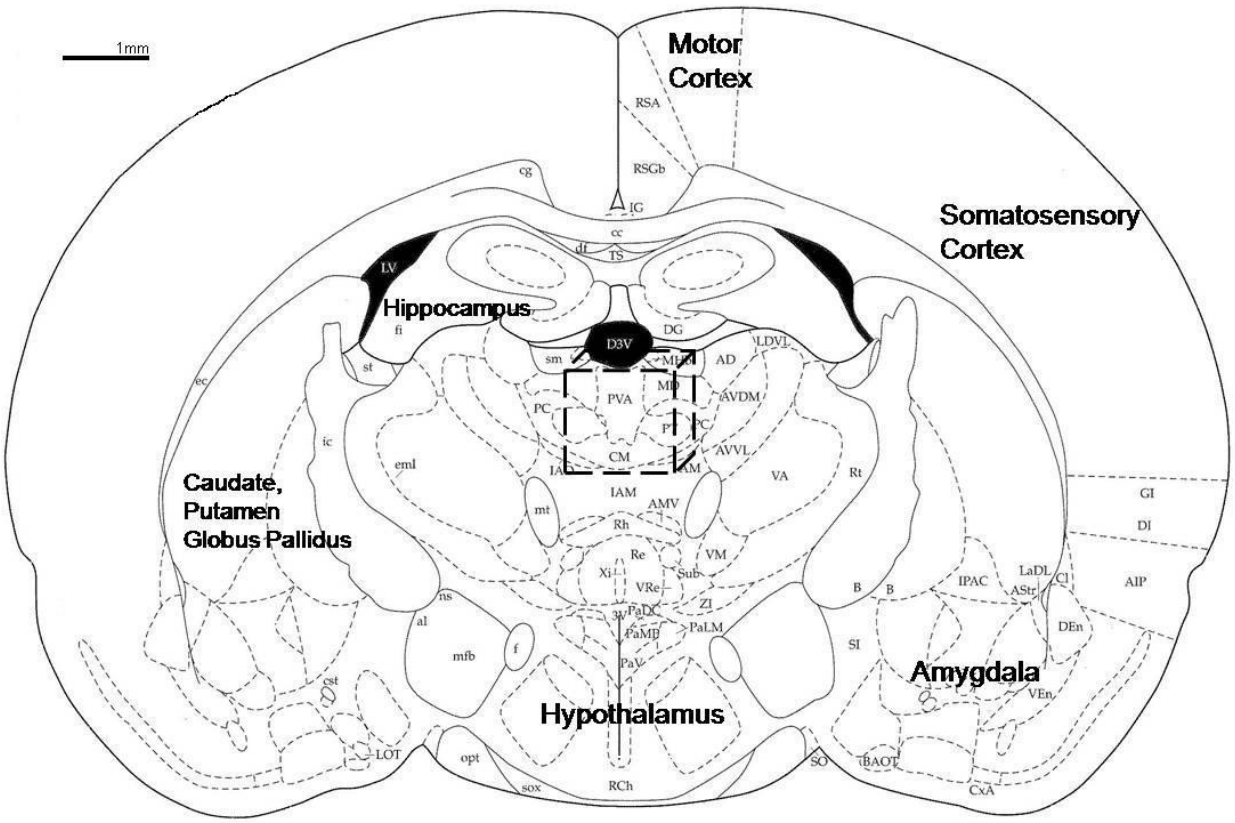

Figure 3-2. Location of collected thalamic tissue sample. Coronal view of the rat brain at Bregma -1.80mm. Dashed box indicates the tissue section (medial thalamus) that was excised for microarray analysis. Modified from (Paxinos and Watson, 1998).

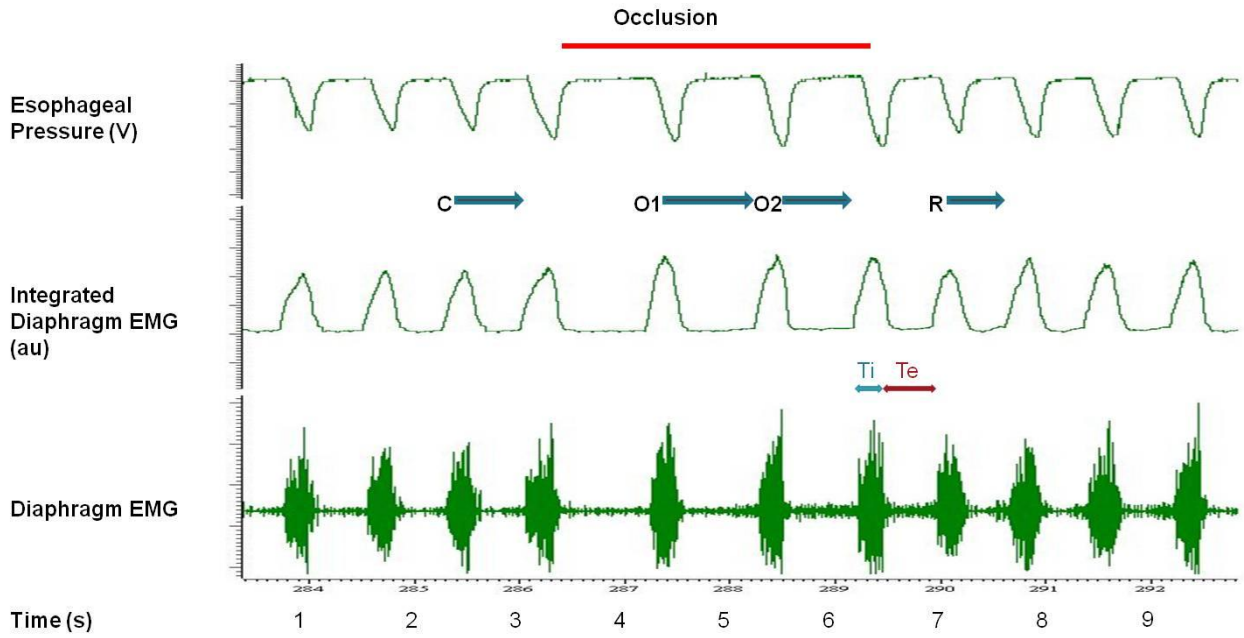

Figure 3-3. Physiological changes as a result of ITTO. Red bar represents application of an occlusion. Identification of control, occlusion, and recovery breaths and determination of Ti and Te are shown. Breath timing (Ttot = Ti + Te) increased mostly due to an increase in Te and esophageal pressure was more negative during occlusion and returned to normal immediately after.

Table 3-1. Control breath comparisons of breath timing, Pes, and ΔEMGdia between experimental and control animals. Control breaths were defined as the last complete breath immediately prior to an occlusion for experimental animals and at matched time points for controls animals. Values are reported as mean ± SD. P-values from one-way ANOVA.

	Experimental Group	Control Group	p-value
Ti (s)	0.228 ± 0.014	0.228 ± 0.014	0.997
Te (s)	0.488 ± 0.104	0.411 ± 0.073	0.277
Ttot (s)	0.715 ± 0.115	0.639 ± 0.073	0.306
P_{es} (V)	-0.038 ± 0.013	-0.038 ± 0.011	0.967
ΔEMG_{dia} (au)	0.697 ± 0.583	0.444 ± 0.246	0.454

Table 3-2. Comparisons between control, occlusion, and recovery breaths in the experimental animals. Values are reported as mean ± SD. Significant differences from one-way repeated measures ANOVA are denoted by: # different from C, * different from R ($p < 0.05$).

	Control breath	Occlusion 1	Occlusion 2	Recovery breath
Ti	0.228 ± 0.014	0.253 ± 0.014*	0.244 ± 0.015	0.211 ± 0.023
Te	0.488 ± 0.104	0.642 ± 0.189#*	0.588 ± 0.155*	0.472 ± 0.128
Ttot	0.715 ± 0.115	0.895 ± 0.193#*	0.832 ± 0.162*	0.683 ± 0.145
P_{es}	-0.038 ± 0.013	-0.053 ± 0.011#*	-0.057 ± 0.012#*	-0.041 ± 0.015
ΔEMG_{dia}	0.697 ± 0.583	0.728 ± 0.570	0.745 ± 0.612	0.717 ± 0.605

Table 3-3. Comparisons between control, occlusion, and recovery breaths in the experimental animals with combined values from O1 and O2. # different from C, * different from R.

	Control	O1+O2	Recovery	p-value
Ti	0.228 ± 0.014	0.248 ± 0.014	0.211 ± 0.023	0.063
Te	0.488 ± 0.104	0.615 ± 0.172#*	0.472 ± 0.128	0.011
Ttot	0.715 ± 0.115	0.864 ± 0.178#*	0.683 ± 0.145	0.010
P_{es}	-0.038 ± 0.013	-0.055 ± 0.012#*	-0.041 ± 0.015	0.002
ΔEMG_{dia}	0.697 ± 0.583	0.736 ± 0.591	0.717 ± 0.605	0.197

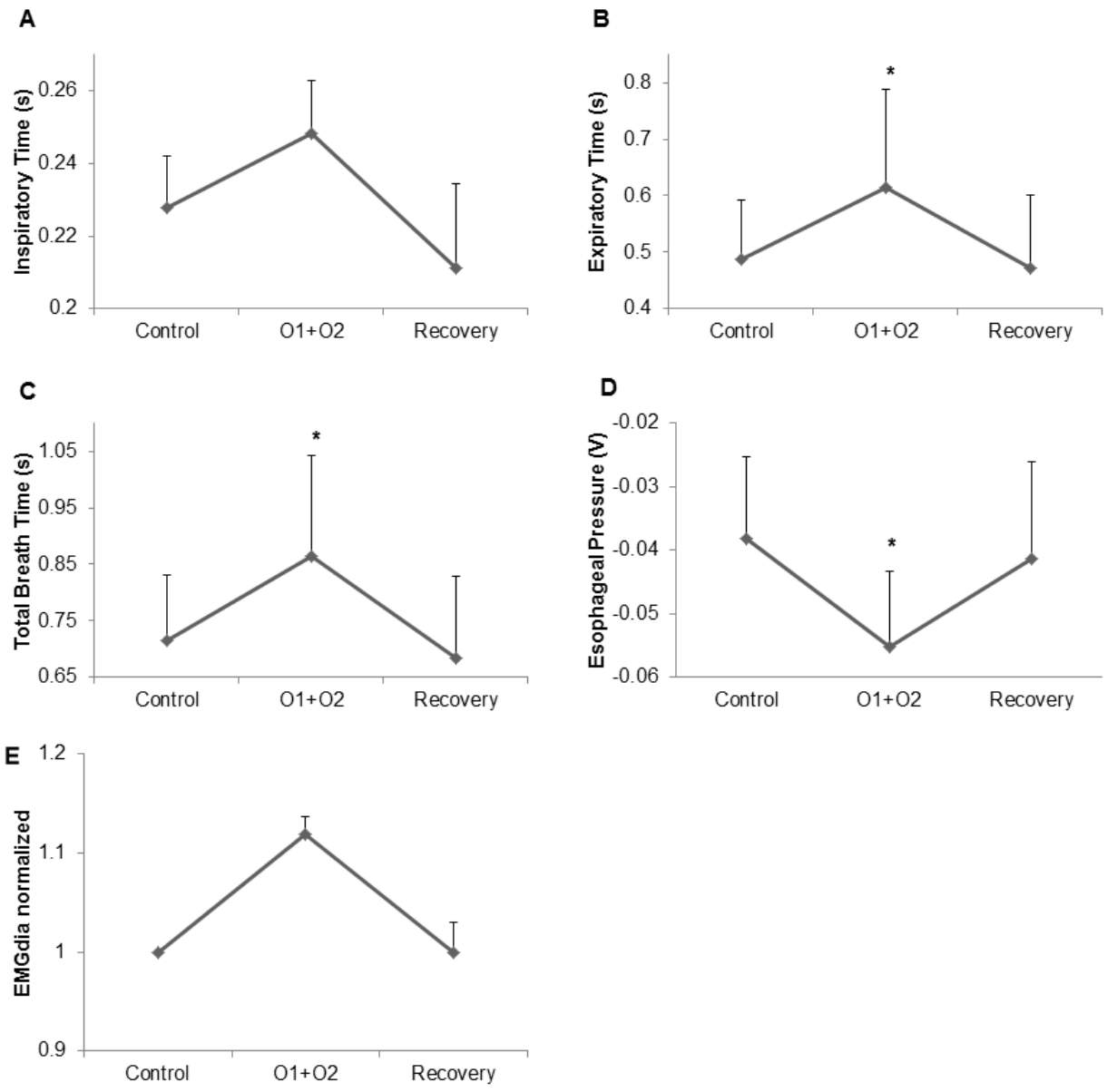

Figure 3-4. Comparisons between control, occlusion, and recovery breaths in the experimental animals. A) Ti, B) Te, C) Ttot, D) P_{es}, E) EMG_{dia}.

Table 3-4. Genes of interest that were significantly regulated following ITTO.

Log fold change	p-value	Gene Symbol	Description
+ 1.30	0.0057	PLAU	Plasminogen activator, urokinase
+ 1.07	0.0425	HTR2A	Serotonin receptor 2A
+ 0.91	0.0060	TNFRSF14	Tumor necrosis factor receptor superfamily
+ 0.75	0.0098	CHRNB1	Cholinergic receptor, nicotinic, beta polypeptide 1
- 0.74	0.0316	KCNJ3	Potassium inwardly-rectifying channel
- 0.71	0.0045	COX6B2	Cytochrome c oxidase subunit
- 0.52	0.0104	DLG4	Discs, large homolog 4
- 0.45	0.0128	DRD1A	Dopamine receptor D1A
- 0.42	0.0271	PRKAA2	Protein kinase alpha 2 catalytic subunit

Table 3-5. Highly regulated biological processes following ITTO were found with gene ontology analysis.

GO ID	GO Name	# of Genes	# of Genes on Array	Fisher p value	FDR
0006916	Anti-apoptosis	25	293	$8.6\ e^{-5}$	0.0497
0006950	Response to stress	93	1780	$9.6\ e^{-5}$	0.0277
0050790	Regulation of enzyme activity	37	575	$4.8\ e^{-4}$	0.0937
0000165	MAPKKK cascade	22	281	$6.6\ e^{-4}$	0.0964
0043066	Negative regulation of apoptosis	28	411	$1.0\ e^{-3}$	0.0998
0043069	Negative regulation of programmed cell death	28	413	$1.1\ e^{-3}$	0.0916

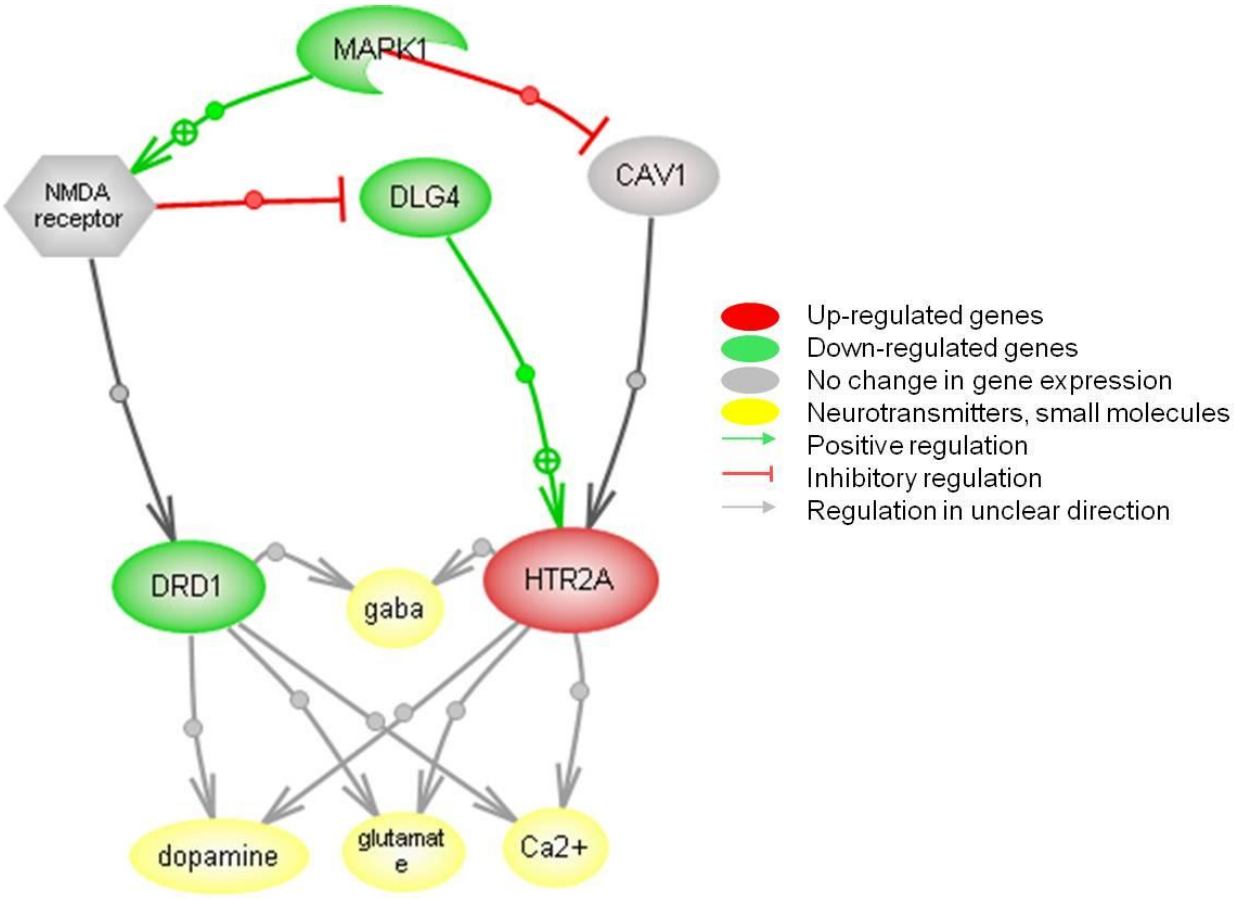

Figure 3-5. Interaction between dopamine (DRD1) and serotonin receptors (HTR2A) under the control of MAPK1. Both DRD1 and HTR2A have actions on the same neurotransmitters and small molecules.

CHAPTER 4
TRACHEAL OCCLUSION CONDITIONING IN CONSCIOUS RATS MODULATES GENE EXPRESSION PROFILE OF MEDIAL THALAMUS

Introduction

Conscious awareness of breathing requires the activation of higher brain centers. The neural control pathway to the higher centers is thought to be a gated process. Only information that is selectively attended to or that is above a certain threshold would be able to pass through the gate to the cortex. The candidate brain structure involved in the gating of various sensory afferents to the cortex is the thalamus (Kimble and Kaufman, 2004); so it is speculated that respiratory sensory information may also be gated and relayed through the thalamus, in particular the medial thalamus. The thalamus integrates many bidirectional connections with virtually every region of the cortex, most notably the prefrontal cortex and the limbic system (Kimble and Kaufman, 2004; Newman, 1995). The thalamus is an integral component in the respiratory cortical neural pathway as tracheal obstruction activates neurons in the cerebral cortex and also in the medial thalamus (Vovk et al., 2006). We have shown that tracheal obstruction in anesthetized animals modulates gene expression in the medial thalamus (Chapter 3). While it is known the repeated exposure to ITTO in conscious states changes load compensation behavior (Pate et al., 2010), it is unknown if neuron plasticity in the medial thalamus is induced by conscious chronic exposure to ITTO. We hypothesized that repeated conscious exposure to ITTO would modulate the gene expression pattern of the medial thalamus.

The thalamus is the largest structure in the diencephalon, located near the center of the brain. Thus, it is situated in an ideal position to receive incoming sensory information and send nerve fibers out to the cerebral cortex in multiple directions.

Functionally, the thalamus is believed to serve as the processing and relay station that sensory information (one known exception is olfaction) must pass before reaching the cortex (Kimble and Kaufman, 2004; McCormick and Bal, 1994; Sherman and Guillery, 2002). It can act as a gate controlling the flow of information to the cortex. For the well-studied visual, auditory, and somatosensory systems different thalamic relay neurons are responsible for relaying the specific information. Visual stimuli pass through the lateral geniculate nucleus, auditory information through the medial geniculate body, and somatosensory stimuli are processed by the ventrobasal complex. It was hypothesized that respiratory afferents also carry lung and airway information to the thalamus, specifically the medial thalamus, where it is processed and relayed to the cortex.

Midline thalamic nuclei receive projections from areas such as the periaqueductal gray (Krout and Loewy, 2000b), the parabrachial nucleus (Krout and Loewy, 2000a), the superior colliculus (Krout et al., 2001), and the brainstem (Krout et al., 2002). Both sensory information as well as arousal signals converge in the thalamus and could explain why even basic sensory information can be distorted under conditions of high arousal, such as in post-traumatic stress disorder (Kimble and Kaufman, 2004). The thalamus has connections to virtually every brain region, most importantly the recurrent loop to and from the cerebral cortex, but also to the amygdala (possibly for emotional processing) and the hippocampus (for learning and memory) (Kimble and Kaufman, 2004). A single thalamic nucleus can send afferents to multiple cortical areas (Herrero et al., 2002). The cortex then feeds back onto different thalamic nuclei to either enhance or suppress information. Indeed, anatomical studies have shown that about 50% of thalamic connections are coming from the cortex. It is believed that corticothalamic

feedback functions in “egocentric selection”, which refers to the ability of cortical neurons to analyze thalamic input, select certain sensory features, and then amplify the transmission of these features by feedback to the thalamus (Suga et al., 2002). Other top-down connections such as from the cingulated gyrus and prefrontal cortex feeding back onto the thalamic neurons help in selecting stimuli that are relevant, salient, and novel (Kimble and Kaufman, 2004). In other instances, the thalamus may impair rather than facilitate the processing of environmental stimuli, such as during extreme stress or trauma (Kimble and Kaufman, 2004).

Sensory information passing through the thalamus is relayed to cortical layer IV from where it is distributed laterally along the cortex. Layer VI sends reciprocal corticothalamic connections back to the thalamic relay and interneurons (McCormick and Bal, 1994). It has been suggested that the cortical neurons analyze the thalamic input and select important features; this information is fed back to the thalamus to enhance thalamic transmission/gating of the selected features. The thalamus consists of three broad classes of neurons, 1) relay neurons, 2) GABAergic interneurons, and 3) GABAergic nRt neurons (McCormick and Bal, 1994). Relay neurons receive both excitatory (glutamatergic) and inhibitory (GABAergic) signals and the balance/ratio between these signals is what determines the response. Other neurotransmitters and neuromodulators also influence thalamic neurons, most notably serotonin from the raphe nucleus (McCormick and Bal, 1994).

Previously, we observed that, with ITTO in anesthetized rats, the serotonin receptor HTR2A was up-regulated ($\log_2$ fold change > 1, $p < 0.05$) (Chapter 3). Serotonin, as well as its receptors and transporter have been implicated in the stress

response, anxiety, and depression (Graeff et al., 1996; Harada et al., 2008; Heisler et al., 2007; Weisstaub et al., 2006). Chronic exposure to tracheal occlusions in conscious, rats is stressful and may show an even greater modulation of serotonin and/or its targets in the thalamus.

It was hypothesized that 10 days of exposure to 10 minute trials of ITTO in chronically instrumented, conscious rats would induce gene expression changes in the medial thalamus; specifically, upregulation of genes that have been implicated in the response to stress, anxiety, and/or depression, such as genes in the serotonergic system.

Materials and Methods

Animals

Eight male Sprague-Dawley rats (299 g ± 43.05) were housed two per cage in a temperature-controlled room (72°F) on a 12:12 light:dark cycle, and with free access to food and water. All animal experiments were approved by the Institutional Animal Care and Use Committee of the University of Florida.

Surgical Procedures

Placement of tracheal occluder

Rats were anesthetized using inhaled isoflurane gas (2-5% in O_2). Buprenorphine (0.01-0.05 mg/kg BW) and carpofen (5mg/kg BW) were administered preoperatively via subcutaneous injection. The eyes were coated with petroleum ointment to prevent drying. Incision sites were shaved and sterilized with povidine-iodine topical antiseptic solution. The trachea was exposed ventrally in the neck via a skin incision and blunt dissection of surrounding connective tissues. An expandable cuff was sutured around the trachea, two cartilage rings caudal to the larynx. The actuating tube was routed

subcutaneously and externalized, between the scapulae. The tube was anchored to the skin using the closing sutures. The neck incision was then closed using an interrupted suture pattern.

Analgesia and postoperative care

Preoperative analgesia consisted of buprenorphine (0.01-0.05 mg/kg BW) and carpofen (5mg/kg BW) administered via subcutaneous injection. Following surgical instrumentation rats were administered warm normal saline (0.01-0.02 ml/g BW) to ensure proper hydration. Postoperative analgesia was provided for at least three days using buprenorphine (0.01-0.05 mg/kg BW given every 12-24 hours) and carprofen (5mg/kg BW given every 24 hours). Rats were closely observed for any signs of distress or pain.

Experimental Protocol

Rats were placed in a plethysmograph and the externalized occlude actuator was connected to a saline-filled syringe (Figure 4-1). The syringe was used to inflate and deflate the cuff bladder. Inflation of the cuff compressed the trachea completely, occluding the airway during both inspiration and expiration. Deflation restored the trachea back to its original condition to allow unobstructed breathing. The control group data collection consisted of 15 min of recording with no experimental manipulation. The experimental group received a 2.5 min background control recording period, followed by a 10 min experimental session of ITTO, and ended with a 2.5 min post-test control period. During the experimental session the rats underwent repeated trials of 3-10 breath occlusions followed by approximately 30 s of recovery (Figure 4-2). Occlusion and control sessions were performed daily for 10 days. On day 10, within 10 min of completing the ITTO trial, the rats were sacrificed via overdose of anesthetic. The

medial thalamus was quickly excised, frozen in liquid nitrogen, and stored at -80°C until further use.

Microarray Analysis

Isolation of total RNA, amplification of RNA, microarray hybridization, statistical analysis, and gene ontology and pathway analysis was performed in the same way as in the previous study (Chapter 2). Genes were considered differentially expressed if the p-value was ≤ 0.05 and the $\log_2$ fold change was ≥ 0.58.

Results

Modulation of Gene Expression Profile Following ITTO

Statistical analysis of the microarray data showed that a total of 661 genes were altered ($p < 0.05$, $\log_2$ fold change ≥ 0.58) following the 10 day occlusion protocol, with 250 down-regulated and 411 up-regulated (Appendix Table C-1). Table 4-1 shows some of the significantly differentially modulated genes. These genes were chosen based on their potential role thalamic neuron functioning, as well as their implication in stress, anxiety, and depression. The glutamic acid decarboxylase subtypes 1 and 2 (GAD1 and GAD2), corticotrophin releasing hormone binding protein (CRHBP), and the serotonin receptor subtypes 1A and 2A (HTR1A and HTR2A) were found to be significantly up-regulated. Down-regulated genes included short stature homeobox 2 (SHOX2), cholecystokinin (CCK), protein kinase C (PRKCG), metabotropic glutamate receptor subtype 4 (GRM4), and a potassium inwardly-rectifying channel (KCNJ9).

Gene Ontology and Pathway Analysis

Table 4-2 shows some of the GO categories for biological processes that were significantly over-represented among the regulated genes (for full list see Appendix

Table D-1). Neurotransmitter signaling and learning and memory were some of the most important differentially modulated processes.

Pathway Studio was used to visualize changes of gene expression following tracheal occlusions. The balance between the activity of up- and down-regulated genes involved in these pathways determines the response. Figure 4-3 shows the significantly regulated genes and pathways involved in learning and/or memory. The up-regulated KCJN and GRM genes promote learning and/or memory, while the down-regulated HTR and GAD genes inhibited these pathways. Counteractive interactions between up- and down-regulated genes exist between the HTR and KCNJ pathways.

Modulated pathways for cellular processes are depicted in Figure 4-4. Cell proliferation is positively regulated by the down-regulated HTR and GAD genes and negatively regulated by the up-regulated GRM4, suggesting that this pathway could be less active following chronic exposure to ITTO. Cell differentiation appears to be promoted due to the positive regulation by DLH4 and the inhibition by GAD2. Several genes are involved in neuroprotection but the exact regulation is unknown. Cell death is inhibited by HTR1A and CRHBP but also by CCK, complicating a prediction on the direction of regulation on this pathway.

Figure 4-5 demonstrates the modulated pathways for cell signaling. Most up-regulated genes, except for GRM4, positively regulate calcium (Ca^{2+}) export, membrane polarization, and synaptic transmission. The up-regulated DLG4 inhibits HTR1A, which was found to be down-regulated. HTR1A and HTR2A have opposing effects on long-term synaptic potentiation, membrane polarization, and synaptic transmission.

Discussion

Thalamic Firing Mode and Sensory Gating

Transmission in the thalamic relay neurons occurs via one of two neuronal firing modes, called tonic and burst (Ramcharan et al., 2000). This response depends on the cells' membrane potential and the activity of T- (transient) and L- (long-lasting) type Ca^{2+} channels (Cheong et al., 2008; Sherman and Guillery, 2002). Tonic firing occurs at relatively depolarized membrane potentials when the T-channels are inactivated, and the firing of single action potentials is dependent on suprathreshold activation. Burst firing occurs when the membrane is hyperpolarized. The T-channels are de-inactivated and the next suprathreshold depolarization activates the channels to produce an inward Ca^{2+} current. This results in a low-threshold, all-or-none voltage spike that is usually large enough to fire a high frequency cluster of action potentials. L-type Ca^{2+} channels are involved in the production of afterhyperpolarization, an important factor in determining the firing rate of neuronal cells. Specifically, Cheong et al. (Cheong et al., 2008) have shown that increased Ca^{2+} influx via these channels augments afterhyperpolarization, which leads to both decreased tonic firing rates in thalamic relay neurons and increased gating of pain stimuli.

It has been proposed that switching between firing modes occurs in order to liberate the cerebral cortex from bothersome interference from the outside world (McCormick and Bal, 1994), or when the organism is attending to a specific stimulus (Sherman, 1996, 2001; Sherman and Guillery, 2002). During tonic firing each depolarization from a sensory stimulus produces one action potential. This linear relationship attains a faithful and accurate transmission of information through the thalamus to the cortex. Burst firing, on the other hand, is non-linear because

spontaneous activity can occur in the absence of a stimulus. This high signal-to-noise ratio improves the initial detectability of a stimulus. Sherman et al. (Sherman and Guillery, 2002) thus hypothesized that thalamic relay cells fire in burst mode when an important stimulus is detected, after which the cell switches to tonic mode for accurate relay of that input. A finding supporting this hypothesis is that tonic firing is increased the more alert the animal is (Ramcharan et al., 2000; Swadlow and Gusev, 2001). Furthermore, increased bursting and decreased tonic firing of thalamic neurons has been shown to reduce pain responses, suggesting that burst firing is associated with gating out of afferent sensory signals (Cheong et al., 2008).

Switching between firing modes requires a shift in membrane potential that is sufficiently sustained to inactivate or de-inactivate the T-channels. Ionotropic receptors are too fast acting to promote this shift; the slow metabotropic receptors are most likely responsible for the sustained voltage change. Specifically, studies have demonstrated that depolarization (inactivate T-channels) occurs through metabotropic glutamate receptors from the cortex and hyperpolarization (de-inactivate T-channels) through GABA receptors from reticular and/or interneuronal inputs (Sherman, 1996, 2001; Sherman and Guillery, 2002). Several neurotransmitters, such as serotonin, glutamate, acetylcholine, and norepinephrine, have been shown to facilitate the transition between thalamic firing modes (McCormick and Bal, 1994). Information on several genes that were found to be significantly modulated following chronic ITTO and that could be important in the thalamic firing and thus gating activity is presented below.

KCNJ9 (or GIRK channel or Cir3 channels, potassium inwardly-rectifying channel, subfamily J, member 9): G-protein inwardly rectifying potassium (GIRK)

channels mediate the synaptic actions of numerous neurotransmitters in the mammalian brain and play an important role in the regulation of neuronal excitability in most brain regions through activation of various G-protein-coupled receptors (Saenz del Burgo et al., 2008). Activation of GIRK channels causes membrane hyperpolarization, and thus the channels play an important role in the inhibitory regulation of neuronal excitability (Kobayashi et al., 2004). GIRK channels are widely expressed in brain nuclei and are co-expressed with serotonergic, GABAergic, glutamatergic, and cholinergic neurons throughout the brain (Saenz del Burgo et al., 2008). Thus, the interplay between the neurotransmitters and GIRK channels in addition to hyperpolarization could result in switching of the thalamic firing mode. GIRK2-deficient mice have been shown to exhibit reduced anxiety and elevated motor activity (Kobayashi et al., 2004); thus an upregulation in GIRK as found in this study could point to increased anxiety.

GRM4 (or mGluR4, metabotropic glutamate receptor 4): Glutamatergic neurotransmission is involved in most aspects of normal brain function and can be perturbed in many neuropathologic conditions. L-glutamate is the major excitatory neurotransmitter in the central nervous system and activates both ionotropic and metabotropic glutamate receptors. Grm4 belongs to group III metabotropic glutamate receptors. Agonists of group III mGluRs have been shown to exert antidepressant-like effects, possibly due to a decrease in excitatory glutamatergic neurotransmission (Klak et al., 2007).

A recent study in protein lipase C-knockout mice demonstrated that switching between tonic and burst firing in thalamic neurons occurs through the simultaneous modulation of T- and L-type Ca^{2+} channels possibly through a transduction cascade that

includes metabotropic glutamate receptors and protein kinase C (Cheong et al., 2008). These mice, which show decreased visceral pain responses, exhibited increased bursting and decreased tonic firing in thalamic neurons, suggesting that burst firing acts as an inhibitor of pain signal transmission to the cortex.

PRKCG (protein kinase C, gamma): Protein kinase C (PRKC) is a family of serine- and threonine-specific protein kinases that can be activated by Ca^{2+} and the second messenger diacylglycerol. These molecules phosphorylate a wide variety of protein targets and are involved in diverse cellular signaling pathways. The gamma subunit of PRKC is expressed solely in neurons in the brain and spinal cord (Saito and Shirai, 2002). This specific kinase has been implicated in several neuronal functions, including long term potentiation and long term depression (Saito and Shirai, 2002). It has also been shown to associate directly with the GluR4 AMPA receptor subunit; GluR4 phosphorylation would allow for regulation of synaptic function and plasticity (Correia et al., 2003). As mentioned above, PRKC is involved in switching between burst and tonic firing. Specifically, down-regulation of PRKC activity in thalamic relay neurons has been attributed to reduced pain responses, or increased sensory gating (Cheong et al., 2008). In the present study, we found an up-regulation of PRKC, suggesting that chronic exposure to ITTO results in decreased gating in the thalamus.

CCK (cholecystokinin): Cholecystokinin is one of the most abundant neuropeptides in the brain and acts as a neurotransmitter and neuromodulator of dopamine, serotonin, endogenous opioids, GABA and excitatory amino acids (Harro and Vasar, 1991). These characteristics support an important role in regulation of many behavioral phenomena, including anxiety and learning and memory. Indeed, CCK

agonists have been shown to be anxiogenic and CCK antagonists are anxiolytic in a variety of animal species (for reviews see (Harro et al., 1993; Rotzinger and Vaccarino, 2003). CCK has also been demonstrated to have close interaction with GABAergic inhibitory neurotransmission, mediated probably through CCK-B receptors, which could be the neurochemical substrate for anxious behavior (Harro and Vasar, 1991).Whole-cell patch clamp experiments have shown that CCK depolarizes somatosensory cortex neurons long-lastingly and thus may lead to prolonged discharge of these corticothalamic glutamatergic neurons and slow depolarization of thalamocortical neurons, shifting the firing mode from burst- to tonic-firing mode, thus being critical in sensory information processing (Chung et al., 2009).

Chronic Exposure to ITTO Modulates Genes Involved in Stress, Anxiety, and Depression

Chronic airway occlusion, as occurs in diseases such as chronic obstructive pulmonary disease, has been implicated in an increased incidence of anxiety and depression (Di Marco et al., 2006; Omachi et al., 2009). In the present study, several genes were found to be significantly altered following tracheal occlusions that play important roles in the development of depressive and other psychological disorders.

GAD1 (or GAD67, glutamate decarboxylase) and GAD2 (or GAD65): GAD1 and GAD2 are two isoforms of glutamate decarboxylase. These enzymes catalyze the reaction to synthesize GABA from glutamate and are responsible for keeping cortical GABA levels at steady state (Soghomonian and Martin, 1998). Thus, a reduced expression of GAD1 and GAD2 may lead to decreased GABA levels and less inhibition of downstream targets. Decreased GAD67 expression has been implicated in schizophrenia and bipolar disorder with psychosis (Guidotti et al., 2000).

CRHBP (corticotrophin releasing hormone – binding protein): CRHBP is an important modulatory protein that negatively regulates corticotrophin releasing hormone (CRH) activity. CRHBP binds to CRH and thus reduces the ability of CRH to activate the CRHR1 and CRHR2 receptors (Jahn et al., 2002). CRHBP is a physiologically relevant reservoir of endogenous CRH, as 40-60% of human brain CRH is bound by CRHBP. CRH is released in response to stress. A reduction in CRHBP would lead to less binding of CRH and more free CRH which can then activate its receptors and elevate the stress response. In a CRHBP-deficient mouse model, Karolyi et al. (Karolyi et al., 1999) have demonstrated increased anxiogenic behavior as tested on the elevated plus maze and open field. A decrease in CRHBP has also been suggested to play a role in the pathogenesis of major depressive disorder by inhibiting the function of CRH (Van Den Eede et al., 2005).

HTR (serotonin receptors): The serotonin system has been shown to play a critical role in a variety of human psychopathological conditions, particularly mood and anxiety disorders (Hensler, 2006). Antidepressant treatment has thus focused on modulating serotonergic neurotransmission (Jones and Blackburn, 2002). One of the challenges of the serotonin system is the sheer complexity of it, with 14 known receptor varieties categorized into seven receptor subtypes (Hoyer et al., 2002).

The HTR1A subtype exists on pre-synaptic neurons in raphe nuclei as well as on post-synaptic neurons in other brain regions, such as the hippocampus and the thalamus. Agonists have different effects depending on the location of the receptors, in that agonists to pre-synaptic receptors result in anxiolytic behaviors while agonists to post-synaptic receptors lead to anti-depressive behaviors (Schreiber and De Vry,

1993)). Kennett et al. (Kennett et al., 1987) have demonstrated that the 5-HTR1A agonist 8-hydroxy-2-(di-n-propylamino) tetralin (8-OH-DPAT) may have rapid antidepressant properties. Partial HTR1A may also be effective in the treatment of generalized anxiety disorder (Jones and Blackburn, 2002) and schizophrenia (Millan, 2000).

HTR1A knockout mice show elevated anxiety levels in open-field, elevated-zero maze, and novel-object assays (Heisler et al., 1998) and are less reactive, more anxious, and possibly less aggressive than the wild-types (Ramboz et al., 1998). Dysfunction of this receptor has been suggested to also play a role in the genesis of major depressive disorder in humans (Savitz et al., 2009). PET studies in patients with posttraumatic stress and panic disorders (Neumeister et al., 2004) and depression (Drevets et al., 1999) have shown reduced HTR1A receptor binding potential and reduced receptor availability (Nash et al., 2008).

In the present study we found a down-regulation of serotonin receptors after 10 days of ITTO. In the previous study (Chapter 3) we have shown that the serotonin receptor HTR2A was rapidly up-regulated with acute occlusions. This is in general agreement with the suggestion that anxiety is the result of a hypersensitive serotonin system; whereas impulsivity and depression is the result of a hyposensitive serotonin system (Schreiber and De Vry, 1993).

Chronic Exposure to ITTO Modulates SHOX2

SHOX2 (or Prx3 or OG12X or SHOT): SHOX2 is a homeobox gene expressed mainly in the thalamus in adult rats, more specifically in those thalamic relay nuclei that coordinate and integrate sensory information to be sent to the sensory cortex (van Schaick et al., 1997). Despite its critical location for gating of sensory information, no

reports have been published on modulated SHOX2 gene expression. Homeobox genes are the largest class of transcription factors instrumental in cell-specific gene expression. Their expression patterns are mostly restricted during development of embryonic brain, and some persist during adult life. Aberrations in homeobox genes can cause several genetic disorders, in the case of SHOX2 it is thought to be responsible for idiopathic short stature in Turner syndrome patients (Rao et al., 1997).

Chronic Exposure to ITTO Modulates Pathways Involved in Learning and Memory, Cell Processes, and Cell Signaling

Ten days of ITTO resulted in a behavioral adaption in order to cope with the stress of the occlusion trials. These adaptations were characterized by decreased exploratory behavior, increased submissive state, and even breath holding (Pate et al., 2010). This finding of learned helplessness and memory of previous occlusion trials is consistent with the altered molecular pathways of learning and/or memory. In the present study, most of the genes that were found to be up-regulated have been shown to increase learning and/or memory.

Modulated cellular processes included cell proliferation, differentiation, neuroprotection, and cell death. A common trend in the analysis of these pathways was the inhibitory regulation of cell death by up-regulated genes, while neuroprotection was positively regulated. Cell proliferation seemed to be down-regulated because the genes that are activating this process showed decreased expression. However, cell differentiation appeared to be increased, both by positive regulation of up-regulated genes as well as by inhibitory regulation of down-regulated ones.

Differentially regulated genes involved in cell signaling were Ca^{2+} transport, membrane polarization, synaptic potentiation and transmission. Involvement of the

various genes is less clear and often in opposite direction. The balance of up- and down-regulation of genes in these pathways seems to be important in determining the final outcome.

Conclusions

Contrary to our hypothesis that repeated ITTO would induce increases in 5-HTR2A gene expression, we found a decrease in the expression of this receptor subtype along with a decrease in 5-HTR1A. This finding could be explained by the opposite action of the serotonergic system depending on the duration of the stress stimulus (Graeff et al., 1997; Schreiber and De Vry, 1993). An acute stress, such as one trial of ITTO, would produce anxiety due to up-regulation of components in the serotonergic system, while chronic exposure to a stress such as repeated trials of ITTO would produce depression-like behavior due to down-regulation of this system.

Repeated ITTO elicited changes in the gene expression profile of the medial thalamus involved in neuronal firing mode, suggesting a modulation of respiratory afferent information gating. A change in gating of information to higher brain centers could result in a different behavioral response to the ITTO respiratory stimulus. The respiratory load compensation response has been shown to be altered in conscious rats and following 10 days of repeated ITTO (Pate et al., 2010). This alteration may be due to a change in the gating pattern that influenced the behavioral control of breathing.

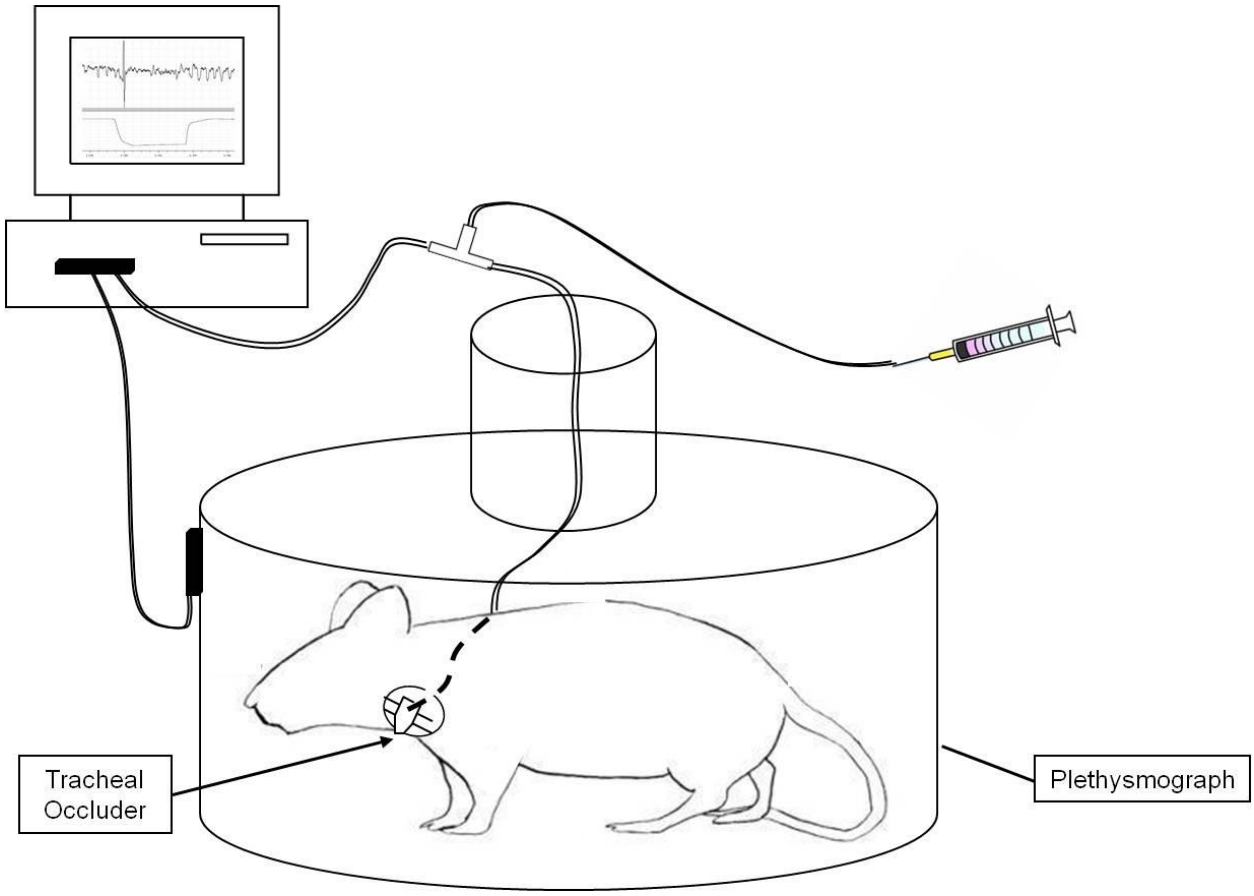

Figure 4-1. Schematic of the experimental protocol for repeated ITTO. Rats were placed in a plethysmograph and the actuator tube of the tracheal cuff was connected to a saline-filled syringe.

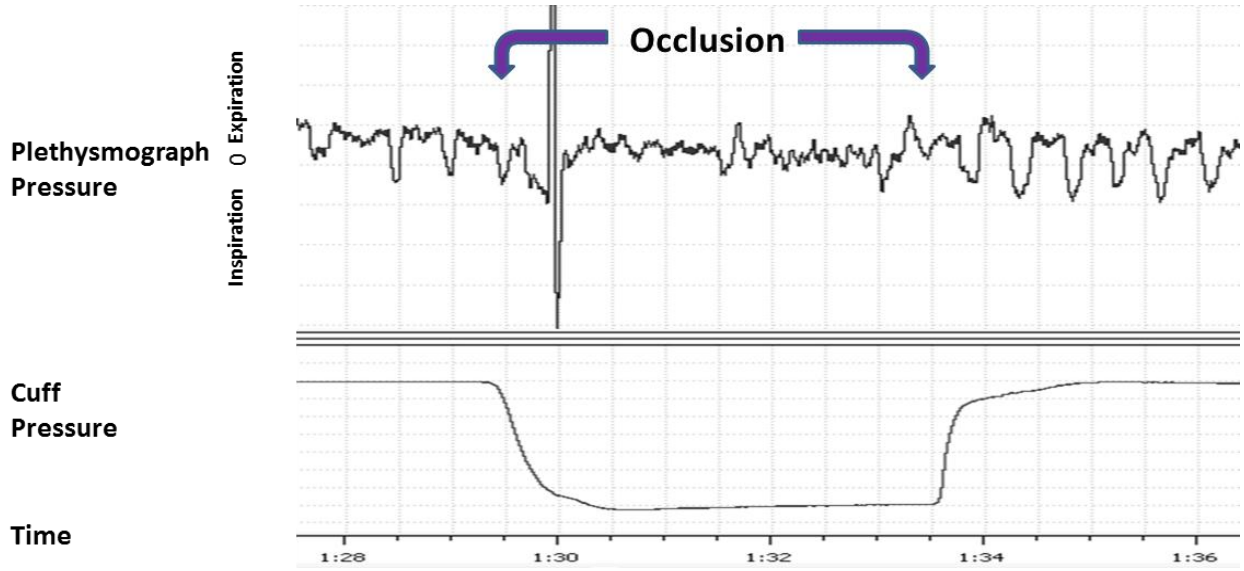

Figure 4-2. Representative plethysmograph pressure traces for one occlusion trial on day 10. Cuff pressure indicates the period of occlusion. The large deflection of the signal at the beginning of occlusion is ascribed to a movement artifact when the rat twitches due to application of occlusion.

Table 4-1. Candidate genes significantly differentially regulated following chronic ITTO.

Log fold change	p-value	Gene Symbol	Description
- 2.14	0.0043	GAD1	Glutamic acid decarboxylase 1
- 1.61	0.0256	GAD2	Glutamic acid decarboxylase 2
- 1.38	0.0039	CRHBP	Corticotropin releasing hormone binding protein
- 0.78	0.0396	HTR1A	Serotonin receptor 1A
- 0.59	0.0023	HTR2A	Serotonin receptor 2A
+ 1.37	0.0009	SHOX2	Short stature homeobox 2
+ 1.36	0.0402	CCK	Cholecystokinin
+ 1.22	0.0040	PRKCG	Protein kinase C, gamma
+ 1.09	0.0085	GRM4	Glutamate receptor, metabotropic 4
+ 1.07	0.0060	KCNJ9	Potassium inwardly-rectifying channel

Table 4-2. Significantly modulated Gene Ontology Biological Processes.

Name	# of Entities	Overlap	p-value
Synaptic transmission	247	17	$2.19\ e^{-12}$
Learning and/or memory	42	5	$1.11\ e^{-5}$
Neurotransmitter Transport	62	5	$7.55\ e^{-5}$
Neurotransmitter Secretion	48	4	$3.60\ e^{-4}$
Regulation of neuronal synaptic plasticity	26	3	$7.85\ e^{-4}$
Regulation of neurotransmitter secretion	27	3	$8.79\ e^{-4}$
Learning	31	3	$1.32\ e^{-3}$

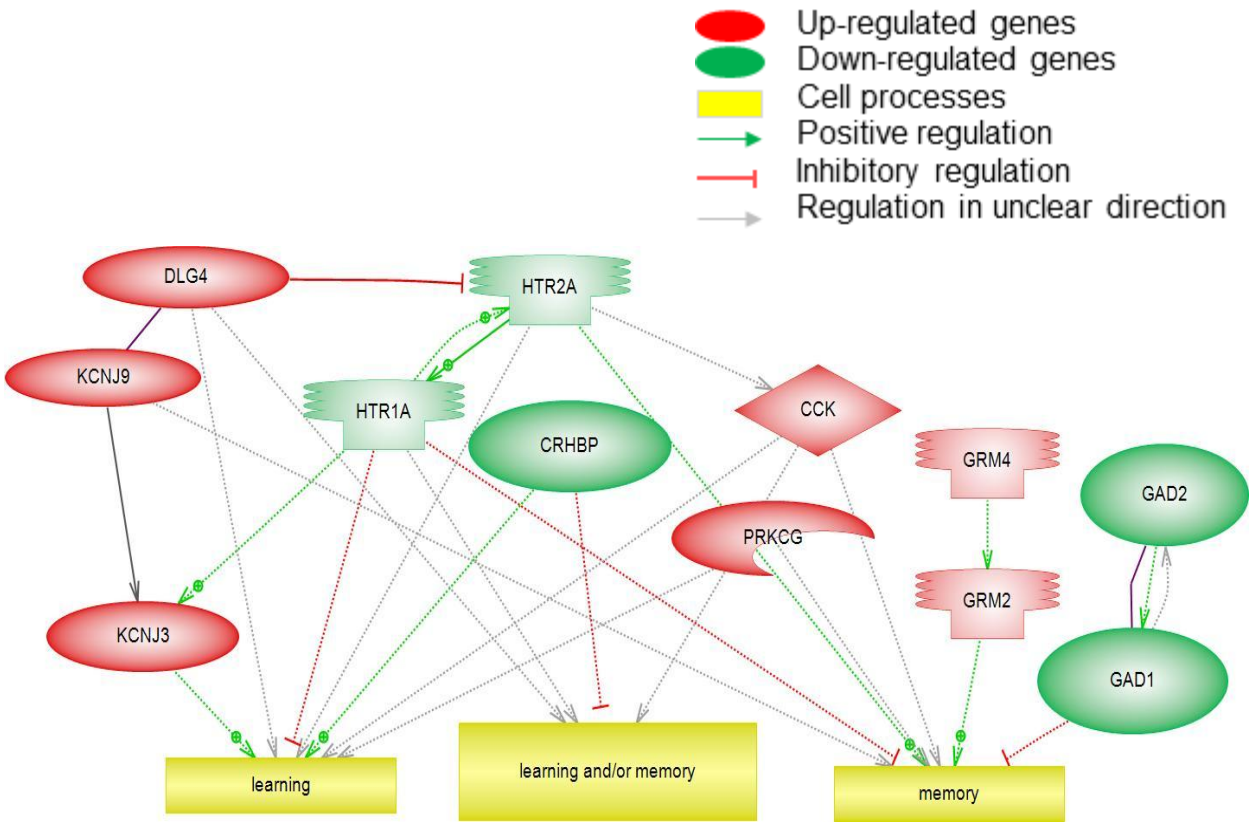

Figure 4-3. Pathway analysis of transcripts ($p < 0.05$) involved in the biological processes of learning and/or memory.

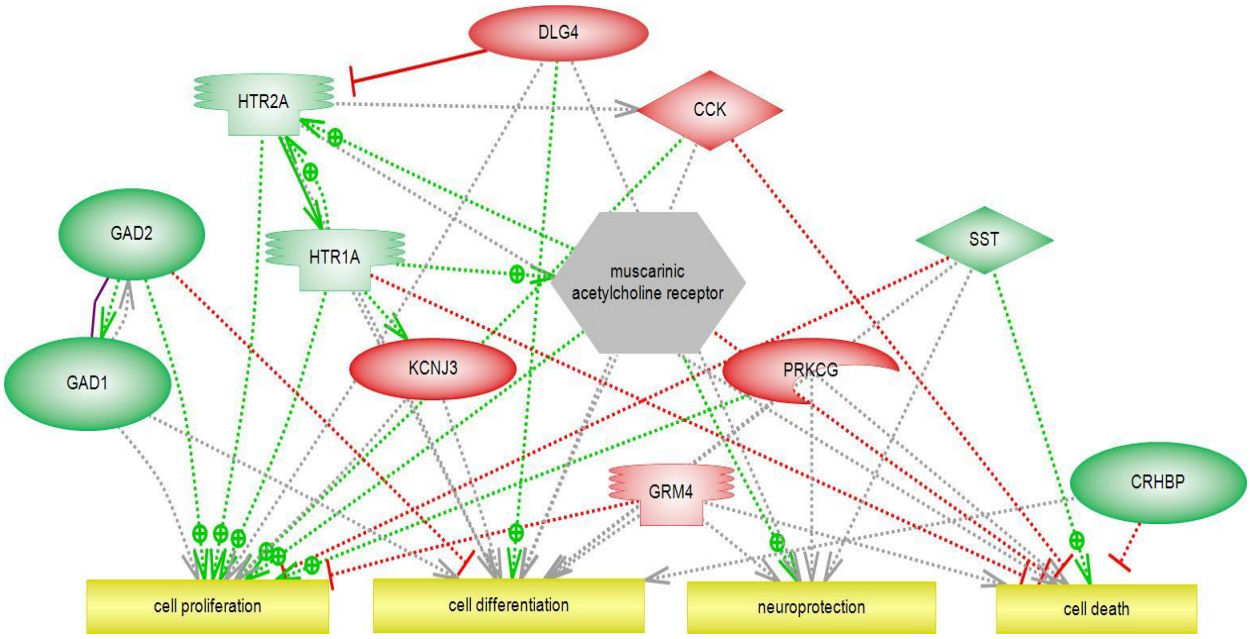

Figure 4-4. Pathway analysis of transcripts ($p < 0.05$) involved in cell processes.

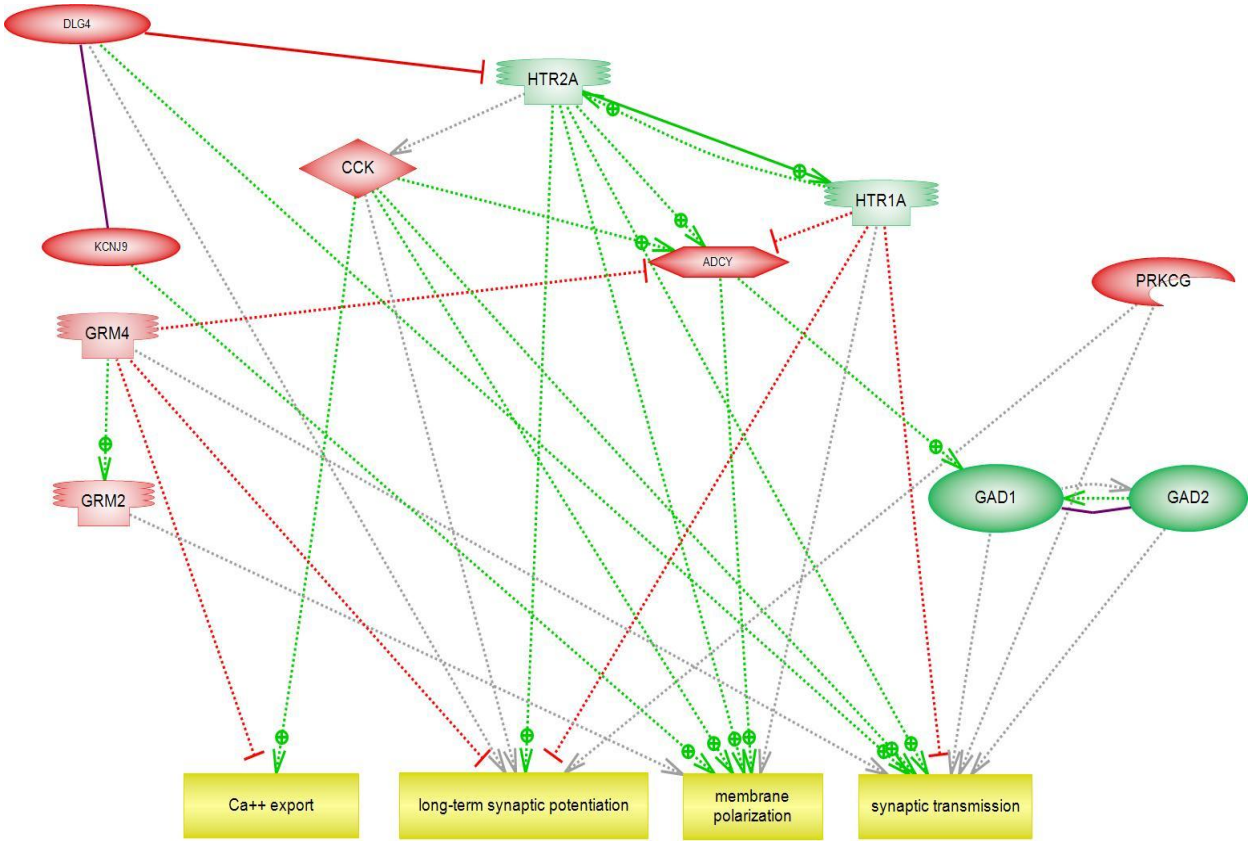

Figure 4-5. Pathway analysis of transcripts ($p < 0.05$) involved in cell signaling.

CHAPTER 5
SUMMARIES AND CONCLUSIONS

Summary of Study Findings

Study #1 Summary

The purpose of this study was to determine the effects of EMST on pulmonary function and maximal expiratory pressure generating capacity, and to determine whether this specific respiratory muscle training affects oxygen consumption during an incremental exercise test, swimming performance, and perception of exertion and breathlessness in highly trained collegiate swimmers. The EMST group was compared to an AFT group that functioned as a placebo control.

The EMST intervention elicited significant increases in MEP but not the other measured pulmonary function variables ($FEV_{1.0}$, FVC, $FEV_{1.0}$/FVC). Post-training, MEP increased by 29.86% in the EMST group and 7.86% in the AFT group. These results demonstrate that the EMST pressure-threshold training device provided a sufficiently strong stimulus to increase expiratory pressure generating capacity in these highly trained swimmers, while the AFT non-resistance air-flow training device did not significantly increase expiratory muscle strength as measure by MEP.

Swimming performance improved more in the EMST than the AFT group. Average swim time during the all-out 6 x 100 meter freestyle interval test decreased by 1.44% in the EMST group and by 0.29% in the AFT group, however, the change was not statistically significantly different between the groups ($p = 0.204$). Post-training, ratings of breathlessness tended to worsen in the AFT group and ratings of perceived exertion tended to improve in the EMST group. The results demonstrate that EMST has a trend to improve swimming times in a maximal effort interval swim test that may give these

highly competitive athletes an improved performance during a swim competition, and EMST has a trend to improve subjective ratings of perceived exertion and breathlessness during maximum effort swimming. EMST is more effective than AFT in conditioning expiratory muscles of highly trained athletes and is an easy method that could be used as an adjunct for swimmer's athletic conditioning. These promising results in improving performance merit further investigation into training of the respiratory system in athletes.

Study #2 Summary

This study evaluated the responses of a 10-minute bout of ITTO on the gene expression profile of the medial thalamus in urethane anaesthetized rats. This study was important to establish a role of the medial thalamus as a component in the respiratory mechanosensory neural pathway. Analyses of breath timing responses to ITTO corroborated the existence of the ventilatory load compensation reflex in the anaesthetized animal. Gene expression profiles were measured using Agilent Technology Oligo Microarrays. Tracheal occlusions modulated a total of 588 genes ($p < 0.05$, $\log_2$ fold change ≥ 0.58), of which 261 were up-regulated and 327 were down-regulated. A significant up-regulation of the serotonin HTR2A receptor and significant down-regulation of the dopamine DRD1 receptor genes were found. Pathway analysis was performed targeting serotonin and dopamine receptor pathways. The MAPK1 gene was significantly down-regulated. MAPK1 is an inhibitory regulator of the serotonin HTR2A receptor and facilitatory regulator for the dopamine DRD1 receptor. Down-regulation of MAPK1 may be related to the up-regulation of HTR2A and down-regulation of DRD1 suggesting an interaction in the medial thalamus serotonin-dopamine pathway elicited by airway obstruction. Gene ontology analysis showed gene expression

changes related to anti-apoptosis, response to stress, and the MAPKKK cascade. The results of this study demonstrate an immediate change in gene expression in thalamic stress/anxiety/depression-pathways, providing evidence for the involvement of the medial thalamus to respond to airway occlusions.

Study #3 Summary

Based on the results of study #2, the experiments in study #3 were undertaken to evaluate the gene expression profile of the medial thalamus following chronic conditioning to ITTO (daily 10-minute occlusion trials for 10 days) in conscious rats. Chronic tracheal obstruction conditioning modulated 611 genes ($p < 0.05$), of which 411 were up-regulated and 250 were down-regulated. There was a significant down-regulation of the genes encoding GAD1, GAD2, CRHBP, HTR1A, and HTR2A. Up-regulated genes included SHOX2, CCK, PRKCG, GRM4, and KCNJ9. Significantly regulated gene ontology categories were learning and/or memory, neurotransmitter synthesis, transport, and secretion, and synaptic transmission and plasticity. Pathway analysis showed the involvement of the significantly modulated genes in learning and/or memory, cell processes, and cell signaling.

The results of this microarray study demonstrate that repeated ITTO in conscious rats elicited changes in the gene expression profile of the medial thalamus involved in neuronal firing mode, suggesting a modulation of respiratory afferent information gating. A change in gating would influence the behavioral control breathing and thus alter the respiratory load compensation response. It further implicated a role of chronic exposure to airway occlusions in development of stress, anxiety, and depression.

Discussion

The Role of Serotonin in Response to Respiratory Stimuli

Any stressor threatening the homeostasis of an organism can initiate neural and behavioral responses to adapt to the specific situation. The activity of neurotransmitters is critical for these changes to occur. Based on the studies in chapters 3 and 4, one of the neurotransmitter systems involved in respiratory stimuli is serotonin. Pharmacologic agents targeting the serotoninergic system are used to treat a variety of disorders; some functions of serotonin include the regulation of mood, appetite, sleep, and memory and learning. Serotonergic fibers from the raphe nucleus travel to midline, intralaminar and association nuclei of the thalamus and from there mostly to limbic forebrain areas and some to sensory and motor cortices, suggesting that serotonergic fibers to the thalamus may exert a significant influence on affective and cognitive functions involved in emotional and cognitive behaviors (Vertes et al., 2010). Modulation of components of the serotonergic system in the thalamus could thus be responsible to changes in affective perception and behavior to a stimulus. In study 2 (Chapter 3), the serotonin receptor HTR2A was found to be *up*-regulated following just one trial of ITTO in anesthetized rats. In study 3 (chapter 4), there was a *down*-regulation of the serotonin receptors subtype HTR2A and HTR1A after ten days of repeated ITTO in conscious animals. These findings are in agreement with other studies that show that serotonin can modulate anxiety and depression in opposite directions, with high serotonergic activity being associated with anxiety and low activity with depression (Graeff et al., 1997; Schreiber and De Vry, 1993).

The Effects of Respiratory Training

The respiratory system could be one of the factors limiting exercise performance in highly trained athletes (Dempsey, 2006). Study 1 corroborates this hypothesis by demonstrating that a specific respiratory muscle strength training slightly, albeit statistically not significant, improved swimming performance. Pulmonary function (FVC, FEV1.0) did not change, which is consistent with the notion that the pulmonary system does not structurally adapt to physical training (Dempsey et al., 1990). However, EMST did significantly increase the maximum expiratory pressure capacity, indicating that the expiratory muscles responded to the training load by an increase in strength. This increase could improve the response to the expiratory flow limitation imposed by the water pressure, and in turn reduce and/or delay the perception of breathlessness.

The results from the animal studies in chapters 3 and 4 using ITTO shed some light on the potential underlying mechanisms for the positive effects of EMST. We found changes on the gene level in the medial thalamus, indicating that the supra-pontine brain areas play a role in influencing the control of breathing. As described in chapter 1, the thalamus is the structure implicated in the gating of sensory information to higher brain centers such as cortical areas and the limbic system (Figure 1-1). Modulation of thalamic function and thus gating could suggest altered feedback to these brain areas and thus a different response pattern to the stimuli. More specifically, the trend of decreased perception of breathlessness and exertion during the interval swim test in the EMST group could have been due to increased gating of the uncomfortable respiratory stimulus.

Breathlessness, either in combination with peripheral muscle fatigue or by itself, is the most common reason for reduction or termination of exercise (Killian and Campbell,

1995). During a maximal effort exercise, the subject is aware of both the increasing central motor command and the decline in power output (Killian and Gandevia, 1996); the awareness of these two factors gives rise to the sensation of fatigue (Jones and Killian, 2000). The sensation of breathlessness likely depends on several different mechanisms that are involved in the regulation of breathing including feed-forward and feedback mechanisms (Figure 2-11) (Chonan et al., 1990b).

Figure 5-1 shows a schematic model of the effects of respiratory muscle training on perception based on my studies. With increasing exercise intensity, there usually is increased feedback from receptors in the respiratory muscles, chest wall, lungs, lower and upper airways, and chemoreceptors to the thalamus. Respiratory muscle training (repeated ITTO) could modulate this feedback due to improved strength of these muscles and thus could result in a change of how the thalamus handles the influx of respiratory information, so that the perception of breathlessness is delayed or reduced. The ITTO animal studies are suggestive of a change in function of the thalamic gating process. The combined factors of reduced feedback and change in gating within the thalamus could lead to decreased signaling to the limbic system and the sensory cortex, and in turn decrease perception.

Methodological Considerations and Directions for Future Studies

The present set of experiments highlighted a potential ergogenic effect of EMST in a group of highly trained swimmers and contributed to a better understanding of the role of the medial thalamus in response to loaded respiratory stimuli. Limitations to these studies and proposals for future experiments that could expand this body of work are discussed below.

Fatigue due to Regular Training

During the EMST study the swimmers were on a three-week training cycle with each week having a different focus such as endurance, sprint, strength, and recovery, which was repeated every three weeks. Accordingly, the swimmers' general fatigue levels varied to some extent within the training cycle. One week of training (Monday through Saturday) consisted of nine two-hour swim sessions at 5,000-8,000 m, plus additional dry land and weight training workouts. Therefore, most of our laboratory testing was performed early in the week to take advantage of the recovery Sunday. The 6 x 100 m swim tests were administered at the beginning of the Tuesday afternoon swim practice after a specific standard warm-up. In order to minimize variability, an interval swim test was chosen instead of a time-trial. Other studies involving highly trained swimmers have used either time-trials (Kilding et al., 2010; Lindh et al., 2008; Vandenbogaerde and Hopkins, 2010) or interval tests (Psycharakis, 2010; Seifert et al., 2010; Wells et al., 2005).

Respiratory Training Stress Stimulus

As seen from study 3 (chapter 4), repeated ITTO induced gene expression changes in the conscious rat that are associated with anxiety and depression. This is consistent with evidence showing an increased rate of anxiety and depression in patients with repeated acute or chronic airway occlusion, such as asthma and COPD (Moussas et al., 2008). It also implicates ITTO as a negative stressor. However, in our experiments the animals were healthy and had no intrinsic respiratory muscle weakness as is characteristic of asthma, COPD, or various neuromuscular diseases (Barbarito et al., 2001). Respiratory muscle training in humans is probably a positive stressor due to the motivation and expectation of the individual; therefore, this training should not

induce anxiety/depression but rather a positive outlook toward improvement of performance. Thus, we cannot be absolutely certain that the respiratory stimulus of ITTO *per se* elicited the changes in gene expression or if feedback from higher brain centers, especially from the limbic system, were involved. However, study 3 also showed an up-regulation of the learning and/or memory pathways and study 2 (chapter 3) demonstrated an up-regulation of the stress response and negative regulation in apoptosis in anesthetized animals immediately following the single trial of ITTO, suggesting that this type of stressor was not necessarily a negative one. To my knowledge, our animal model is the first to examine gene expression changes in a subcortical area in response to an intrinsic respiratory stimulus that has been shown to induce respiratory muscle hypertrophy (Smith et al., 2010).

$\dot{V}O_2$max Testing

The incremental $\dot{V}O_2$ test on the swim ergometer was not a true maximal test, but submaximal because most swimmers were able to complete the testing protocol before the characteristic plateau phase of the $\dot{V}O_2$ curve was reached. To my knowledge, this particular swim ergometer has never been used in previous studies, even though it has some important advantages to other ergometers as discussed in chapter 2. For a future study, adjustments to stroke frequency and/or time spent at each resistance level should be made, depending on the fitness level of the participant group. In this case with highly trained swimmers, a slightly higher constant stroke frequency may be more appropriate to assess a true $\dot{V}O_2$ max value.

Prevalence of Respiratory Disease in Swimmers

Asthma is a common occurrence in elite athletes, especially in endurance sport such as swimming. The most recent study of 200 top Finnish swimmers revealed that the prevalence of asthma was higher in these swimmers than in the general population (Paivinen et al., 2010). The study found that physician-diagnosed asthma was reported by 32 swimmers (16%), including 24 (12%) with exercise-induced asthma. Asthmatic symptoms during swimming were described by 84 subjects (42%) with most symptoms occurring when swimming exceeded speeds corresponding to the lactic/anaerobic threshold. In our study with UF swimmers, exclusion criteria included the occurrence of bronchoconstriction and taking medication for respiratory disease. Unfortunately, these criteria complicated the recruiting process since about one third of the swimmers asked had physician-diagnosed asthma and were taking medication. Future studies should include asthmatic athletes to see the possibly different effect of EMST in this population.

Specificity of Medial Thalamic Nuclei

The medial thalamus consists of multiple nuclei, midline and intralaminar nuclei, that may have different specific functions. Furthermore, the medial thalamus contains a variety of anatomically and functionally heterogeneous neurons (Benarroch, 2008), such as glutamatergic projection neurons, inhibitory interneurons, and relay neurons. The thalamic microarray sample in the experiments presented here was not targeted to a specific nucleus or group of neurons, thus gene expression may be multifactorial. Future studies may be carried out to determine the different type of neurons comprising the midline and intralaminar nuclei and the connectivity between other brain areas and these specific neurons.

Genomics Versus Proteomics

The use of microarray technology has become a popular method to study changes in gene expression in pathologies and following specific stimulus interventions. However, a change in mRNA levels of a particular gene does not necessarily translate into the same change in protein levels of that gene. Most microarray studies that use protein validation (in the form of Western blots, for example) show modulation of mRNA and protein in the same direction and with similar fold changes. Some studies, however, have demonstrated distinctly different fold changes or even opposite regulation of mRNA and the associated protein. Thus, in future studies, proteomics could be used to assess protein changes in certain brain regions involved in the respiratory control network.

Conclusions

The three studies presented in this dissertation examined the effects of respiratory muscle training in humans and in a rat model. EMST in swimmers showed a significant increase in expiratory pressure generating capacity and trends for improvements in swimming performance and feelings of breathlessness and perceived exertion. Tracheal occlusions in anesthetized and conscious rats showed changes in the gene expression profile of the medial thalamus, indicating that this brain area responds to respiratory loading and may be involved in gating and relaying respiratory information to higher brain centers.

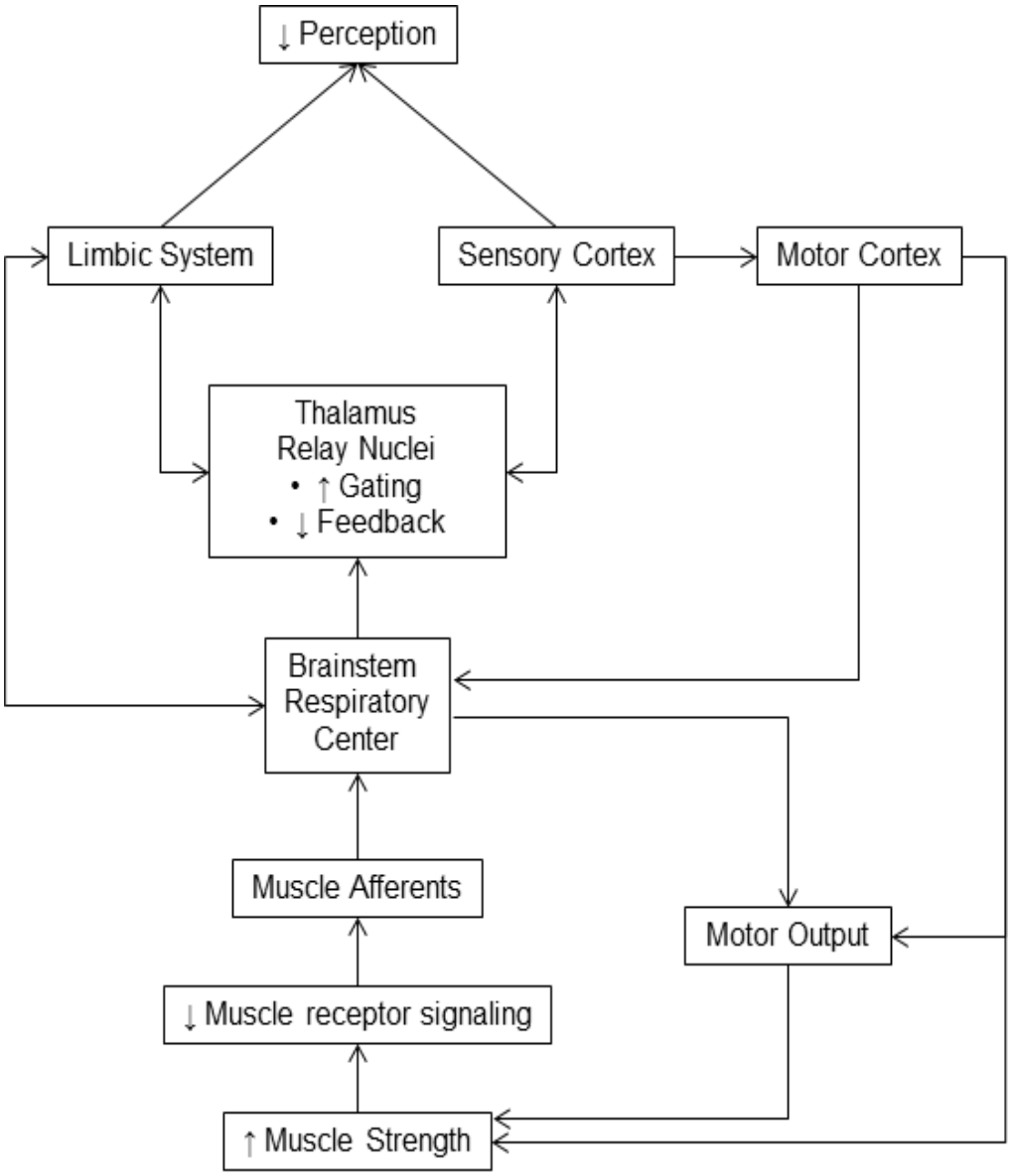

Figure 5-1. Model for possible effects of respiratory muscle training on perception.

APPENDIX A
RATING SCALES

Perceived Exertion Scale

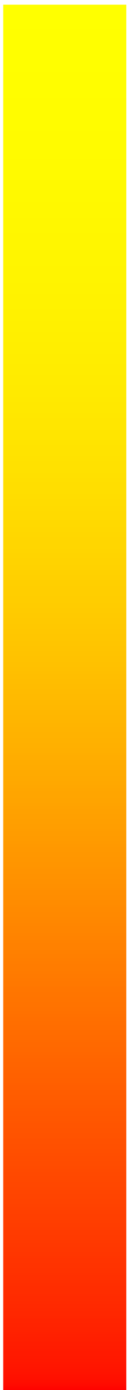

0	None
0.5	Extremely light
1	Very light
2	Fairly light
3	Moderate
4	Somewhat hard
5	Hard
6	
7	Very hard
8	
9	Extremely hard
10	Maximal

Breathlessness Scale

0	None
0.5	Extremely mild
1	Very mild
2	Fairly mild
3	Moderate
4	Somewhat strong
5	Strong
6	
7	Very strong
8	
9	Extremely strong
10	Maximal

APPENDIX B
LIST OF MODULATED GENES FOLLOWING ACUTE ITTO

Table B-1. List of modulated genes following acute ITTO, $p < 0.05$ and $\log_2$ fold change ≥ 0.4

$\log_2$ FC	p-value	TargetID	Symbol	Name
-2.99	0.0466	AA899244		
-1.48	0.0196	ENSRNOT00000047881		
-1.43	0.0418	AA900238		
-1.33	0.0004	AW143927		
-1.33	0.0388	XM_237191	Fzd7_predicted	frizzled homolog 7 (Drosophila) (predicted)
-1.31	0.0474	CB547739		
-1.29	0.0377	NM_001025147	Gpr160	G protein-coupled receptor 160
-1.28	0.0011	BQ196489		
-1.28	0.0220	AI102771		
-1.27	0.0214	BC099085		
-1.25	0.0436	XM_001077586	LOC691293	similar to reproductive homeobox on chromosome X, 7
-1.25	0.0414	NM_013167	Ucp3	uncoupling protein 3 (mitochondrial, proton carrier)
-1.23	0.0144	TC541367		
-1.20	0.0249	D84486		
-1.20	0.0401	NM_147165	Gpx6	glutathione peroxidase 6
-1.15	0.0200	BI291339		
-1.13	0.0019	NM_153721	Cxcl7	chemokine (C-X-C motif) ligand 7
-1.12	0.0300	XM_577774	LOC502310	similar to Cytochrome P450 2B12 (CYPIIB12)
-1.12	0.0304	AI555248		
-1.10	0.0063	XM_222561		
-1.09	0.0265	NM_147213	LOC259245	alpha-2u globulin PGCL5
-1.08	0.0026	AA997228		
-1.08	0.0345	AA956566		
-1.08	0.0011	BF391695		
-1.08	0.0098	AA818571		
-1.06	0.0429	NM_133533	Cd79b	CD79B antigen
-1.06	0.0209	A_44_P473318		
-1.06	0.0411	XM_001076906	LOC687057	similar to Calponin-2 (Calponin H2, smooth muscle) (Neutral calponin)
-1.06	0.0069	NM_001025628	Ropn1	ropporin, rhophilin associated protein 1
-1.05	0.0109	BI296967		
-1.05	0.0117	TC541883		
-1.04	0.0444	XM_217136	Cd3g	CD3 antigen, gamma polypeptide
-1.04	0.0432	A_44_P319138		
-1.03	0.0215	BF559727		
-1.02	0.0407	BE097028		
-0.99	0.0059	XM_340956	LOC360684	similar to eyes absent 4 isoform a
-0.99	0.0102	NM_012969	Irs1	insulin receptor substrate 1
-0.98	0.0310	BI296249		
-0.98	0.0472	NM_031537	LOC24906	Robo-1
-0.98	0.0395	BF396663		
-0.98	0.0121	AA944970		

-0.97	0.0278	BI296064		
-0.96	0.0134	XM_001069898	LOC684331	hypothetical protein LOC684331
-0.96	0.0430	AA800882		
-0.95	0.0184	BF281960		
-0.95	0.0300	TC530472		
-0.93	0.0389	BI282122		
-0.93	0.0124	A_44_P527770		
-0.91	0.0390	XM_344756	Pou4f2	POU domain, class 4, transcription factor 2
-0.91	0.0270	XM_001075247	LOC686680	similar to membrane-spanning 4-domains, subfamily A, member 5
-0.91	0.0392	XM_344473		
-0.91	0.0270	BE115850		
-0.91	0.0456	XM_345276		
-0.91	0.0064	XM_001053946	LOC679957	similar to G protein-coupled receptor 18
-0.91	0.0489	NM_175755	Ppm1f	protein phosphatase 1F (PP2C domain containing)
-0.90	0.0018	NM_012629	Prl	prolactin
-0.90	0.0411	A_44_P340418		
-0.89	0.0495	XM_001072511	LOC684923	similar to chromosome 9 open reading frame 79
-0.88	0.0350	AA926044		
-0.88	0.0382	BE113640		
-0.88	0.0087	AA850212		
-0.88	0.0430	XM_225068	Irx4_predicted	Iroquois related homeobox 4 (Drosophila) (predicted)
-0.88	0.0221	AJ224441		
-0.87	0.0101	A_44_P889765		
-0.87	0.0247	CB547880		
-0.86	0.0128	BI293639		
-0.86	0.0077	NM_138898	Phlpb	phospholipase B
-0.85	0.0177	AA925378		
-0.85	0.0477	BF409820		
-0.85	0.0182	AW530584		
-0.83	0.0433	NM_147139		
-0.83	0.0361	TC548367		
-0.83	0.0018	TC548927		
-0.83	0.0165	NM_012741	LOC25087	K-kininogen
-0.83	0.0421	AI406624		
-0.83	0.0197	NM_001014058	Usp18	ubiquitin specific peptidase 18
-0.82	0.0125	XM_232952		
-0.82	0.0241	AI072433		
-0.82	0.0279	NM_198727	LOC288750	hypothetical protein
-0.82	0.0058	TC537158		
-0.81	0.0438	AA819842		
-0.81	0.0350	XM_345868	Hdac7a	histone deacetylase 7A
-0.81	0.0050	AY325249		
-0.80	0.0016	CB547640		
-0.80	0.0272	XM_232342	Cd163_predicted	CD163 antigen (predicted)
-0.80	0.0088	TC543535		
-0.79	0.0109	XM_001079735	LOC687705	similar to misshapen-like kinase 1 isoform 1

-0.78	0.0312	AA924420		
-0.78	0.0058	AI175421		
-0.77	0.0468	XM_343922	Polr2a_mapped	polymerase (RNA) II (DNA directed) polypeptide A (mapped)
-0.77	0.0247	XM_222215	RGD1565800_predicted	similar to hypothetical protein FLJ20674 (predicted)
-0.77	0.0163	BE108142		
-0.76	0.0109	XM_341912	Xylt1	xylosyltransferase 1
-0.76	0.0348	XM_573321	LOC498113	similar to This CDS feature is included to show the translation of the corresponding V_region. Presently translation qualifiers on V_region features are illegal
-0.76	0.0184	NM_001024782	Lrrc8	leucine-rich repeat-containing 8
-0.76	0.0452	TC544952		
-0.75	0.0399	NM_053398	Gfra3	glial cell line derived neurotrophic factor family receptor alpha 3
-0.75	0.0113	CB547650		
-0.75	0.0173	XM_214313	Fcho1_predicted	FCH domain only 1 (predicted)
-0.75	0.0207	NM_001003401	Enc1	ectodermal-neural cortex 1
-0.74	0.0283	BF563208		
-0.74	0.0448	BF285026		
-0.74	0.0316	NM_031610	Kcnj3	potassium inwardly-rectifying channel, subfamily J, member 3
-0.73	0.0472	BQ207264		
-0.73	0.0242	NM_021669	Ghrl	ghrelin precursor
-0.72	0.0362	A_44_P598999		
-0.72	0.0432	CF109839		
-0.72	0.0351	A_44_P255625		
-0.72	0.0031	A_44_P984772		
-0.71	0.0192	BC089106		
-0.71	0.0045	NM_001039085	Cox6b2	cytochrome c oxidase subunit VIb testes-specific isoform precursor
-0.71	0.0495	NM_031697	St3gal3	ST3 beta-galactoside alpha-2,3-sialyltransferase 3
-0.71	0.0316	AA849518		
-0.71	0.0327	BF408914		
-0.70	0.0242	NM_001001368	Olr943_predicted	olfactory receptor 943 (predicted)
-0.70	0.0035	AI012782		
-0.70	0.0218	XM_345112		
-0.70	0.0231	NM_138536	Ttl	tubulin tyrosine ligase
-0.70	0.0170	NM_001003929	Cntfr	ciliary neurotrophic factor receptor
-0.70	0.0269	NM_001030034	Rhbdf1	rhomboid family 1 (Drosophila)
-0.69	0.0361	XM_220699	Rutbc1_predicted	RUN and TBC1 domain containing 1 (predicted)
-0.69	0.0178	BF417211		
-0.68	0.0389	XM_220330	RGD1309452_predicted	similar to RIKEN cDNA 9530066K23 (predicted)
-0.67	0.0389	XM_230039	Dusp19_predicted	dual specificity phosphatase 19 (predicted)
-0.67	0.0407	BE106909		
-0.67	0.0126	NM_198727	LOC288750	hypothetical protein
-0.67	0.0368	ENSRNOT00000020530		

-0.67	0.0010	XM_216563	Eif4g3_predicted	eukaryotic translation initiation factor 4 gamma, 3 (predicted)
-0.67	0.0388	XM_232283	Plxnd1_predicted	plexin D1 (predicted)
-0.67	0.0009	BE102282		
-0.66	0.0415	NM_001001518	Sucnr1	succinate receptor 1
-0.66	0.0477	NM_053599	Efna1	ephrin A1
-0.66	0.0449	TC541702		
-0.65	0.0167	BI295759		
-0.65	0.0481	TC565418		
-0.65	0.0191	NM_017094	Ghr	growth hormone receptor
-0.65	0.0462	CA505868		
-0.65	0.0210	XM_220629	Pitpnm3_predicted	PITPNM family member 3 (predicted)
-0.65	0.0223	AI012480		
-0.64	0.0352	AA818997		
-0.64	0.0491	NM_001010964	Klrb1a_mapped	killer cell lectin-like receptor subfamily B, member 1A (mapped)
-0.63	0.0490	TC548986		
-0.63	0.0487	BI290548		
-0.63	0.0131	NM_001009357	Rqcd1	rcd1 (required for cell differentiation) homolog 1 (S. pombe)
-0.63	0.0185	AA801136		
-0.63	0.0422	NM_022944	Inppl1	inositol polyphosphate phosphatase-like 1
-0.63	0.0324	A_44_P168942		
-0.62	0.0472	XM_237839	Mfi2_predicted	antigen p97 (melanoma associated) identified by monoclonal antibodies 133.2 and 96.5 (predicted)
-0.62	0.0469	AABR03116794		
-0.62	0.0151	TC566831		
-0.62	0.0494	ENSRNOT00000020846		
-0.62	0.0267	XM_235115	RGD1306259_predicted	similar to neuron navigator 3; pore membrane and/or filament interacting like protein 1; steerin 3 (predicted)
-0.62	0.0257	AI176773		
-0.62	0.0291	AI408734		
-0.61	0.0176	A_44_P130936		
-0.61	0.0346	NM_012965	Hrh2	histamine receptor H 2
-0.61	0.0260	AA891571		
-0.61	0.0481	A_44_P405733		
-0.61	0.0460	BE115992		
-0.60	0.0156	A_44_P815267		
-0.60	0.0054	AY387092		
-0.60	0.0363	AI180288		
-0.60	0.0005	XM_341856	Ppfia3	protein tyrosine phosphatase, receptor type, f polypeptide (PTPRF), interacting protein (liprin), alpha 3
-0.60	0.0159	NM_001012062	Map3k7ip2	mitogen-activated protein kinase kinase kinase 7 interacting protein 2
-0.59	0.0093	XM_341901	LOC361623	similar to transcriptional intermediary factor 1 delta
-0.59	0.0288	AY325158		
-0.59	0.0213	XM_236321	Fem1b_predicte	feminization 1 homolog b (C. elegans)

			d	(predicted)
-0.58	0.0061	XM_243040	Clstn1	calsyntenin 1
-0.58	0.0410	AA925246		
-0.58	0.0456	XM_001079501	LOC687643	similar to 60S ribosomal protein L13 (A52)
-0.58	0.0040	TC562460		
-0.58	0.0368	AA800318		
-0.58	0.0140	AI008687		
-0.57	0.0230	NM_001030042	Rad9b	RAD9 homolog B (S. cerevisiae)
-0.57	0.0438	NM_053788	Stx1a	syntaxin 1A (brain)
-0.56	0.0255	NM_032613	Lasp1	LIM and SH3 protein 1
-0.55	0.0457	XM_343168	RGD1307067_predicted	LOC362840 (predicted)
-0.55	0.0359	TC532979		
-0.55	0.0112	NM_001014089	Lrrc35	leucine rich repeat containing 35
-0.55	0.0292	XM_217026	Irak4_predicted	interleukin-1 receptor-associated kinase 4 (predicted)
-0.54	0.0172	U42423	Kcnj3	potassium inwardly-rectifying channel, subfamily J, member 3
-0.54	0.0143	AI029408		
-0.54	0.0043	XM_234543	RGD1307503_predicted	similar to Hypothetical protein KIAA0297/KIAA0329 (predicted)
-0.54	0.0470	TC525304		
-0.54	0.0042	AI233717		
-0.54	0.0342	XM_214968	Mtap7_predicted	microtubule-associated protein 7 (predicted)
-0.54	0.0495	XM_235049	Pctk2	PCTAIRE-motif protein kinase 2
-0.54	0.0367	AI179957		
-0.54	0.0489	XM_343492	LOC363153	similar to cyclic AMP-regulated phosphoprotein, 21 isoform 2
-0.53	0.0262	XM_221216	Cd7_predicted	CD7 antigen (predicted)
-0.53	0.0427	ENSRNOT00000034929		
-0.53	0.0122	AI411183		
-0.53	0.0046	XM_343483	Dag1	dystroglycan 1
-0.53	0.0371	NM_022853	Slc30a1	solute carrier family 30 (zinc transporter), member 1
-0.53	0.0456	BF549324		
-0.53	0.0120	XM_001055528	LOC679267	hypothetical protein LOC679267
-0.53	0.0151	NM_053535	Enpp1	ectonucleotide pyrophosphatase/phosphodiesterase 1
-0.53	0.0393	XM_574352	RGD1566222_predicted	similar to HSU79303 protein (predicted)
-0.53	0.0390	CO406134		
-0.52	0.0198	XM_226561	Pgbd5_predicted	piggyBac transposable element derived 5 (predicted)
-0.52	0.0186	A_44_P621328		
-0.52	0.0138	XM_233829	RGD1560519_predicted	similar to thyroid adenoma associated (predicted)
-0.52	0.0105	NM_019621	Dlgh4	discs, large homolog 4 (Drosophila)
-0.52	0.0374	XM_221189	LOC287867	similar to myosin, heavy polypeptide 9, non-muscle
-0.52	0.0270	NM_001033691	Irf7	interferon regulatory factor 7
-0.52	0.0213	XM_001055574	LOC680076	similar to ankyrin repeat and SOCS box-containing protein 14
-0.51	0.0385	TC551983		

-0.51	0.0374	NM_001000604	Olr784_predicted	olfactory receptor 784 (predicted)
-0.51	0.0138	NM_001012345	Dgat2	diacylglycerol O-acyltransferase homolog 2 (mouse)
-0.51	0.0279	XR_007436	LOC302833	similar to CG2691-PA
-0.51	0.0280	XM_226431	RGD1310170_predicted	similar to beta-1,3-galactosyltransferase-related protein (predicted)
-0.51	0.0372	XM_219785	Gldc_predicted	glycine decarboxylase (predicted)
-0.50	0.0063	NM_177931	Orc1l	origin recognition complex, subunit 1-like (S.cereviaiae)
-0.50	0.0147	A_44_P370411		
-0.50	0.0390	A_44_P985259		
-0.50	0.0295	AI104089		
-0.50	0.0484	XM_217409	Bmpr2	bone morphogenic protein receptor, type II (serine/threonine kinase)
-0.50	0.0234	AA946181		
-0.50	0.0283	XM_225138	Dapk1_predicted	death associated protein kinase 1 (predicted)
-0.49	0.0314	XM_001080050	LOC365985	similar to adenylate kinase 5 isoform 1
-0.49	0.0238	XM_220163		
-0.49	0.0342	AW914780		
-0.49	0.0136	AW532611		
-0.49	0.0036	NM_001033706	LOC361571	similar to RIKEN cDNA 2410004H02
-0.49	0.0329	AI101330		
-0.49	0.0131	XM_001053570	LOC679578	similar to Protein C18orf1
-0.49	0.0258	AI232943		
-0.48	0.0081	AA817769		
-0.48	0.0095	BM392264		
-0.48	0.0064	XM_224841	Odz3_predicted	odd Oz/ten-m homolog 3 (Drosophila) (predicted)
-0.48	0.0188	XM_219341		
-0.48	0.0305	BQ211663		
-0.48	0.0212	NM_031070	Nell2	nel-like 2 homolog (chicken)
-0.47	0.0145	AI011604		
-0.47	0.0381	NM_023991	Prkaa2	protein kinase, AMP-activated, alpha 2 catalytic subunit
-0.47	0.0297	TC565055		
-0.47	0.0136	CK598443		
-0.47	0.0490	XM_222179		
-0.47	0.0223	XM_001070874	Dusp7	dual specificity phosphatase 7
-0.47	0.0417	NM_053535	Enpp1	ectonucleotide pyrophosphatase/phosphodiesterase 1
-0.47	0.0205	XM_001079870	LOC687711	similar to small nuclear ribonucleoprotein D3
-0.47	0.0255	XM_213769	Vps37b_predicted	vacuolar protein sorting 37B (yeast) (predicted)
-0.47	0.0252	XM_230784	RGD1562262_predicted	similar to centrosomal Nek2-associated protein 1 (predicted)
-0.46	0.0413	NM_023991	Prkaa2	protein kinase, AMP-activated, alpha 2 catalytic subunit
-0.46	0.0451	NM_053788	Stx1a	syntaxin 1A (brain)
-0.46	0.0414	XM_001054112	RGD1561985_predicted	similar to dystrobrevin alpha isoform 1 (predicted)
-0.46	0.0124	XM_226089		

-0.46	0.0287	CO562195		
-0.46	0.0341	AI171999		
-0.46	0.0443	XM_001064905	RGD1560736_predicted	similar to solute carrier family 9 (sodium/hydrogen exchanger), isoform 9 (predicted)
-0.46	0.0451	NM_001000178	Olr176_predicted	olfactory receptor 176 (predicted)
-0.45	0.0284	NM_019621	Dlgh4	discs, large homolog 4 (Drosophila)
-0.45	0.0255	NM_001014217	LOC363251	similar to 1700029B21Rik protein
-0.45	0.0059	XM_228778		
-0.45	0.0339	AW920552		
-0.45	0.0136	NM_198749	Rab15	RAB15, member RAS onocogene family
-0.45	0.0129	NM_012546	Drd1a	dopamine receptor D1A
-0.45	0.0324	ENSRNOT00000046703		
-0.45	0.0173	NM_001013121	Snapc2	small nuclear RNA activating complex, polypeptide 2
-0.45	0.0133	XM_221964	RGD1311314	similar to RIKEN cDNA 6530401C20
-0.45	0.0086	XM_340870	RGD1305547_predicted	similar to RIKEN cDNA 2810417D08 (predicted)
-0.45	0.0330	AI233855		
-0.44	0.0134	BM986218		
-0.44	0.0229	XM_228196	Ptk9l_predicted	protein tyrosine kinase 9-like (A6-related protein) (predicted)
-0.44	0.0078	AW918520		
-0.44	0.0283	NM_023991	Prkaa2	protein kinase, AMP-activated, alpha 2 catalytic subunit
-0.44	0.0350	BF410589		
-0.44	0.0486	NM_080691	Cacng3	calcium channel, voltage-dependent, gamma subunit 3
-0.44	0.0330	TC541972		
-0.44	0.0435	AW914778		
-0.44	0.0385	XM_575106	LOC499768	similar to TBC1 domain family, member 13
-0.44	0.0245	NM_175762	Ldlr	low density lipoprotein receptor
-0.44	0.0378	NM_023991	Prkaa2	protein kinase, AMP-activated, alpha 2 catalytic subunit
-0.43	0.0334	NM_080585	Napa	N-ethylmaleimide sensitive fusion protein attachment protein alpha
-0.43	0.0137	XM_001070611	Celsr2	cadherin EGF LAG seven-pass G-type receptor 2
-0.43	0.0485	NM_019621	Dlgh4	discs, large homolog 4 (Drosophila)
-0.43	0.0433	NM_031027	Dpyd	dihydropyrimidine dehydrogenase
-0.43	0.0499	NM_001000566	Olr542_predicted	olfactory receptor 542 (predicted)
-0.43	0.0153	XM_243980	RGD1561652_predicted	similar to oxysterol-binding protein-like protein 10 (predicted)
-0.43	0.0129	AY234417		
-0.43	0.0080	M15402		
-0.43	0.0150	NM_001014093	Parp16	poly (ADP-ribose) polymerase family, member 16
-0.43	0.0388	XM_001069774	LOC684297	similar to PHD finger protein 8
-0.43	0.0211	NM_053535	Enpp1	ectonucleotide pyrophosphatase/phosphodiesterase 1
-0.43	0.0020	ENSRNOT00000030885		

-0.43	0.0284	XM_225214	Diras2_predicted	DIRAS family, GTP-binding RAS-like 2 (predicted)
-0.43	0.0402	NM_001024331	Rab43	Ras-related protein RAB43
-0.42	0.0290	NM_001007656	Mapre3	microtubule-associated protein, RP/EB family, member 3
-0.42	0.0267	BI286685		
-0.42	0.0130	NM_017093	Akt2	thymoma viral proto-oncogene 2
-0.42	0.0272	NM_023991	Prkaa2	protein kinase, AMP-activated, alpha 2 catalytic subunit
-0.42	0.0271	A_44_P536567		
-0.42	0.0453	NM_001003711	Jph4	junctophilin 4
-0.42	0.0279	XM_001070712	LOC689414	similar to alternative testis transcripts open reading frame A CG4241-PA, isoform A
-0.42	0.0369	NM_134351	Mat2a	methionine adenosyltransferase II, alpha
-0.42	0.0286	XM_001058968	LOC680806	similar to Transcription initiation factor TFIID 105 kDa subunit (TAFII-105) (TAFII105)
-0.42	0.0030	CF111640		
-0.42	0.0469	NM_172022	Prosapip1	ProSAPiP1 protein
-0.42	0.0286	XM_001072657	Efna3	ephrin A3
-0.42	0.0467	AA955473		
-0.42	0.0450	XM_227627	RGD1309567_predicted	similar to hypothetical protein FLJ20300 (predicted)
-0.41	0.0247	XM_342700	Herc6	potential ubiquitin ligase
-0.41	0.0115	XM_347344	LOC368190	similar to Williams-Beuren syndrome critical region 18
-0.41	0.0078	XM_234904	Shc2_predicted	src homology 2 domain-containing transforming protein C2 (predicted)
-0.41	0.0391	NM_001009667	RGD1308031	similar to RIKEN cDNA 2510048L02
-0.41	0.0193	BF565121		
-0.41	0.0192	XM_219703	RGD1563721_predicted	similar to Cezanne 2 protein (predicted)
-0.41	0.0416	XM_230722	Tcf15_predicted	transcription factor 15 (predicted)
-0.41	0.0495	TC558413		
-0.41	0.0116	XM_575540		
-0.41	0.0224	XM_238302	RGD1562883_predicted	similar to livin inhibitor of apoptosis isoform beta (predicted)
-0.41	0.0418	NM_173101	Myo1e	myosin IE
-0.41	0.0376	XM_236747	Cdcp1_predicted	CUB domain containing protein 1 (predicted)
-0.41	0.0497	NM_017222	Slc10a2	solute carrier family 10, member 2
-0.41	0.0321	TC560423		
-0.41	0.0055	A_44_P354420		
-0.40	0.0326	AY325217		
-0.40	0.0173	AI013472		
-0.40	0.0266	XM_574558	RGD1562278_predicted	similar to KTSR5831 (predicted)
-0.40	0.0174	NM_053535	Enpp1	ectonucleotide pyrophosphatase/phosphodiesterase 1
-0.40	0.0072	TC543636		
-0.40	0.0191	NM_053984	Gjb4	gap junction membrane channel protein beta 4
-0.40	0.0158	XM_217432	Arpc2_predicted	actin related protein 2/3 complex, subunit 2 (predicted)

-0.40	0.0055	AW143308		
-0.40	0.0280	BF390070		
-0.40	0.0261	NM_017025	Ldha	lactate dehydrogenase A
-0.40	0.0208	NM_130829	Palm	paralemmin
2.42	0.0100	XM_218843	RGD1562653_predicted	similar to hypothetical protein D030069K18 (predicted)
2.22	0.0031	XM_001055017	LOC501126	similar to hypothetical protein MGC26733
1.85	0.0158	XM_235839		
1.84	0.0001	XM_234720	Dnah11	dynein, axonemal, heavy polypeptide 11
1.79	0.0334	NM_012630	Prlr	prolactin receptor
1.78	0.0325	TC562412		
1.78	0.0104	TC523276		
1.76	0.0223	XM_214760	RGD1310945_predicted	similar to hypothetical protein FLJ23305 (predicted)
1.59	0.0071	XM_218574	RGD1308141_predicted	similar to BC013491 protein (predicted)
1.57	0.0083	AI599504		
1.56	0.0429	NM_057184	Chrna6	cholinergic receptor, nicotinic, alpha polypeptide 6
1.48	0.0124	XM_343290	Dmc1h_predicted	disrupted meiotic cDNA 1 homolog (yeast) (predicted)
1.47	0.0321	AA817758		
1.46	0.0056	AA925518		
1.41	0.0095	AI178246		
1.41	0.0182	NM_001012176	Tsga2	testis specific gene A2
1.36	0.0255	NM_001004263	Itgb6	integrin, beta 6
1.35	0.0118	AI111365		
1.35	0.0183	XM_576582	RGD1565062_predicted	similar to PF20 (predicted)
1.33	0.0140	NM_012630	Prlr	prolactin receptor
1.32	0.0102	XM_236597	RGD1564871_predicted	similar to Thioredoxin domain containing protein 6 (Thioredoxin-like protein 2) (predicted)
1.30	0.0057	NM_013085	Plau	plasminogen activator, urokinase
1.28	0.0333	BQ194305		
1.27	0.0001	AI044662		
1.26	0.0117	XM_344019	RGD1559942_predicted	similar to hypothetical protein (predicted)
1.24	0.0091	NM_053526	Cpn1	carboxypeptidase N, polypeptide 1, 50kD
1.22	0.0346	BE107038		
1.22	0.0148	NP516904		
1.19	0.0113	XM_001063975	LOC500700	similar to chromosome 14 open reading frame 145
1.19	0.0448	A_44_P347283		
1.17	0.0003	CB606444		
1.15	0.0418	NM_030865	Myoc	myocilin
1.14	0.0321	XM_345077		
1.11	0.0459	AA998060		
1.11	0.0210	NM_001003977	Gk11	glandular kallikrein 11
1.10	0.0277	XM_344863	Cabp5_predicted	calcium binding protein 5 (predicted)
1.10	0.0358	XM_342904	RGD1560700_predicted	similar to palmitoyl-protein thioesterase (predicted)

1.07	0.0491	XM_001055031	LOC680102	similar to mab-21-like 2
1.07	0.0425	NM_017254	Htr2a	5-hydroxytryptamine (serotonin) receptor 2A
1.06	0.0465	XM_236991	Tdrd6_predicted	tudor domain containing 6 (predicted)
1.05	0.0209	NM_001030043	RGD1311300	similar to T cell receptor V delta 6
1.05	0.0482	NM_017144	Tnni3	troponin I type 3 (cardiac)
1.05	0.0178	AI575619		
1.04	0.0198	NM_001007721	Emp2	epithelial membrane protein 2
1.03	0.0252	XM_236325	Cln6_predicted	ceroid-lipofuscinosis, neuronal 6 (predicted)
1.03	0.0262	XM_237386	RGD1305311_predicted	similar to hypothetical protein FLJ22527 (predicted)
1.03	0.0151	U81826		
1.03	0.0412	BF389308		
1.03	0.0312	A_44_P408197		
1.02	0.0104	BF286372		
1.02	0.0170	XM_343481	RGD1306603_predicted	similar to RIKEN cDNA D330022A01 gene (predicted)
1.01	0.0390	TC525017		
1.01	0.0278	CV795283		
1.01	0.0093	XM_217031	RGD1305928_predicted	hypothetical LOC300207 (predicted)
0.99	0.0139	BF416970		
0.99	0.0290	NM_023962	Pdgfd	platelet-derived growth factor, D polypeptide
0.99	0.0313	AA925922		
0.99	0.0320	AI170067		
0.98	0.0493	AI031036		
0.97	0.0482	ENSRNOT00000002541		
0.97	0.0024	BF282074		
0.97	0.0470	NM_023969	Edg7	putative G protein-coupled receptor snGPCR32
0.96	0.0318	NM_173045	Zc3hav1	zinc finger CCCH type, antiviral 1
0.96	0.0158	XM_345792		
0.96	0.0148	BU758972		
0.96	0.0185	XM_220513	Cias1_predicted	cold autoinflammatory syndrome 1 homolog (human) (predicted)
0.96	0.0493	AI007821		
0.95	0.0258	NM_001007692	Nfatc2ip	nuclear factor of activated T-cells, cytoplasmic, calcineurin-dependent 2 interacting protein
0.94	0.0146	XM_001057993	LOC680611	similar to B-cell leukemia/lymphoma 3
0.94	0.0126	BF550234		
0.93	0.0270	XM_232620	Mybl1_predicted	myeloblastosis oncogene-like 1 (predicted)
0.93	0.0339	AI413060		
0.93	0.0335	XM_001059031	Hoxa5	homeo box A5
0.92	0.0294	XM_220008	Pik3ap1_predicted	phosphoinositide-3-kinase adaptor protein 1 (predicted)
0.92	0.0375	XM_341392	Bm259	BM259 protein
0.92	0.0305	XM_001065586	RGD1562236_predicted	similar to breast cancer membrane protein 101 (predicted)
0.92	0.0178	A_44_P858612		
0.92	0.0430	A_44_P368416		
0.91	0.0412	XM_234755		
0.91	0.0260	NM_001033688	Dsc2	desmocollin 2

0.91	0.0164	XM_219738	RGD1565442_predicted	similar to X-linked lymphocyte regulated gene 4 (predicted)
0.91	0.0060	NM_001015034	Tnfrsf14	tumor necrosis factor receptor superfamily, member 14 (herpesvirus entry mediator)
0.91	0.0498	XM_001073797	Tll1_predicted	tolloid-like 1 (predicted)
0.90	0.0361	NM_001008823	Ka39	type I keratin KA39
0.90	0.0495	NR_002149	E030032D13Rik	E030032D13Rik gene
0.90	0.0478	XM_577934	RGD1563918_predicted	similar to putative homeobox protein (predicted)
0.90	0.0148	BQ209930		
0.90	0.0337	NM_053408	Chst3	carbohydrate (chondroitin 6/keratan) sulfotransferase 3
0.89	0.0216	NM_001014158	LOC361487	similar to KRAB-containing zinc-finger protein KRAZ1
0.88	0.0425	AW915462		
0.88	0.0274	NM_013136	Mak	male germ cell-associated kinase
0.87	0.0139	AA819090		
0.87	0.0388	BE115639		
0.87	0.0168	XM_001063356	RGD1311381_predicted	similar to hypothetical protein FLJ20037 (predicted)
0.87	0.0372	AA924018		
0.87	0.0058	XM_001075395	RGD1564575_predicted	RGD1564575 (predicted)
0.86	0.0093	BF403009		
0.86	0.0416	AA997400		
0.85	0.0123	TC525592		
0.85	0.0121	CA507495	S100a8	S100 calcium binding protein A8 (calgranulin A)
0.85	0.0458	AI171652		
0.85	0.0071	XM_222983	RGD1561133_predicted	similar to putative pheromone receptor (Go-VN2) (predicted)
0.84	0.0149	XM_215934	Wfdc5_predicted	WAP four-disulfide core domain 5 (predicted)
0.84	0.0366	XM_001053211	LOC678739	similar to phosphorylase kinase alpha 2
0.83	0.0151	AI228628		
0.82	0.0149	AI029401		
0.82	0.0461	AI070915		
0.82	0.0395	CB547054		
0.81	0.0387	XM_236331	RGD1310670_predicted	similar to hypothetical protein FLJ12476 (predicted)
0.80	0.0366	XM_215558	RGD1307595_predicted	similar to RIKEN cDNA 1700018B24 (predicted)
0.80	0.0405	XM_223116		
0.80	0.0248	AI145286		
0.79	0.0116	BF289433		
0.79	0.0251	AA956634		
0.79	0.0489	BF548111		
0.78	0.0324	XM_216310	Casc1_predicted	cancer susceptibility candidate 1 (predicted)
0.78	0.0373	NM_033485	Pawr	PRKC, apoptosis, WT1, regulator
0.78	0.0467	AA900966		
0.78	0.0072	NM_181376	Spats1	spermatogenesis associated, serine-rich 1
0.77	0.0080	XM_225779		

0.77	0.0241	NM_001009271	Nt5dc2	5'-nucleotidase domain containing 2
0.77	0.0131	CB547106		
0.76	0.0380	NM_001000090	Olr1626_predicted	olfactory receptor 1626 (predicted)
0.75	0.0098	NM_012528	Chrnb1	cholinergic receptor, nicotinic, beta polypeptide 1 (muscle)
0.75	0.0382	NM_133291	Sval2	seminal vesicle antigen-like 2
0.75	0.0215	BF283053		
0.74	0.0301	NM_001013965	Tekt4	tektin 4
0.74	0.0212	BF542793		
0.73	0.0444	NM_001000995	Olr1590_predicted	olfactory receptor 1590 (predicted)
0.73	0.0125	XM_576393	RGD1565120_predicted	similar to brain-specific homeodomain protein (predicted)
0.71	0.0221	CF108537		
0.70	0.0462	A_44_P245767		
0.70	0.0277	BU759617		
0.70	0.0129	XM_226231	RGD1563840_predicted	similar to 60S ribosomal protein L26 (predicted)
0.69	0.0393	XM_001076148	LOC687361	hypothetical protein LOC687361
0.69	0.0193	NM_030985	Agtr1a	angiotensin II receptor, type 1 (AT1A)
0.68	0.0291	XM_575663	LOC500312	similar to putative pheromone receptor V2R1b
0.67	0.0038	A_44_P380365		
0.67	0.0195	AA893180		
0.67	0.0379	NM_022221	Mmp8	matrix metallopeptidase 8
0.67	0.0334	AA899922		
0.66	0.0246	XM_230593	RGD1561442_predicted	similar to Vinculin (Metavinculin) (predicted)
0.66	0.0335	A_44_P450259		
0.65	0.0044	XM_001077632	LOC687232	similar to CG12393-PA, isoform A
0.65	0.0147	AA819337		
0.64	0.0391	XM_346983		
0.64	0.0460	XM_574231	RGD1565341_predicted	similar to translin-associated factor X (Tsnax) interacting protein 1 (predicted)
0.63	0.0155	AA944251		
0.63	0.0329	XM_229173		
0.62	0.0361	AA963008		
0.62	0.0214	XM_001081628	Sox9	SRY-box containing gene 9
0.62	0.0006	BQ209483		
0.62	0.0336	XM_345798		
0.62	0.0422	AY142709	Kcnip1	Kv channel-interacting protein 1
0.62	0.0478	AI555498		
0.61	0.0278	NM_001039337	Fubp3	far upstream element (FUSE) binding protein 3
0.61	0.0296	AI010195		
0.61	0.0193	BF560819		
0.59	0.0376	AI112329		
0.57	0.0180	XM_222564	LOC288979	similar to Cerebellin-2 precursor (Cerebellin-like protein)
0.57	0.0332	AA923854		
0.57	0.0083	AI229269		

0.57	0.0152	TC524716		
0.56	0.0121	XM_001081628	Sox9	SRY-box containing gene 9
0.56	0.0272	AW143519		
0.56	0.0116	AI059089		
0.56	0.0272	XM_227622	Sdfr2_predicted	stromal cell derived factor receptor 2 (predicted)
0.56	0.0049	AA924721		
0.56	0.0060	AI170621		
0.56	0.0364	XM_216733	RGD1565716_predicted	similar to RIKEN cDNA 4921529O18 (predicted)
0.55	0.0229	TC555070		
0.55	0.0131	NM_020101	Centa2	centaurin, alpha 2
0.55	0.0486	XR_006043	LOC681331	similar to apoptosis inhibitor 5
0.55	0.0273	XM_341550	Akr1cl1_predicted	aldo-keto reductase family 1, member C-like 1 (predicted)
0.55	0.0432	TC566391		
0.55	0.0465	AI177135		
0.54	0.0010	XM_001068622	RGD1561916_predicted	similar to testes development-related NYD-SP22 isoform 1 (predicted)
0.54	0.0321	AW253256		
0.54	0.0385	AW920939		
0.54	0.0217	XM_001072036	LOC684554	similar to Thrombospondin-3 precursor
0.54	0.0190	XM_001053365	RGD1561975_predicted	similar to TGFB-induced factor 2 (predicted)
0.54	0.0231	TC519685		
0.54	0.0405	NM_001000473	Olr1325_predicted	olfactory receptor 1325 (predicted)
0.54	0.0466	A_44_P791333		
0.53	0.0370	XM_236675	Glb1_mapped	galactosidase, beta 1 (mapped)
0.53	0.0385	NM_001034139	Lrrc8e	leucine rich repeat containing 8 family, member E
0.53	0.0122	XM_225947	Trim36_predicted	tripartite motif protein 36 (predicted)
0.52	0.0183	XM_230509	RGD1566077_predicted	similar to RIKEN cDNA A130038L21 (predicted)
0.51	0.0287	AI233208		
0.51	0.0481	TC546713		
0.51	0.0446	TC519466		
0.51	0.0428	CB742296		
0.51	0.0467	NM_198772	MGC72974	Unknown (protein for MGC:72974)
0.51	0.0137	AI043958		
0.50	0.0103	NM_053619	C5r1	complement component 5, receptor 1
0.50	0.0339	BQ783165		
0.50	0.0320	XM_342281	Muc1	mucin 1, transmembrane
0.50	0.0294	XM_218644	Klk12_predicted	kallikrein 12 (predicted)
0.49	0.0097	NM_001024800	Txndc1	thioredoxin domain containing 1
0.49	0.0472	XM_001063356	RGD1311381_predicted	similar to hypothetical protein FLJ20037 (predicted)
0.49	0.0444	AI406369		
0.48	0.0444	AA924847		
0.48	0.0280	XM_345338		
0.48	0.0482	TC519225		

0.48	0.0287	XM_221343	RGD1305614_predicted	similar to IGF-II mRNA-binding protein 2 (predicted)
0.48	0.0492	XM_216518		
0.48	0.0497	XM_216331	RGD1305828_predicted	similar to hypothetical protein (predicted)
0.48	0.0166	BM391896		
0.47	0.0020	NM_013091	Tnfrsf1a	tumor necrosis factor receptor superfamily, member 1a
0.47	0.0260	NM_001014051	LOC311548	similar to RIKEN cDNA 4930509O20
0.47	0.0220	NM_001001016	Olr1174_predicted	olfactory receptor 1174 (predicted)
0.47	0.0391	XM_232320	RGD1562038_predicted	similar to putative voltage-gated calcium channel alpha(2)delta-4 subunit (predicted)
0.47	0.0045	NM_001011997	Tmod3	tropomodulin 3
0.47	0.0443	AA925130		
0.46	0.0271	NM_023981	Csf1	colony stimulating factor 1 (macrophage)
0.46	0.0256	CF111186		
0.46	0.0106	TC542803		
0.46	0.0377	NM_001013944	RGD1309051	similar to chromosome 14 open reading frame 50
0.46	0.0371	NM_019273	Kcnmb1	potassium large conductance calcium-activated channel, subfamily M, beta member 1
0.46	0.0426	XM_001077512	RGD1565716_predicted	similar to RIKEN cDNA 4921529O18 (predicted)
0.46	0.0070	XM_001058665	LOC681839	hypothetical protein LOC681839
0.45	0.0405	NM_207601	Plp2_mapped	proteolipid protein 2 (mapped)
0.45	0.0286	AY064511	Ua20	putative UA20 protein
0.45	0.0487	XM_223527	Sh3tc1_predicted	SH3 domain and tetratricopeptide repeats 1 (predicted)
0.45	0.0248	XM_343728		
0.45	0.0068	NM_172223	Pxmp4	peroxisomal membrane protein 4
0.45	0.0136	NM_138848	Podxl	podocalyxin-like
0.45	0.0407	NM_012620	Serpine1	serine (or cysteine) peptidase inhibitor, clade E, member 1
0.44	0.0085	TC556623		
0.44	0.0373	NM_214828	Olr1378_predicted	olfactory receptor 1378 (predicted)
0.44	0.0149	XM_227540	Rsbn1_predicted	rosbin, round spermatid basic protein 1 (predicted)
0.44	0.0496	NM_001025039	LOC499602	hypothetical protein LOC499602
0.44	0.0314	XM_213813	Lrrc43	leucine rich repeat containing 43
0.44	0.0147	XM_217218	RGD1311381_predicted	similar to hypothetical protein FLJ20037 (predicted)
0.43	0.0178	XM_346182		
0.43	0.0350	NM_012824	Apoc1	apolipoprotein C-I
0.43	0.0210	TC523657		
0.43	0.0426	NM_130741	Lcn2	lipocalin 2
0.42	0.0004	XM_001081958	Fyttd1	forty-two-three domain containing 1
0.42	0.0316	AW525988		
0.42	0.0188	AI169706		
0.42	0.0234	NM_001009650	Taar5	trace amine associated receptor 5
0.42	0.0241	AI030156		

0.41	0.0330	NM_053399	Nrtn	neurturin
0.41	0.0057	XM_236938	RGD1310693_predicted	similar to RIKEN cDNA 1700027N10 (predicted)
0.41	0.0089	XM_001065902	Syncrip	synaptotagmin binding, cytoplasmic RNA interacting protein
0.41	0.0304	AW916350		
0.41	0.0113	NM_012735	Hk2	hexokinase 2
0.41	0.0347	XM_222564	LOC288979	similar to Cerebellin-2 precursor (Cerebellin-like protein)
0.41	0.0499	XM_576074	RGD1560978_predicted	similar to hypothetical protein (predicted)
0.40	0.0419	XM_343348		
0.40	0.0449	BF407782		
0.40	0.0345	NM_017064	Stat5a	signal transducer and activator of transcription 5A
0.40	0.0307	NM_183326	Gabra1	gamma-aminobutyric acid A receptor, alpha 1
0.40	0.0460	NM_031003	Abat	4-aminobutyrate aminotransferase
0.40	0.0270	NM_001012235	Impact	imprinted and ancient
0.40	0.0110	TC523460		
0.40	0.0305	XM_214962	Tm2d3_predicted	TM2 domain containing 3 (predicted)
0.40	0.0148	XM_343652		
0.40	0.0261	XM_342959	RGD1310427_predicted	similar to KIAA0090 protein (predicted)
0.40	0.0182	XM_001079851	LOC691849	hypothetical protein LOC691849

APPENDIX C
LIST OF MODULATED GENES FOLLOWING REPEATED ITTO

Table C-1. List of modulated genes following repeated ITTO, $p < 0.05$ and $\log_2$ fold change ≥ 0.58

Log_2 FC	p-value	TargetID	Symbol	Description
-2.830	0.019	NM_012881	Spp1	secreted phosphoprotein 1
-2.787	0.022	NM_012881	Spp1	secreted phosphoprotein 1
-2.722	0.019	NM_012881	Spp1	secreted phosphoprotein 1
-2.719	0.024	NM_012881	Spp1	secreted phosphoprotein 1
-2.698	0.020	NM_012881	Spp1	secreted phosphoprotein 1
-2.676	0.027	NM_012881	Spp1	secreted phosphoprotein 1
-2.665	0.023	NM_012881	Spp1	secreted phosphoprotein 1
-2.617	0.026	NM_012881	Spp1	secreted phosphoprotein 1
-2.601	0.020	NM_012881	Spp1	secreted phosphoprotein 1
-2.601	0.027	NM_012881	Spp1	secreted phosphoprotein 1
-2.138	0.004	NM_017007	Gad1	glutamic acid decarboxylase 1
-2.126	0.001	ENSRNOT00000012564	RGD1564797_predicted	similar to empty spiracles-like protein 2 (predicted)
-2.062	0.009	NM_031782	Slc32a1	solute carrier family 32 (GABA vesicular transporter), member 1
-1.741	0.038	NM_181370	Hs3st2	heparan sulfate (glucosamine) 3-O-sulfotransferase 2
-1.669	0.002	TC617840	-	-
-1.614	0.026	NM_012563	Gad2	glutamic acid decarboxylase 2
-1.525	0.012	NM_017007	Gad1	glutamic acid decarboxylase 1
-1.463	0.002	NM_001014183	RGD1306991	similar to Protein C20orf103 precursor
-1.401	0.011	NM_013007	Pnoc	prepronociceptin
-1.398	0.003	NM_017122	Hpca	hippocalcin
-1.382	0.004	NM_139183	Crhbp	corticotropin releasing hormone binding protein
-1.342	0.016	CB327622	-	-
-1.305	0.010	NM_001037351	Tnnc2	troponin C type 2 (fast)
-1.294	0.025	NM_001008880	Scn4b	sodium channel, voltage-gated, type IV, beta
-1.232	0.037	ENSRNOT00000001048	Man1a_predicted	mannosidase 1, alpha (predicted)
-1.184	0.006	NM_001047973	LOC503325	hypothetical protein LOC503325
-1.132	0.000	DY471163	-	-
-1.120	0.006	TC603004	-	-
-1.109	0.025	NM_017007	Gad1	glutamic acid decarboxylase 1
-1.077	0.018	TC626556	-	-
-1.074	0.011	NM_012798	Mal	myelin and lymphocyte protein, T-cell differentiation protein
-1.074	0.013	NM_057196	Baiap2	brain-specific angiogenesis inhibitor 1-associated protein 2
-1.066	0.008	NM_032071	Synj2	synaptojanin 2
-1.052	0.004	NM_001077201	Caln1_predicted	calneuron 1 (predicted)
-1.048	0.005	NM_031736	Slc27a2	solute carrier family 27 (fatty acid transporter),

				member 2
-1.043	0.002	TC645081	-	-
-1.038	0.021	TC633482	Pde6h	phosphodiesterase 6H, cGMP-specific, cone, gamma
-1.031	0.017	NM_001033656	Man1a_predicted	mannosidase 1, alpha (predicted)
-1.010	0.000	NM_001037206	Bphl	biphenyl hydrolase-like (serine hydrolase, breast epithelial mucin-associated antigen)
-0.985	0.008	TC603491	-	-
-0.980	0.038	NM_053976	Krt1-18	keratin complex 1, acidic, gene 18
-0.976	0.019	XM_578417	RGD1562829_predicted	similar to RAS-like, estrogen-regulated, growth-inhibitor (predicted)
-0.976	0.006	NM_031059	Msx1	homeo box, msh-like 1
-0.970	0.012	DV722143	-	-
-0.964	0.026	BF287496	-	-
-0.956	0.021	ENSRNOT00000031175	Crabp1	cellular retinoic acid binding protein 1
-0.952	0.003	ENSRNOT00000010623	RGD1561357_predicted	similar to LIM domain only 3 (predicted)
-0.952	0.023	TC600004	-	-
-0.943	0.021	NM_012752	Cd24	CD24 antigen
-0.943	0.010	XM_232202	Adamts9_predicted	a disintegrin-like and metalloprotease (reprolysin type) with thrombospondin type 1 motif, 9 (predicted)
-0.939	0.036	NM_031742	Kcnh1	potassium voltage-gated channel, subfamily H (eag-related), member 1
-0.939	0.013	XM_001070642	RGD1564871_predicted	similar to Thioredoxin domain containing protein 6 (Thioredoxin-like protein 2) (predicted)
-0.921	0.000	ENSRNOT00000049507	RGD1560658_predicted	similar to serine (or cysteine) proteinase inhibitor, clade B, member 1b (predicted)
-0.908	0.023	TC631315	-	-
-0.905	0.018	NM_012733	Rbp1	retinol binding protein 1, cellular
-0.905	0.011	ENSRNOT00000016433	RGD1310371	similar to RIKEN cDNA 1700026D08
-0.903	0.004	XM_217250	Ephb1	Eph receptor B1
-0.899	0.000	NM_031834	Sult1a1	sulfotransferase family 1A, phenol-preferring, member 1
-0.897	0.014	XM_213354	Dnah9	dynein, axonemal, heavy polypeptide 9
-0.894	0.018	NM_012825	Aqp4	aquaporin 4
-0.885	0.022	BF567171	LOC689106	hypothetical protein LOC689106
-0.880	0.008	BF556399	-	-
-0.877	0.004	ENSRNOT00000023378	Capsl_predicted	calcyphosine-like (predicted)
-0.865	0.039	ENSRNOT00000010850	Cnr1	cannabinoid receptor 1 (brain)
-0.860	0.007	NM_012825	Aqp4	aquaporin 4
-0.856	0.007	ENSRNOT00000010623	RGD1561357_predicted	similar to LIM domain only 3 (predicted)
-0.856	0.010	NM_001013953	RGD1305351	hypothetical LOC300663
-0.838	0.005	NM_001024882	Ccdc19	coiled-coil domain containing 19
-0.836	0.021	NM_053878	Cplx2	complexin 2
-0.835	0.016	ENSRNOT0	Rshl3_predi	radial spokehead-like 3 (predicted)

		0000036449	cted	
-0.833	0.033	NM_199093	Serping1	serine (or cysteine) peptidase inhibitor, clade G, member 1
-0.831	0.022	NM_001012235	Impact	imprinted and ancient
-0.830	0.021	NM_057196	Baiap2	brain-specific angiogenesis inhibitor 1-associated protein 2
-0.826	0.014	NM_024140	Nrgn	neurogranin
-0.825	0.049	NM_001033656	Man1a_predicted	mannosidase 1, alpha (predicted)
-0.824	0.006	NM_001005765	Rap1a	RAS-related protein 1a
-0.820	0.012	BC092207	LOC365476	similar to chromosome 10 open reading frame 79
-0.811	0.008	TC611803	-	-
-0.806	0.014	NM_031736	Slc27a2	solute carrier family 27 (fatty acid transporter), member 2
-0.804	0.043	NM_017210	Dio3	deiodinase, iodothyronine, type III
-0.800	0.002	ENSRNOT00000016911	Efhb_predicted	EF hand domain family, member B (predicted)
-0.795	0.003	NM_012825	Aqp4	aquaporin 4
-0.793	0.020	XM_001054111	LOC689106	hypothetical protein LOC689106
-0.791	0.030	XM_343481	RGD1306603_predicted	similar to RIKEN cDNA D330022A01 gene (predicted)
-0.789	0.006	NM_031509	Gsta3	glutathione S-transferase A3
-0.783	0.006	ENSRNOT00000038579	RGD1560137_predicted	similar to expressed sequence AU021034 (predicted)
-0.777	0.040	J05276	Htr1a	5-hydroxytryptamine (serotonin) receptor 1A
-0.774	0.035	ENSRNOT00000013483	LOC679875	similar to MAGE-like protein 2 (Protein nS7)
-0.773	0.026	TC598708	-	-
-0.772	0.023	XR_007590	RGD1563002_predicted	similar to hypothetical protein DKFZp434O0527 (predicted)
-0.769	0.007	NM_012825	Aqp4	aquaporin 4
-0.765	0.011	AW915033	Traf3_predicted	Tnf receptor-associated factor 3 (predicted)
-0.764	0.013	ENSRNOT00000012469	Amn_predicted	amnionless (predicted)
-0.755	0.011	XM_573504	RGD1562658_predicted	similar to RIKEN cDNA 1700009P17 (predicted)
-0.754	0.013	NM_145880	Lhx1	LIM homeobox protein 1
-0.754	0.000	NM_001025664	Wsb1	WD repeat and SOCS box-containing 1
-0.749	0.020	ENSRNOT00000024222	Ccdc37_predicted	coiled-coil domain containing 37 (predicted)
-0.749	0.026	BC092207	LOC365476	similar to chromosome 10 open reading frame 79
-0.748	0.006	NM_012825	Aqp4	aquaporin 4
-0.745	0.015	NM_001013953	RGD1305351	hypothetical LOC300663
-0.743	0.028	TC607764	-	-
-0.742	0.038	ENSRNOT00000010850	Cnr1	cannabinoid receptor 1 (brain)
-0.741	0.018	XM_341694	Dynlrb2_predicted	dynein light chain roadblock-type 2 (predicted)

-0.729	0.028	BC107936	-	-
-0.724	0.003	NM_053688	Pde6h	phosphodiesterase 6H, cGMP-specific, cone, gamma
-0.723	0.011	CX569250	-	-
-0.723	0.010	ENSRNOT00000003841	RGD1561932_predicted	similar to novel protein (predicted)
-0.717	0.025	CK366954	LOC691455	similar to calmodulin-like 4
-0.716	0.049	TC584035	-	-
-0.715	0.047	ENSRNOT00000010850	Cnr1	cannabinoid receptor 1 (brain)
-0.713	0.021	XM_341952	RGD1562437_predicted	similar to transcription elongation regulator 1-like (predicted)
-0.705	0.039	TC596255	-	-
-0.701	0.049	ENSRNOT00000010850	Cnr1	cannabinoid receptor 1 (brain)
-0.697	0.029	BF556560	-	-
-0.697	0.006	ENSRNOT00000007789	Nnmt_predicted	nicotinamide N-methyltransferase (predicted)
-0.696	0.001	NM_001012176	Tsga2	testis specific gene A2
-0.694	0.041	ENSRNOT00000016433	RGD1310371	similar to RIKEN cDNA 1700026D08
-0.694	0.042	ENSRNOT00000010850	Cnr1	cannabinoid receptor 1 (brain)
-0.690	0.042	ENSRNOT00000010850	Cnr1	cannabinoid receptor 1 (brain)
-0.690	0.017	ENSRNOT00000036374	RGD1310677_predicted	similar to RIKEN cDNA 4632412N22 gene (predicted)
-0.689	0.011	NM_012825	Aqp4	aquaporin 4
-0.688	0.015	TC634886	-	-
-0.685	0.004	NM_023020	Tmeff1	transmembrane protein with EGF-like and two follistatin-like domains 1
-0.684	0.005	TC607399	Arnt2	aryl hydrocarbon receptor nuclear translocator 2
-0.682	0.003	XM_001080361	LOC691960	similar to solute carrier family 28, member 2
-0.682	0.036	XM_342561	RGD1305725_predicted	similar to chromosome 20 open reading frame 102 (predicted)
-0.681	0.005	ENSRNOT00000008005	Pole4_predicted	polymerase (DNA-directed), epsilon 4 (p12 subunit) (predicted)
-0.680	0.011	ENSRNOT00000027055	RGD1307059_predicted	similar to RIKEN cDNA 1110035L05 (predicted)
-0.680	0.007	NM_001009920	Yc2	glutathione S-transferase Yc2 subunit
-0.679	0.009	NM_012825	Aqp4	aquaporin 4
-0.677	0.038	NM_017258	Btg1	B-cell translocation gene 1, anti-proliferative
-0.676	0.008	NM_138506	Adra2c	adrenergic receptor, alpha 2c
-0.673	0.005	XM_220252	-	-
-0.672	0.023	NM_212541	Slc44a4	solute carrier family 44, member 4
-0.672	0.007	XM_575803	RGD1561916_predicted	similar to testes development-related NYD-SP22 isoform 1 (predicted)
-0.672	0.035	ENSRNOT00000029587	Dpysl4	dihydropyrimidinase-like 4
-0.672	0.045	NM_001000388	Olr417_predicted	olfactory receptor 417 (predicted)

-0.670	0.006	NM_145786	Iiig9	IIIG9 protein
-0.669	0.023	TC617303	-	-
-0.669	0.009	BC092654	Col16a1	procollagen, type XVI, alpha 1
-0.668	0.014	NM_013099	Mc4r	melanocortin 4 receptor
-0.668	0.018	TC599619	-	-
-0.667	0.025	ENSRNOT00000044831	Ttll2_predicted	tubulin tyrosine ligase-like family, member 2 (predicted)
-0.667	0.022	NM_012667	Tacr1	tachykinin receptor 1
-0.666	0.005	NM_001031647	Dnali1	dynein, axonemal, light intermediate polypeptide 1
-0.666	0.004	NM_053018	Cd9	CD9 antigen
-0.664	0.016	NM_001025293	Mbp	myelin basic protein
-0.663	0.006	ENSRNOT00000026491	RGD1305311_predicted	similar to hypothetical protein FLJ22527 (predicted)
-0.663	0.024	TC614187	-	-
-0.661	0.010	ENSRNOT00000035948	RGD1565611_predicted	RGD1565611 (predicted)
-0.660	0.001	NM_053660	Gng10	guanine nucleotide binding protein (G protein), gamma 10
-0.660	0.003	CV102938	-	-
-0.658	0.003	TC624015	-	-
-0.657	0.018	AI113235	-	-
-0.656	0.049	CX571008	Pla2g3_predicted	phospholipase A2, group III (predicted)
-0.656	0.035	BI297059	Ibrdc3_predicted	IBR domain containing 3 (predicted)
-0.655	0.016	NM_031140	Vim	vimentin
-0.655	0.003	ENSRNOT00000020568	Crtac1	cartilage acidic protein 1
-0.654	0.002	TC617271	-	-
-0.653	0.047	A_44_P729134	-	-
-0.652	0.030	XM_343747	LOC363424	similar to spermatogenesis associated glutamate (E)-rich protein 2
-0.652	0.029	TC603496	-	-
-0.651	0.002	ENSRNOT00000033449	Samd7_predicted	sterile alpha motif domain containing 7 (predicted)
-0.651	0.002	NM_001079701	RGD1310641	similar to hypothetical protein
-0.650	0.023	NM_133293	Gata3	GATA binding protein 3
-0.649	0.047	TC633399	-	-
-0.649	0.024	ENSRNOT00000017847	Bm259	BM259 protein
-0.648	0.049	XM_001067026	RGD1566097_predicted	similar to Anillin (predicted)
-0.648	0.046	NM_012667	Tacr1	tachykinin receptor 1
-0.647	0.007	TC593623	-	-
-0.647	0.005	ENSRNOT00000012490	RGD1561171_predicted	similar to RIKEN cDNA 6330407D12 (predicted)
-0.647	0.018	XM_229809	-	-
-0.646	0.005	TC643803	-	-
-0.644	0.013	NM_012825	Aqp4	aquaporin 4

-0.644	0.033	NM_012667	Tacr1	tachykinin receptor 1
-0.644	0.014	ENSRNOT00000047663	LOC689415	similar to Metallothionein-2 (MT-2) (Metallothionein-II) (MT-II)
-0.642	0.041	TC578855	Ptger2	prostaglandin E receptor 2, subtype EP2
-0.641	0.028	NM_021703	Akap14	A kinase (PRKA) anchor protein 14
-0.641	0.023	NM_053330	Rpl21	ribosomal protein L21
-0.640	0.016	NM_022620	Kpl2	KPL2 protein
-0.640	0.016	NM_012825	Aqp4	aquaporin 4
-0.638	0.001	ENSRNOT00000026491	RGD1305311_predicted	similar to hypothetical protein FLJ22527 (predicted)
-0.638	0.015	NM_053456	Plcl1	phospholipase C-like 1
-0.636	0.019	NM_001012235	Impact	imprinted and ancient
-0.635	0.004	TC583130	-	-
-0.635	0.012	TC601388	-	-
-0.634	0.028	ENSRNOT00000037023	RGD1562705_predicted	similar to Shb-like adapter protein, Shf - human (predicted)
-0.632	0.035	NM_019168	Arg2	arginase 2
-0.629	0.037	NM_053832	Foxj1	forkhead box J1
-0.626	0.026	NM_001024367	LOC501619	similar to 40S ribosomal protein S29
-0.625	0.041	ENSRNOT00000010850	Cnr1	cannabinoid receptor 1 (brain)
-0.625	0.007	ENSRNOT00000027261	RGD1565856_predicted	similar to Hypothetical 55.1 kDa protein F09G8.5 in chromosome III (predicted)
-0.625	0.015	NM_012825	Aqp4	aquaporin 4
-0.625	0.012	XR_008801	Elmod1_predicted	ELMO domain containing 1 (predicted)
-0.625	0.027	NM_012667	Tacr1	tachykinin receptor 1
-0.624	0.037	XM_342195	RGD1307735_predicted	similar to hypothetical protein FLJ11795 (predicted)
-0.623	0.024	NM_138837	Pou3f3	POU domain, class 3, transcription factor 3
-0.621	0.020	NM_001012235	Impact	imprinted and ancient
-0.621	0.010	NM_001031647	Dnali1	dynein, axonemal, light intermediate polypeptide 1
-0.621	0.000	XM_218313	Gpr126_predicted	G protein-coupled receptor 126 (predicted)
-0.620	0.016	NM_012825	Aqp4	aquaporin 4
-0.620	0.017	AW915353	Anp32e	acidic (leucine-rich) nuclear phosphoprotein 32 family, member E
-0.620	0.015	ENSRNOT00000057692	Slitrk5_predicted	SLIT and NTRK-like family, member 5 (predicted)
-0.620	0.001	TC587992	RGD1310623	similar to RIKEN cDNA 2010005O13
-0.619	0.016	DV729125	-	-
-0.619	0.011	TC622410	Bbox1	butyrobetaine (gamma), 2-oxoglutarate dioxygenase 1 (gamma-butyrobetaine hydroxylase)
-0.618	0.040	NM_213627	Zdhhc23	zinc finger, DHHC domain containing 23
-0.616	0.014	NM_012809	Cnp1	cyclic nucleotide phosphodiesterase 1
-0.615	0.020	NM_001014221	LOC363337	similar to RIKEN cDNA 1700081O22
-0.614	0.017	XM_576882	LOC501474	similar to Myosin-9B (Myosin IXb) (Unconventional myosin-9b)

-0.613	0.013	NM_001013151	Gna14	guanine nucleotide binding protein, alpha 14
-0.612	0.005	A_44_P358649	-	-
-0.612	0.012	XR_009412	RGD1563000_predicted	similar to hypothetical protein MGC26856 (predicted)
-0.612	0.024	ENSRNOT00000045285	RGD1564852_predicted	similar to hypothetical protein FLJ14503 (predicted)
-0.611	0.018	NM_053019	Avpr1a	arginine vasopressin receptor 1A
-0.611	0.010	NM_001004269	Jam3	junctional adhesion molecule 3
-0.608	0.002	TC647877	-	-
-0.607	0.001	NM_031339	Parg	poly (ADP-ribose) glycohydrolase
-0.606	0.033	AA801133	RGD1563109_predicted	RGD1563109 (predicted)
-0.606	0.045	ENSRNOT00000017151	Mlf1_predicted	myeloid leukemia factor 1 (predicted)
-0.603	0.009	AI236782	RGD1308324_predicted	similar to RIKEN cDNA 5730469D23 (predicted)
-0.602	0.020	NM_019291	Ca2	carbonic anhydrase 2
-0.600	0.037	TC646852	-	-
-0.599	0.006	NM_001005765	Rap1a	RAS-related protein 1a
-0.598	0.023	NM_001044277	MGC94891	hypothetical protein LOC681210
-0.597	0.033	NM_001007710	Acpl2	acid phosphatase-like 2
-0.597	0.028	NM_022202	Grm8	glutamate receptor, metabotropic 8
-0.597	0.020	DV717011	-	-
-0.597	0.009	NM_022629	Bbox1	butyrobetaine (gamma), 2-oxoglutarate dioxygenase 1 (gamma-butyrobetaine hydroxylase)
-0.596	0.012	XR_005527	LOC679620	similar to CG4329-PA, isoform A
-0.596	0.031	NM_001004080	Gsn	gelsolin
-0.594	0.004	NM_001047912	RGD1307739	similar to CG3306-PA
-0.594	0.001	ENSRNOT00000001728	LOC690211	similar to Disco-interacting protein 2 homolog
-0.594	0.026	NM_001033893	RGD1308356	similar to Hypothetical protein KIAA0341
-0.593	0.003	CF109910	-	-
-0.592	0.011	A_44_P490025	-	-
-0.589	0.018	NM_012614	Npy	neuropeptide Y
-0.587	0.009	NM_031322	Lrp4	low density lipoprotein receptor-related protein 4
-0.586	0.045	NM_012667	Tacr1	tachykinin receptor 1
-0.586	0.041	ENSRNOT00000044595	Lrrc4c_predicted	leucine rich repeat containing 4C (predicted)
-0.585	0.002	ENSRNOT00000013408	Htr2a	5-hydroxytryptamine (serotonin) receptor 2A
-0.584	0.019	BC092654	Col16a1	procollagen, type XVI, alpha 1
-0.583	0.020	ENSRNOT00000012061	RGD1563441_predicted	similar to RIKEN cDNA A030009H04 (predicted)
-0.583	0.031	ENSRNOT0	Slc24a4_pre	solute carrier family 24 (sodium/potassium/calcium

		0000008886	dicted	exchanger), member 4 (predicted)
-0.583	0.041	NM_012667	Tacr1	tachykinin receptor 1
-0.582	0.026	TC596776	-	-
-0.582	0.004	NM_181366	Gpr64	G protein-coupled receptor 64
-0.582	0.020	NM_001013949	Ribc2	RIB43A domain with coiled-coils 2
-0.582	0.037	NM_012721	P2rxl1	purinergic receptor P2X-like 1, orphan receptor
-0.582	0.047	NM_012667	Tacr1	tachykinin receptor 1
1.693	0.031	XM_343196	Mybpc1	myosin binding protein C, slow type
1.683	0.024	NM_012681	Ttr	transthyretin
1.593	0.016	ENSRNOT00000019931	RGD1564779_predicted	similar to Synaptopodin-2 (Myopodin) (predicted)
1.574	0.014	BC128755	LOC296935	similar to leiomodin 2 (cardiac)
1.516	0.021	BG665051	-	-
1.504	0.012	NM_017289	Gabrd	gamma-aminobutyric acid A receptor, delta
1.475	0.020	AI045171	Casq2	calsequestrin 2
1.451	0.008	XM_001057045	LOC680404	similar to Complement C1q-like protein 3 precursor (Gliacolin)
1.422	0.015	NM_020100	Ramp3	receptor (calcitonin) activity modifying protein 3
1.373	0.001	NM_013028	Shox2	short stature homeobox 2
1.361	0.040	NM_012829	Cck	cholecystokinin
1.359	0.024	TC585827	-	-
1.308	0.012	NM_130429	Lef1	lymphoid enhancer binding factor 1
1.304	0.009	TC640931	-	-
1.302	0.005	NM_013028	Shox2	short stature homeobox 2
1.299	0.002	ENSRNOT00000058820	Rcsd1_predicted	RCSD domain containing 1 (predicted)
1.277	0.007	XM_574162	RGD1564431_predicted	similar to heart alpha-kinase (predicted)
1.274	0.030	NM_012829	Cck	cholecystokinin
1.255	0.005	TC612190	-	-
1.241	0.008	NM_001005540	Ppm1j	protein phosphatase 1J
1.235	0.029	NM_016991	Adra1b	adrenergic receptor, alpha 1b
1.233	0.048	NM_012829	Cck	cholecystokinin
1.220	0.008	ENSRNOT00000038486	RGD1562107_predicted	similar to class-alpha glutathione S-transferase (predicted)
1.219	0.049	NM_012829	Cck	cholecystokinin
1.219	0.000	TC615198	-	-
1.217	0.004	NM_012628	Prkcc	protein kinase C, gamma
1.215	0.018	TC619679	-	-
1.207	0.042	NM_012829	Cck	cholecystokinin
1.182	0.045	NM_012829	Cck	cholecystokinin
1.157	0.011	ENSRNOT00000009406	RGD1564459_predicted	similar to hypothetical protein DKFZp434G156 (predicted)
1.150	0.004	NM_012914	Atp2a3	ATPase, Ca++ transporting, ubiquitous
1.148	0.000	ENSRNOT00000018058	RGD1309360	hypothetical LOC294715
1.142	0.009	NM_017131	Casq2	calsequestrin 2
1.141	0.004	XM_227605	RGD1563465_predicted	similar to netrin G1 (predicted)
1.136	0.009	ENSRNOT0	Cidea_predi	cell death-inducing DNA fragmentation factor,

		0000024968	cted	alpha subunit-like effector A (predicted)
1.134	0.003	TC596653	-	-
1.124	0.015	TC614984	-	-
1.115	0.025	NM_016991	Adra1b	adrenergic receptor, alpha 1b
1.113	0.039	BC103629	Ptpn3	protein tyrosine phosphatase, non-receptor type 3
1.107	0.011	NM_053699	Cited4	Cbp/p300-interacting transactivator, with Glu/Asp-rich carboxy-terminal domain, 4
1.096	0.012	TC610674	-	-
1.089	0.008	NM_022666	Grm4	glutamate receptor, metabotropic 4
1.081	0.002	CB547657	-	-
1.079	0.020	XM_343196	Mybpc1	myosin binding protein C, slow type
1.075	0.006	NM_019340	Rgs3	regulator of G-protein signalling 3
1.069	0.006	NM_053834	Kcnj9	potassium inwardly-rectifying channel, subfamily J, member 9
1.060	0.016	AW917391	-	-
1.050	0.014	AF366899	Adra2b	adrenergic receptor, alpha 2b
1.047	0.033	AW143334	-	-
1.044	0.037	TC601767	-	-
1.041	0.029	ENSRNOT0 0000009406	RGD156445 9_predicted	similar to hypothetical protein DKFZp434G156 (predicted)
1.040	0.007	XM_343983	-	-
1.037	0.015	NM_017214	Rgs4	regulator of G-protein signaling 4
1.037	0.017	ENSRNOT0 0000018677	RGD130490 4_predicted	similar to mitochondrial glycerol 3-phosphate acyltransferase (predicted)
1.037	0.011	NM_001013 032	Npy1r	neuropeptide Y receptor Y1
1.020	0.036	XM_001072 492	LOC684921	similar to Complement C1q-like protein 3 precursor (Gliacolin)
1.017	0.003	BE101695	-	-
1.010	0.012	NM_016991	Adra1b	adrenergic receptor, alpha 1b
1.003	0.037	ENSRNOT0 0000005072	LOC498289	similar to Opsin-3 (Encephalopsin) (Panopsin)
1.002	0.022	AW916327	RGD130739 6_predicted	similar to RIKEN cDNA 6330406I15 (predicted)
0.996	0.007	NM_001002 829	Rasl11a	RAS-like family 11 member A
0.990	0.004	TC601560	-	-
0.983	0.007	NM_053506	Hrh3	histamine receptor H3
0.981	0.016	XM_001058 055	LOC681708	similar to transmembrane protein 41a
0.981	0.048	ENSRNOT0 0000004193	RGD131016 6_predicted	similar to Chromodomain-helicase-DNA-binding protein 1 (CHD-1) (predicted)
0.973	0.004	ENSRNOT0 0000008692	Fstl4_predic ted	follistatin-like 4 (predicted)
0.969	0.010	TC645916	-	-
0.966	0.004	TC626053	-	-
0.965	0.003	ENSRNOT0 0000021471	LOC679812	similar to Pleckstrin homology domain-containing family G member 1
0.963	0.002	NM_173138	Dlgap3	discs, large (Drosophila) homolog-associated protein 3
0.959	0.006	ENSRNOT0 0000007993	LOC679668	similar to leucine-rich repeat transmembrane neuronal 1
0.959	0.040	BF393607	LOC689147	hypothetical protein LOC689147

0.959	0.011	NM_053613	Rtn4r	reticulon 4 receptor
0.958	0.010	TC608608	-	-
0.950	0.008	AF039218	Cit	citron
0.946	0.015	TC585018	-	-
0.938	0.014	NM_024354	Chrna4	cholinergic receptor, nicotinic, alpha polypeptide 4
0.937	0.008	BI395573	-	-
0.934	0.017	XM_342800	Tox_predicted	thymocyte selection-associated HMG box gene (predicted)
0.934	0.010	ENSRNOT00000042872	LOC689770	similar to osteoclast inhibitory lectin
0.931	0.049	NM_013157	Ass	argininosuccinate synthetase
0.929	0.038	ENSRNOT00000018058	RGD1309360	hypothetical LOC294715
0.929	0.009	CF107721	-	-
0.924	0.002	A_44_P723917	-	-
0.924	0.041	NM_023960	Kcnmb4	potassium large conductance calcium-activated channel, subfamily M, beta member 4
0.923	0.013	NM_017214	Rgs4	regulator of G-protein signaling 4
0.922	0.029	AW919694	LOC679158	similar to SRY (sex determining region Y)-box 3
0.920	0.026	TC598660	-	-
0.919	0.015	TC623297	-	-
0.916	0.020	XM_219747	Trpm6	transient receptor potential cation channel, subfamily M, member 6
0.915	0.011	NM_019230	Slc22a3	solute carrier family 22, member 3
0.914	0.028	TC594011	-	-
0.913	0.020	NM_053402	Wnt4	wingless-related MMTV integration site 4
0.909	0.003	NM_057142	Lrrc7	leucine rich repeat containing 7
0.905	0.005	ENSRNOT00000014661	Tox_predicted	thymocyte selection-associated HMG box gene (predicted)
0.903	0.005	NM_001011974	Akap2	A kinase (PRKA) anchor protein 2
0.899	0.010	NM_053788	Stx1a	syntaxin 1A (brain)
0.898	0.008	ENSRNOT00000003568	Ptpn4	protein tyrosine phosphatase, non-receptor type 4
0.898	0.001	NM_001025145	Zfp365	zinc finger protein 365
0.893	0.011	ENSRNOT00000001205	RGD1307396_predicted	similar to RIKEN cDNA 6330406I15 (predicted)
0.892	0.004	TC630382	-	-
0.887	0.021	AW142807	-	-
0.887	0.033	BF523192	-	-
0.883	0.015	NM_053804	Kcnk4	potassium channel, subfamily K, member 4
0.881	0.015	ENSRNOT00000004963	Usp43_predicted	ubiquitin specific protease 43 (predicted)
0.881	0.011	NM_001037492	Slc41a3	solute carrier family 41, member 3
0.879	0.007	NM_031826	Fbn2	fibrillin 2
0.878	0.010	NM_021676	Shank3	SH3/ankyrin domain gene 3
0.878	0.040	XM_344544	Angpt2	angiopoietin 2
0.874	0.013	NM_053788	Stx1a	syntaxin 1A (brain)
0.871	0.007	M92075	Grm2	glutamate receptor, metabotropic 2
0.870	0.020	NM_080587	Gabra4	gamma-aminobutyric acid (GABA-A) receptor,

				subunit alpha 4
0.868	0.019	NM_001012101	Coro2a	coronin, actin binding protein 2A
0.867	0.009	ENSRNOT00000046812	RGD1563465_predicted	similar to netrin G1 (predicted)
0.866	0.016	NM_138502	Mgll	monoglyceride lipase
0.865	0.013	TC600845	Ptger3	prostaglandin E receptor 3 (subtype EP3)
0.860	0.014	TC637759	Adarb1	adenosine deaminase, RNA-specific, B1
0.858	0.027	NM_139217	Kcnc2	potassium voltage gated channel, Shaw-related subfamily, member 2
0.854	0.028	NM_001007611	RGD1359691	hypothetical LOC287534
0.853	0.001	AI502122	-	-
0.853	0.017	NM_184045	Srpk3	serine/arginine-rich protein specific kinase 3
0.853	0.009	XM_235546	Upk3a_predicted	uroplakin 3A (predicted)
0.849	0.002	U90444	Adarb1	adenosine deaminase, RNA-specific, B1
0.847	0.024	TC622940	-	-
0.846	0.004	ENSRNOT00000029415	Tnrc9_predicted	trinucleotide repeat containing 9 (predicted)
0.846	0.017	NM_019372	Ppm2c	protein phosphatase 2C, magnesium dependent, catalytic subunit
0.844	0.014	NM_053788	Stx1a	syntaxin 1A (brain)
0.842	0.043	XM_223087	Lamb3	laminin, beta 3
0.840	0.023	NM_022302	Efcbp1	EF hand calcium binding protein 1
0.840	0.027	NM_022297	Ddah1	dimethylarginine dimethylaminohydrolase 1
0.836	0.044	CR469283	-	-
0.835	0.013	NM_053788	Stx1a	syntaxin 1A (brain)
0.834	0.015	ENSRNOT00000051793	RGD1310117_predicted	hypothetical LOC298591 (predicted)
0.832	0.016	DV713993	-	-
0.829	0.026	NM_031686	Scn7a	sodium channel, voltage-gated, type VII, alpha
0.829	0.016	ENSRNOT00000051566	LOC679869	similar to transcription factor 7-like 2, T-cell specific, HMG-box
0.828	0.008	DV718743	-	-
0.827	0.015	NM_053788	Stx1a	syntaxin 1A (brain)
0.827	0.015	NM_053788	Stx1a	syntaxin 1A (brain)
0.826	0.026	BG673684	-	-
0.825	0.044	TC600862	Rnf152_predicted	ring finger protein 152 (predicted)
0.819	0.002	BF522086	-	-
0.819	0.016	ENSRNOT00000026262	RGD1561144_predicted	similar to N-acetylglucosamine 6-O-sulfotransferase (predicted)
0.819	0.026	NM_053788	Stx1a	syntaxin 1A (brain)
0.818	0.005	NM_012704	Ptger3	prostaglandin E receptor 3 (subtype EP3)
0.818	0.036	ENSRNOT00000020727	Cpne7_predicted	copine VII (predicted)
0.817	0.025	TC608942	-	-
0.816	0.022	CK603271	LOC681708	similar to transmembrane protein 41a
0.815	0.003	NM_031826	Fbn2	fibrillin 2
0.815	0.015	TC590536	-	-
0.814	0.006	AW142828	LOC293589	putative GTP-binding protein
0.812	0.011	AA957183	Cit	citron

0.812	0.004	NM_138909	Foxe1	forkhead box E1 (thyroid transcription factor 2)
0.808	0.003	L04739	-	-
0.804	0.016	ENSRNOT00000050400	Gpr123_predicted	G protein-coupled receptor 123 (predicted)
0.803	0.006	TC586471	-	-
0.802	0.023	NM_053788	Stx1a	syntaxin 1A (brain)
0.802	0.025	XM_344130	Inhbb	inhibin beta-B
0.800	0.046	ENSRNOT00000022774	Angpt2	angiopoietin 2
0.800	0.021	NM_053788	Stx1a	syntaxin 1A (brain)
0.798	0.045	XM_001072408	LOC684906	similar to zinc finger, matrin type 4
0.797	0.002	NM_080482	Dbccr1	deleted in bladder cancer chromosome region candidate 1 (human)
0.797	0.008	AW143275	-	-
0.795	0.001	CB545680	-	-
0.794	0.012	ENSRNOT00000021253	Chst9_predicted	carbohydrate (N-acetylgalactosamine 4-0) sulfotransferase 9 (predicted)
0.794	0.033	NM_153473	Myo7a	myosin VIIA
0.793	0.026	NM_001004268	RGD1303271	similar to chromosome 1 open reading frame 172
0.789	0.011	NM_001007235	Itpr1	inositol 1,4,5-triphosphate receptor 1
0.788	0.002	NM_031977	Src	Rous sarcoma oncogene
0.788	0.008	AW920092	-	-
0.786	0.017	TC576606	Coro2a	coronin, actin binding protein 2A
0.784	0.008	NM_053917	Inpp4b	inositol polyphosphate-4-phosphatase, type II
0.783	0.006	NM_001003401	Enc1	ectodermal-neural cortex 1
0.783	0.013	NM_001000779	Olr1424_predicted	olfactory receptor 1424 (predicted)
0.782	0.031	TC620908	-	-
0.782	0.028	TC616402	-	-
0.781	0.005	ENSRNOT00000056116	LOC690366	similar to vang, van gogh-like 1
0.780	0.012	ENSRNOT00000021432	Vil1_predicted	villin 1 (predicted)
0.778	0.028	AW917894	-	-
0.778	0.008	XM_341784	Cdc42ep5_predicted	CDC42 effector protein (Rho GTPase binding) 5 (predicted)
0.777	0.019	NM_057190	Nelf	nasal embryonic LHRH factor
0.774	0.025	TC623960	-	-
0.773	0.002	NM_031977	Src	Rous sarcoma oncogene
0.773	0.028	DV725289	-	-
0.771	0.013	ENSRNOT00000007242	RGD1308745_predicted	similar to E430002G05Rik protein (predicted)
0.771	0.021	NM_013026	Sdc1	syndecan 1
0.771	0.012	AA997148	Morf4l1	mortality factor 4 like 1
0.764	0.048	NM_001024791	Epn3	epsin 3
0.762	0.003	ENSRNOT00000009896	Cyp46a1_predicted	cytochrome P450, family 46, subfamily a, polypeptide 1 (predicted)
0.762	0.003	NM_001033	Slc6a17	solute carrier family 6 (neurotransmitter

		079		transporter), member 17
0.761	0.019	BF563765	-	-
0.760	0.022	A_44_P417133	-	-
0.759	0.022	NM_001012056	LOC307660	carboxylesterase 615
0.758	0.015	TC599342	-	-
0.758	0.047	ENSRNOT00000026419	Gbx2	gastrulation brain homeobox 2
0.758	0.031	NM_017288	Scn1b	sodium channel, voltage-gated, type I, beta
0.757	0.011	NM_031085	Prkch	protein kinase C, eta
0.757	0.006	NM_053698	Cited2	Cbp/p300-interacting transactivator, with Glu/Asp-rich carboxy-terminal domain, 2
0.757	0.000	TC620686	-	-
0.754	0.006	NM_001007235	Itpr1	inositol 1,4,5-triphosphate receptor 1
0.753	0.008	ENSRNOT00000002498	Pkp2	plakophilin 2
0.750	0.019	NM_017230	Padi3	peptidyl arginine deiminase, type III
0.749	0.002	NM_001034855	Gpr153	G protein-coupled receptor 153
0.747	0.038	ENSRNOT00000012757	Papln_predicted	papilin, proteoglycan-like sulfated glycoprotein (predicted)
0.747	0.011	NM_001007235	Itpr1	inositol 1,4,5-triphosphate receptor 1
0.745	0.034	NM_053981	Kcnj12	potassium inwardly-rectifying channel, subfamily J, member 12
0.744	0.044	CB546657	-	-
0.743	0.009	NM_001007235	Itpr1	inositol 1,4,5-triphosphate receptor 1
0.742	0.015	NM_001007235	Itpr1	inositol 1,4,5-triphosphate receptor 1
0.742	0.021	ENSRNOT00000021036	Cda_predicted	cytidine deaminase (predicted)
0.742	0.007	TC610464	-	-
0.741	0.035	NM_138849	Bk	brain and kidney protein
0.740	0.013	ENSRNOT00000044039	RGD1565245_predicted	similar to Histone H2B 291B (predicted)
0.739	0.008	NM_001034933	Arsa	arylsulfatase A
0.738	0.008	A_44_P918476	-	-
0.737	0.014	XM_231560	-	-
0.735	0.006	NM_001029911	Cit	citron
0.734	0.002	NM_031977	Src	Rous sarcoma oncogene
0.734	0.011	NM_001007235	Itpr1	inositol 1,4,5-triphosphate receptor 1
0.731	0.006	TC599051	-	-
0.731	0.027	TC596940	-	-
0.730	0.004	NM_031977	Src	Rous sarcoma oncogene
0.729	0.004	NM_031977	Src	Rous sarcoma oncogene
0.727	0.011	NM_031730	Kcnd2	potassium voltage gated channel, Shal-related family, member 2

0.724	0.038	A_44_P323955	-	-
0.722	0.033	NM_172224	Impa2	inositol (myo)-1(or 4)-monophosphatase 2
0.720	0.023	NM_053311	Atp2b1	ATPase, Ca++ transporting, plasma membrane 1
0.719	0.029	ENSRNOT00000039225	RGD1310037_predicted	similar to RIKEN cDNA C230093N12 (predicted)
0.719	0.001	AF468695	Plekha5	pleckstrin homology domain containing, family A member 5
0.718	0.011	A_44_P199343	-	-
0.715	0.008	NM_001007235	Itpr1	inositol 1,4,5-triphosphate receptor 1
0.714	0.002	NM_001014035	LOC309957	similar to myocyte enhancer factor 2C
0.714	0.009	TC580645	LOC685491	similar to retinoblastoma binding protein 4
0.712	0.012	NM_012596	Lepr	leptin receptor
0.711	0.019	XM_219476	Ifitm6_predicted	interferon induced transmembrane protein 6 (predicted)
0.710	0.020	NM_001024999	RGD1307787	similar to RIKEN cDNA 9130017C17 gene
0.710	0.021	A_44_P792124	RGD1560587_predicted	similar to Eph receptor A4 (predicted)
0.710	0.040	ENSRNOT00000044378	Grid2ip_predicted	glutamate receptor, ionotropic, delta 2 (Grid2) interacting protein 1 (predicted)
0.709	0.050	NM_133307	Prkcd	protein kinase C, delta
0.709	0.002	NM_173145	Dlgap4	discs, large homolog-associated protein 4 (Drosophila)
0.709	0.013	XM_216761	-	-
0.709	0.008	NM_001007235	Itpr1	inositol 1,4,5-triphosphate receptor 1
0.708	0.016	ENSRNOT00000019442	Shc3	src homology 2 domain-containing transforming protein C3
0.708	0.050	BF565038	-	-
0.707	0.011	CB547706	-	-
0.707	0.006	TC597957	-	-
0.705	0.005	NM_031977	Src	Rous sarcoma oncogene
0.705	0.000	CF110435	-	-
0.704	0.039	XM_345977	Cpne4_predicted	copine IV (predicted)
0.704	0.001	ENSRNOT00000012219	Rab6b_predicted	RAB6B, member RAS oncogene family (predicted)
0.703	0.008	ENSRNOT00000023084	Lrrn6a	leucine rich repeat neuronal 6A
0.703	0.017	TC601674	-	-
0.703	0.017	NM_001007235	Itpr1	inositol 1,4,5-triphosphate receptor 1
0.702	0.023	ENSRNOT00000009883	Il12rb2	interleukin 12 receptor, beta 2
0.702	0.041	AJ617619	Syt1	synaptotagmin I
0.699	0.021	NM_030841	Nptxr	neuronal pentraxin receptor
0.698	0.023	NM_031684	Slc29a1	solute carrier family 29 (nucleoside transporters), member 1
0.697	0.013	NM_001007235	Itpr1	inositol 1,4,5-triphosphate receptor 1

0.696	0.001	XM_346384	Grin2a	glutamate receptor, ionotropic, N-methyl D-aspartate 2A
0.692	0.014	AA943125	-	-
0.692	0.006	A_44_P668786	-	-
0.691	0.008	NM_199381	NAPE-PLD	N-acyl-phosphatidylethanolamine-hydrolyzing phospholipase D
0.691	0.014	NM_001025680	Gpr4	G protein-coupled receptor 4
0.691	0.016	NM_012517	Cacna1c	calcium channel, voltage-dependent, L type, alpha 1C subunit
0.690	0.037	NM_199402	Spata20	spermatogenesis associated 20
0.689	0.017	TC605809	-	-
0.689	0.020	ENSRNOT00000056721	Galnt9_predicted	UDP-N-acetyl-alpha-D-galactosamine:polypeptide N-acetylgalactosaminyltransferase 9 (predicted)
0.687	0.020	DY471743	-	-
0.685	0.003	XM_001077297	LOC691506	similar to Tetratricopeptide repeat protein 19 (TPR repeat protein 19)
0.684	0.029	TC601709	-	-
0.683	0.018	NM_207598	Abca7	ATP-binding cassette, sub-family A (ABC1), member 7
0.682	0.006	XM_344728	Nkd1_predicted	naked cuticle 1 homolog (Drosophila) (predicted)
0.682	0.026	XR_007322	RGD1563459_predicted	RGD1563459 (predicted)
0.681	0.038	AW534376	-	-
0.681	0.033	TC598660	-	-
0.680	0.008	NM_031321	Slit3	slit homolog 3 (Drosophila)
0.678	0.016	AW143756	Amotl1_predicted	angiomotin-like 1 (predicted)
0.677	0.017	ENSRNOT00000005176	Wnt3_predicted	wingless-type MMTV integration site family, member 3 (predicted)
0.675	0.032	BG663107	Akap12	A kinase (PRKA) anchor protein (gravin) 12
0.674	0.042	NM_017238	Vipr2	vasoactive intestinal peptide receptor 2
0.673	0.015	TC633364	-	-
0.672	0.037	A_44_P921044	-	-
0.671	0.030	ENSRNOT00000046700	Trpc3	transient receptor potential cation channel, subfamily C, member 3
0.671	0.033	BF286307	-	-
0.670	0.002	TC598831	-	-
0.669	0.002	NM_001011989	Gns	glucosamine (N-acetyl)-6-sulfatase
0.668	0.017	TC599772	-	-
0.668	0.007	AW142827	RGD1306212_predicted	similar to hypothetical protein DKFZp566N034 (predicted)
0.667	0.006	NM_001034131	Foxp1	forkhead box P1
0.667	0.007	CB608947	-	-
0.666	0.014	ENSRNOT00000010620	Sema7a_predicted	sema domain, immunoglobulin domain (Ig), and GPI membrane anchor, (semaphorin) 7A (predicted)
0.665	0.021	TC611170	-	-
0.663	0.026	NM_053311	Atp2b1	ATPase, Ca++ transporting, plasma membrane 1

0.662	0.015	NM_053774	Usp2	ubiquitin specific peptidase 2
0.661	0.013	NM_199381	NAPE-PLD	N-acyl-phosphatidylethanolamine-hydrolyzing phospholipase D
0.660	0.004	NM_053945	Rims2	regulating synaptic membrane exocytosis 2
0.659	0.007	BI395616	-	-
0.658	0.008	NM_012971	Kcna4	potassium voltage-gated channel, shaker-related subfamily, member 4
0.657	0.022	NM_012517	Cacna1c	calcium channel, voltage-dependent, L type, alpha 1C subunit
0.654	0.010	NM_133559	Pcsk4	proprotein convertase subtilisin/kexin type 4
0.653	0.039	BC089892	RGD1566180_predicted	RGD1566180 (predicted)
0.653	0.018	TC646523	-	-
0.652	0.002	TC631242	-	-
0.652	0.003	ENSRNOT00000001182	Auts2_predicted	autism susceptibility candidate 2 (predicted)
0.651	0.043	AI511358	-	-
0.650	0.008	TC647640	-	-
0.648	0.021	NM_012517	Cacna1c	calcium channel, voltage-dependent, L type, alpha 1C subunit
0.648	0.004	AW144045	Slc9a3r1	solute carrier family 9 (sodium/hydrogen exchanger), isoform 3 regulator 1
0.646	0.010	BM986517	Nudt4	nudix (nucleoside diphosphate linked moiety X)-type motif 4
0.645	0.006	ENSRNOT00000015795	RGD1308153_predicted	similar to RIKEN cDNA 2700085M18 (predicted)
0.644	0.006	NM_019329	Cntn3	contactin 3
0.643	0.028	A_44_P812699	Hrsp12	heat-responsive protein 12
0.643	0.016	ENSRNOT00000013009	Slitrk3_predicted	SLIT and NTRK-like family, member 3 (predicted)
0.643	0.003	NM_031977	Src	Rous sarcoma oncogene
0.641	0.005	NM_012886	Timp3	tissue inhibitor of metalloproteinase 3 (Sorsby fundus dystrophy, pseudoinflammatory)
0.641	0.012	BC086332	Adprtl1	ADP-ribosyltransferase (NAD+; poly (ADP-ribose) polymerase)-like 1
0.641	0.007	TC596471	-	-
0.641	0.011	ENSRNOT00000040110	LOC691335	similar to septin 6
0.640	0.016	NM_019344	Rgs8	regulator of G-protein signaling 8
0.639	0.045	XM_230765	E2f1	E2F transcription factor 1
0.638	0.039	NM_053788	Stx1a	syntaxin 1A (brain)
0.638	0.004	NM_031977	Src	Rous sarcoma oncogene
0.634	0.001	XM_343260	Bai1_predicted	brain-specific angiogenesis inhibitor 1 (predicted)
0.633	0.004	NM_012727	Camk4	calcium/calmodulin-dependent protein kinase IV
0.632	0.028	TC590363	-	-
0.631	0.008	NM_001014271	LOC367515	similar to RIKEN cDNA 1700081O22
0.631	0.005	ENSRNOT00000049753	Mgat5b_predicted	mannoside acetylglucosaminyltransferase 5, isoenzyme B (predicted)
0.630	0.002	CO399814	-	-
0.629	0.014	ENSRNOT00000002498	Pkp2	plakophilin 2

0.629	0.028	NM_199381	NAPE-PLD	N-acyl-phosphatidylethanolamine-hydrolyzing phospholipase D
0.629	0.020	NM_053931	5-Sep	septin 5
0.628	0.037	TC600452	-	-
0.627	0.044	XR_009350	RGD1561060_predicted	similar to hypothetical protein 4930474N05 (predicted)
0.627	0.026	TC606407	-	-
0.627	0.022	NM_178021	Hspa5bp1	heat shock 70kDa protein 5 binding protein 1
0.626	0.012	NM_199381	NAPE-PLD	N-acyl-phosphatidylethanolamine-hydrolyzing phospholipase D
0.626	0.014	ENSRNOT00000025516	Elmo1_predicted	engulfment and cell motility 1, ced-12 homolog (C. elegans) (predicted)
0.624	0.013	AI008119	-	-
0.624	0.007	XM_217648	Hspa12a_predicted	heat shock 70kDa protein 12A (predicted)
0.624	0.011	NM_199381	NAPE-PLD	N-acyl-phosphatidylethanolamine-hydrolyzing phospholipase D
0.621	0.005	ENSRNOT00000035826	RGD1304563_predicted	similar to RIKEN cDNA 4831426I19 (predicted)
0.621	0.018	AW142951	-	-
0.620	0.019	NM_012517	Cacna1c	calcium channel, voltage-dependent, L type, alpha 1C subunit
0.619	0.013	NM_053698	Cited2	Cbp/p300-interacting transactivator, with Glu/Asp-rich carboxy-terminal domain, 2
0.618	0.033	XM_341147	Rcsd1_predicted	RCSD domain containing 1 (predicted)
0.618	0.009	NM_031977	Src	Rous sarcoma oncogene
0.616	0.025	NM_199381	NAPE-PLD	N-acyl-phosphatidylethanolamine-hydrolyzing phospholipase D
0.614	0.040	ENSRNOT00000040706	RGD1309808_predicted	similar to apolipoprotein L2; apolipoprotein L-II (predicted)
0.613	0.010	ENSRNOT00000035926	Arhgap22_predicted	Rho GTPase activating protein 22 (predicted)
0.611	0.018	XM_342632	Pftk1_predicted	PFTAIRE protein kinase 1 (predicted)
0.610	0.001	NM_021658	Hcn4	hyperpolarization-activated, cyclic nucleotide-gated K+ 4
0.609	0.005	AJ617619	Syt1	synaptotagmin I
0.608	0.015	AW251647	-	-
0.608	0.013	NM_012517	Cacna1c	calcium channel, voltage-dependent, L type, alpha 1C subunit
0.607	0.001	AI059890	RGD1560744_predicted	similar to ring finger protein 111 (predicted)
0.607	0.021	NM_012746	Pcsk2	proprotein convertase subtilisin/kexin type 2
0.607	0.013	NM_012517	Cacna1c	calcium channel, voltage-dependent, L type, alpha 1C subunit
0.606	0.006	NM_019179	Tyms	thymidylate synthase
0.606	0.004	TC636367	-	-
0.606	0.039	NM_012517	Cacna1c	calcium channel, voltage-dependent, L type, alpha 1C subunit
0.606	0.008	TC602078	-	-
0.605	0.001	NM_053949	Kcnh2	potassium voltage-gated channel, subfamily H (eag-related), member 2
0.604	0.020	NM_001039	Zdhhc18	zinc finger, DHHC domain containing 18

		339		
0.604	0.036	TC625842	-	-
0.604	0.003	XM_001066889	RGD1561030_predicted	similar to DEP domain containing 6 (predicted)
0.604	0.031	NM_053351	Cacng2	calcium channel, voltage-dependent, gamma subunit 2
0.603	0.012	BE107979	-	-
0.603	0.037	ENSRNOT00000054890	Inpp5a_predicted	inositol polyphosphate-5-phosphatase A (predicted)
0.602	0.018	NM_012746	Pcsk2	proprotein convertase subtilisin/kexin type 2
0.601	0.015	ENSRNOT00000019408	Zfhx3_predicted	zinc finger homeobox 3 (predicted)
0.601	0.011	A_44_P989601	-	-
0.601	0.013	NM_199381	NAPE-PLD	N-acyl-phosphatidylethanolamine-hydrolyzing phospholipase D
0.600	0.004	TC594701	-	-
0.599	0.023	TC592480	-	-
0.598	0.025	NM_012517	Cacna1c	calcium channel, voltage-dependent, L type, alpha 1C subunit
0.597	0.022	XM_342320	-	-
0.596	0.010	NM_053851	Cacnb2	calcium channel, voltage-dependent, beta 2 subunit
0.595	0.000	AW523545	Btbd3_predicted	BTB (POZ) domain containing 3 (predicted)
0.594	0.024	NM_199381	NAPE-PLD	N-acyl-phosphatidylethanolamine-hydrolyzing phospholipase D
0.594	0.021	TC644730	-	-
0.594	0.021	XM_341223	RGD1562860_predicted	similar to RIKEN cDNA 2310045A20 (predicted)
0.593	0.012	ENSRNOT00000057506	Rora_predicted	RAR-related orphan receptor alpha (predicted)
0.593	0.005	XM_001076955	RGD1565556_predicted	similar to cajalin 2 isoform a (predicted)
0.591	0.033	ENSRNOT00000019956	Sema4g_predicted	sema domain, immunoglobulin domain (Ig), transmembrane domain (TM) and short cytoplasmic domain, (semaphorin) 4G (predicted)
0.591	0.002	NM_139333	Prpf19	PRP19/PSO4 pre-mRNA processing factor 19 homolog (S. cerevisiae)
0.588	0.010	NM_053698	Cited2	Cbp/p300-interacting transactivator, with Glu/Asp-rich carboxy-terminal domain, 2
0.588	0.003	ENSRNOT00000022469	Loxl2_predicted	lysyl oxidase-like 2 (predicted)
0.587	0.027	TC612255	-	-
0.587	0.013	NM_017032	Pde4d	phosphodiesterase 4D, cAMP specific
0.587	0.005	TC627587	-	-
0.587	0.028	CB547681	-	-
0.587	0.007	TC596530	-	-
0.587	0.023	NM_017345	L1cam	L1 cell adhesion molecule
0.587	0.007	NM_012588	Igfbp3	insulin-like growth factor binding protein 3
0.587	0.007	NM_134373	Avpi1	arginine vasopressin-induced 1
0.587	0.030	TC619875	-	-
0.586	0.006	NM_001034855	Gpr153	G protein-coupled receptor 153
0.586	0.007	ENSRNOT0	LOC685076	similar to phosphoglucomutase 2-like 1

		0000022963		
0.585	0.039	AI111924	RGD1562963_predicted	similar to chromosome 6 open reading frame 52 (predicted)
0.585	0.003	XM_341506	RGD1306058_predicted	similar to RIKEN cDNA 1110007C09 (predicted)
0.584	0.025	AI237691	LOC314964	similar to PHD finger protein 20-like 1 isoform 1
0.584	0.038	NM_199381	NAPE-PLD	N-acyl-phosphatidylethanolamine-hydrolyzing phospholipase D
0.584	0.023	NM_031977	Src	Rous sarcoma oncogene
0.584	0.002	AJ617619	Syt1	synaptotagmin I
0.583	0.014	NM_031601	Cacna1g	calcium channel, voltage-dependent, T type, alpha 1G subunit
0.583	0.001	XM_576480	LOC501065	similar to chemokine-like factor super family 7
0.583	0.004	ENSRNOT00000046486	Tiam1	T-cell lymphoma invasion and metastasis 1
0.583	0.036	BF563262	-	-
0.582	0.037	ENSRNOT00000009178	Stk32c_predicted	serine/threonine kinase 32C (predicted)
0.582	0.016	NM_031610	Kcnj3	potassium inwardly-rectifying channel, subfamily J, member 3
0.581	0.027	BC086332	Adprtl1	ADP-ribosyltransferase (NAD+; poly (ADP-ribose) polymerase)-like 1

APPENDIX D
LIST OF MODULATED GENE ONTOLOGY BIOLOGICAL PROCESSES FOLLOWING REPEATED ITTO

Table D-1. List of modulated GO groups following repeated ITTO with $p < 0.01$

Name	# of Entities	Expanded # of Entities	Over lap	p-value
Synaptic transmission	247	247	17	2.189 e-12
Melanogenesis	51	687	29	6.496 e-9
Gap junction regulation	51	644	26	1.317 e-7
Neuropeptide signaling pathway	127	127	9	2.965 e-7
Ion transport	619	619	18	4.204 e-7
Elevation of cytosolic calcium ion concentration	99	99	8	5.032 e-7
Nervous system development	441	441	15	5.834 e-7
Signal transduction	3207	3207	46	1.515 e-6
Skeletal myogenesis control	70	558	21	9.190 e-6
Cation transport	106	106	7	1.017 e-5
Learning and-or memory	42	42	5	1.112 e-5
Feeding behavior	44	44	5	1.403 e-5
Cell-cell signaling	334	334	11	2.612 e-5
Gonadotrope cell activation	71	702	23	3.048 e-5
Multicellular organismal development	1100	1100	21	3.303 e-5
Dentate gyrus development	2	2	2	4.898 e-5
Negative regulation of fibroblast growth factor receptor signaling pathway	2	2	2	4.898 e-5
Glutamate decarboxylation to succinate	2	2	2	4.898 e-5
Ectoderm formation	2	2	2	4.898 e-5
Response to drug	190	190	8	6.203 e-5
Neurotransmitter transport	62	62	5	7.550 e-5
Calcium ion transport	145	145	7	7.66 e-5
Drinking behavior	13	13	3	9.235 e-5
Response to glucocorticoid stimulus	67	67	5	1.095 e-4
G-protein signaling, coupled to cyclic nucleotide second messenger	42	42	4	2.134 e-4
Transport	1962	1962	28	2.621 e-4
Striated muscle contraction	45	45	4	2.794 e-4
Negative regulation of appetite	4	4	2	2.912 e-4
Embryonic epithelial tube formation	4	4	2	2.912 e-4
Negative regulation of blood pressure	19	19	3	3.033 e-4
Negative regulation of adenylate cyclase activity	19	19	3	3.033 e-4
Axonogenesis	84	84	5	3.180 e-4
Regulation of cell migration	47	47	4	3.309 e-4
Neurotransmitter secretion	48	48	4	3.590 e-4
Negative regulation of bone mineralization	5	5	2	4.830 e-4
Behavior	52	52	4	4.887 e-4
Inner ear morphogenesis	52	52	4	4.887 e-4
Kidney development	53	53	4	5.257 e-4
Intracellular signaling cascade	472	472	11	5.352 e-4
Opioidr -> CREB/ELK-SRF/STAT3 signaling	32	51	5	5.560 e-4
Negative regulation of neuron differentiation	24	24	3	6.174 e-4
Embryonic limb morphogenesis	56	56	4	6.490 e-4

Regulation of bone remodeling	6	6	2	7.212 e-4
Embryonic digestive tract morphogenesis	6	6	2	7.212 e-4
Regulation of neuronal synaptic plasticity	26	26	3	7.850 e-4
Cell death	60	60	4	8.427 e-4
Regulation of neurotransmitter secretion	27	27	3	8.785 e-4
Hemocyte development	7	7	2	0.0010
Regulation of synaptic transmission, glutamatergic	7	7	2	0.0010
Response to steroid hormone stimulus	29	29	3	0.0011
Regulation of transcription	521	521	11	0.0012
Regulation of blood pressure	67	67	4	0.0013
Learning	31	31	3	0.0013
Monoamine transport	8	8	2	0.0013
Adrenergicra -> STAT3 signaling	22	38	4	0.0016
Adrenergicrb -> CREB signaling	28	64	5	0.0016
Behavioral response to cocaine	9	9	2	0.0017
Regulation of cytoskeleton organization and biogenesis	9	9	2	0.0017
Mast cell degranulation	9	9	2	0.0017
Cholecystokininr -> ELK-SRF signaling	23	39	4	0.0017
Negative regulation of transcription from RNA polymerase II promoter	247	247	7	0.0019
Anatomical structure formation	35	35	3	0.0019
VIPR -> CREB/CEBP signaling	31	67	5	0.0019
Thyroid hormone metabolic process	10	10	2	0.0021
Thyroid hormone generation	10	10	2	0.0021
Adrenergicra -> ELK-SRF signaling	26	42	4	0.0023
Forebrain development	79	79	4	0.0023
Anterior-posterior pattern formation	79	79	4	0.0023
Prostaglandinir -> ATF1/ELK-SRF/CREB signaling	35	70	5	0.0023
T-cell receptor -> ATF/CREB signaling pathway	49	71	5	0.0025
Positive regulation of cell cycle	11	11	2	0.0026
Vasopressinr1 -> STAT signaling	16	44	4	0.0027
Regulation of G-protein coupled receptor protein signaling pathway	41	41	3	0.0030
Neurotransmitter biosynthetic process	12	12	2	0.0031
Neurite development	43	43	3	0.0034
Prostaglandinfr -> ATF1/ELK-SRF/CREB signaling	28	47	4	0.0035
Tube morphogenesis	13	13	2	0.0036
Regulation of Wnt receptor signaling pathway	13	13	2	0.0036
Cell differentiation	691	691	12	0.0037
Adenosiner -> NF-kb signaling	19	49	4	0.0040
Epithelial cell differentiation	46	46	3	0.0041
Regulation of ossification	14	14	2	0.0042
Cerebellum development	14	14	2	0.0042
Dorsal-ventral pattern formation	47	47	3	0.0044
Heart development	156	156	5	0.0050
GHR -> ELK-SRF/MYC signaling	25	53	4	0.0053
Vasopressinr2 -> CREB/ELK-SRF/AP-1/EGR signaling	56	121	6	0.0055
Response to estradiol stimulus	16	16	2	0.0055
Organ morphogenesis	228	228	6	0.0056
Response to nutrient	104	104	4	0.0063
KIT -> MITF signaling	28	56	4	0.0065

Hair follicle morphogenesis	18	18	2	0.0070
Midbrain-hindbrain boundary morphogenesis	1	1	1	0.0070
Hard palate development	1	1	1	0.0070
Positive regulation of mitochondrial depolarization	1	1	1	0.0070
Negative regulation of serotonin secretion	1	1	1	0.0070
Negative regulation of gamma-aminobutyric acid secretion	1	1	1	0.0070
Negative regulation of glycogen catabolic process	1	1	1	0.0070
Negative regulation of collateral sprouting of intact axon in response to injury	1	1	1	0.0070
Negative regulation of hepatocyte growth factor biosynthetic process	1	1	1	0.0070
Positive regulation of mismatch repair	1	1	1	0.0070
Positive regulation of circadian sleep-wake cycle, REM sleep	1	1	1	0.0070
Positive regulation of insulin receptor signaling pathway	1	1	1	0.0070
Positive regulation of epinephrine secretion	1	1	1	0.0070
Positive regulation of protein oligomerization	1	1	1	0.0070
Positive regulation of collagen biosynthetic process	1	1	1	0.0070
Histamine uptake	1	1	1	0.0070
Vasoconstriction of artery involved in baroreceptor response to lowering of systemic arterial blood pressure	1	1	1	0.0070
Phagolysosome formation	1	1	1	0.0070
Keratan sulfate biosynthetic process	1	1	1	0.0070
5-phosphoribose 1-diphosphate biosynthetic process	1	1	1	0.0070
Protein-pyridoxal-5-phosphate linkage	1	1	1	0.0070
Rhombomere 2 development	1	1	1	0.0070
Synaptic vesicle amine transport	1	1	1	0.0070
Voluntary musculoskeletal movement	1	1	1	0.0070
Prolactinr -> STAT signaling	10	10	2	0.0075
Neuroprotection	19	19	2	0.0077
Lamellipodium biogenesis	19	19	2	0.0077
Lipid metabolic process	327	327	7	0.0085
Positive regulation of cell adhesion	20	20	2	0.0086
Inactivation of MAPK activity	20	20	2	0.0086
Endoderm development	20	20	2	0.0086
Fciger -> ELK-SRF signaling	34	62	4	0.0093
Nk cell activation	59	525	14	0.0094
IL8R -> CREB/EGR signaling	33	33	3	0.0095

LIST OF REFERENCES

1995. Standardization of Spirometry, 1994 Update. American Thoracic Society. Am J Respir Crit Care Med 152, 1107-1136.

1999. Dyspnea. Mechanisms, assessment, and management: a consensus statement. American Thoracic Society. Am J Respir Crit Care Med 159, 321-340.

Aaron, E.A., Seow, K.C., Johnson, B.D., Dempsey, J.A., 1992. Oxygen cost of exercise hyperpnea: implications for performance. J Appl Physiol 72, 1818-1825.

Alitto, H.J., Usrey, W.M., 2003. Corticothalamic feedback and sensory processing. Curr Opin Neurobiol 13, 440-445.

Aliverti, A., 2008. Lung and chest wall mechanics during exercise: Effects of expiratory flow limitation. Respir Physiol Neurobiol.

Amonette, W.E., Dupler, T.L., 2002. The effects of respiratory muscle training on VO2max, the ventilatory threshold and pulmonary function. J Exerc Physiol Online 5, 29-35.

Arias-Carrion, O., Poppel, E., 2007. Dopamine, learning, and reward-seeking behavior. Acta Neurobiol Exp (Wars) 67, 481-488.

Armour, J., Donnelly, P.M., Bye, P.T., 1993. The large lungs of elite swimmers: an increased alveolar number? Eur Respir J 6, 237-247.

Armstrong, N., Davies, B., 1981. An ergometric analysis of age group swimmers. Br J Sports Med 15, 20-26.

Athanasopoulos, D., Louvaris, Z., Cherouveim, E., Andrianopoulos, V., Roussos, C., Zakynthinos, S.G., Vogiatzis, I., 2010. Expiratory muscle loading increases intercostal muscle blood flow during leg exercise in healthy humans. J Appl Physiol.

Babcock, M.A., Pegelow, D.F., McClaran, S.R., Suman, O.E., Dempsey, J.A., 1995. Contribution of diaphragmatic power output to exercise-induced diaphragm fatigue. J Appl Physiol 78, 1710-1719.

Baker, S., Davenport, P., Sapienza, C., 2005. Examination of strength training and detraining effects in expiratory muscles. J Speech Lang Hear Res 48, 1325-1333.

Barbarito, N., Ceriana, P., Nava, S., 2001. Respiratory muscles in chronic obstructive pulmonary disease and asthma. Minerva Anestesiol 67, 653-658.

Benarroch, E.E., 2008. The midline and intralaminar thalamic nuclei: anatomic and functional specificity and implications in neurologic disease. Neurology 71, 944-949.

Bishop, B., Settle, S., Hirsch, J., 1981. Single motor unit activity in the diaphragm of cat during pressure breathing. J Appl Physiol 50, 348-357.

Borg, G., 2008. A general scale to rate symptoms and feelings related to problems of ergonomic and organizational importance. G Ital Med Lav Ergon 30, A8-10.

Botteron, K.N., Raichle, M.E., Drevets, W.C., Heath, A.C., Todd, R.D., 2002. Volumetric reduction in left subgenual prefrontal cortex in early onset depression. Biol Psychiatry 51, 342-344.

Boutellier, U., Buchel, R., Kundert, A., Spengler, C., 1992. The respiratory system as an exercise limiting factor in normal trained subjects. Eur J Appl Physiol Occup Physiol 65, 347-353.

Bradley, G.W., 1972. The response of the respiratory system to elastic loading in cats. Respir Physiol 16, 142-160.

Bremner, J.D., Narayan, M., Anderson, E.R., Staib, L.H., Miller, H.L., Charney, D.S., 2000. Hippocampal volume reduction in major depression. Am J Psychiatry 157, 115-118.

Bullitt, E., 1990. Expression of c-fos-like protein as a marker for neuronal activity following noxious stimulation in the rat. J Comp Neurol 296, 517-530.

Campbell, E.J., Gandevia, S.C., Killian, K.J., Mahutte, C.K., Rigg, J.R., 1980. Changes in the perception of inspiratory resistive loads during partial curarization. J Physiol 309, 93-100.

Carlsson, A., Waters, N., Carlsson, M.L., 1999. Neurotransmitter interactions in schizophrenia-therapeutic implications. Eur Arch Psychiatry Clin Neurosci 249 Suppl 4, 37-43.

Carvalho, N.S., Ribeiro, P.R., Ribeiro, M., Nunes Mdo, P., Cukier, A., Stelmach, R., 2007. Comparing asthma and chronic obstructive pulmonary disease in terms of symptoms of anxiety and depression. J Bras Pneumol 33, 1-6.

Chan, P.Y., Davenport, P.W., 2008. Respiratory-related evoked potential measures of respiratory sensory gating. J Appl Physiol 105, 1106-1113.

Charney, D.S., Woods, S.W., Goodman, W.K., Heninger, G.R., 1987. Serotonin function in anxiety. II. Effects of the serotonin agonist MCPP in panic disorder patients and healthy subjects. Psychopharmacology (Berl) 92, 14-24.

Chen, Z., Eldridge, F.L., Wagner, P.G., 1992. Respiratory-associated thalamic activity is related to level of respiratory drive. Respir Physiol 90, 99-113.

Cheong, E., Lee, S., Choi, B.J., Sun, M., Lee, C.J., Shin, H.S., 2008. Tuning thalamic firing modes via simultaneous modulation of T- and L-type Ca2+ channels controls pain sensory gating in the thalamus. J Neurosci 28, 13331-13340.

Chiara, T., Martin, A.D., Davenport, P.W., Bolser, D.C., 2006. Expiratory muscle strength training in persons with multiple sclerosis having mild to moderate disability: effect on maximal expiratory pressure, pulmonary function, and maximal voluntary cough. Arch Phys Med Rehabil 87, 468-473.

Chonan, T., Altose, M.D., Cherniack, N.S., 1990a. Effects of expiratory resistive loading on the sensation of dyspnea. J Appl Physiol 69, 91-95.

Chonan, T., Mulholland, M.B., Leitner, J., Altose, M.D., Cherniack, N.S., 1990b. Sensation of dyspnea during hypercapnia, exercise, and voluntary hyperventilation. J Appl Physiol 68, 2100-2106.

Chung, L., Moore, S.D., Cox, C.L., 2009. Cholecystokinin action on layer 6b neurons in somatosensory cortex. Brain Res 1282, 10-19.

Clanton, T.L., Dixon, G.F., Drake, J., Gadek, J.E., 1987. Effects of swim training on lung volumes and inspiratory muscle conditioning. J Appl Physiol 62, 39-46.

Clark, F.J., von Euler, C., 1972. On the regulation of depth and rate of breathing. J Physiol 222, 267-295.

Cordain, L., Tucker, A., Moon, D., Stager, J.M., 1990. Lung volumes and maximal respiratory pressures in collegiate swimmers and runners. Res Q Exerc Sport 61, 70-74.

Corfield, D.R., Fink, G.R., Ramsay, S.C., Murphy, K., Harty, H.R., Watson, J.D., Adams, L., Frackowiak, R.S., Guz, A., 1995. Evidence for limbic system activation during CO2-stimulated breathing in man. J Physiol 488 (Pt 1), 77-84.

Correia, S.S., Duarte, C.B., Faro, C.J., Pires, E.V., Carvalho, A.L., 2003. Protein kinase C gamma associates directly with the GluR4 alpha-amino-3-hydroxy-5-methyl-4-isoxazole propionate receptor subunit. Effect on receptor phosphorylation. J Biol Chem 278, 6307-6313.

Corry, I., Powers, N., 1982. Maximal aerobic power measurement in runners and swimmers. Br J Sports Med 16, 154-160.

Davenport, P.W., Frazier, D.T., Zechman, F.W., Jr., 1981. The effect of the resistive loading of inspiration and expiration on pulmonary stretch receptor discharge. Respir Physiol 43, 299-314.

Davenport, P.W., Freed, A.N., Rex, K.A., 1984. The effect of sulfur dioxide on the response of rabbits to expiratory loads. Respir Physiol 56, 359-368.

Davenport, P.W., Reep, R.L., Thompson, F.J., 2010. Phrenic nerve afferent activation of neurons in the cat SI cerebral cortex. J Physiol 588, 873-886.

Davenport, P.W., Vovk, A., 2009. Cortical and subcortical central neural pathways in respiratory sensations. Respir Physiol Neurobiol 167, 72-86.

Davenport, P.W., Wozniak, J.A., 1986. Effect of expiratory loading on expiratory duration and pulmonary stretch receptor discharge. J Appl Physiol 61, 1857-1863.

Dempsey, J.A., 1986. J.B. Wolffe memorial lecture. Is the lung built for exercise? Med Sci Sports Exerc 18, 143-155.

Dempsey, J.A., 2006. Is the healthy respiratory system (always) built for exercise? J Physiol 576, 339-340.

Dempsey, J.A., Johnson, B.D., Saupe, K.W., 1990. Adaptations and limitations in the pulmonary system during exercise. Chest 97, 81S-87S.

Dempsey, J.A., Miller, J.D., Romer, L., Amann, M., Smith, C.A., 2008. Exercise-induced respiratory muscle work: effects on blood flow, fatigue and performance. Adv Exp Med Biol 605, 209-212.

Dempsey, J.A., Romer, L., Rodman, J., Miller, J., Smith, C., 2006. Consequences of exercise-induced respiratory muscle work. Respir Physiol Neurobiol 151, 242-250.

Di Chiara, G., Bassareo, V., 2007. Reward system and addiction: what dopamine does and doesn't do. Curr Opin Pharmacol 7, 69-76.

Di Marco, F., Verga, M., Reggente, M., Maria Casanova, F., Santus, P., Blasi, F., Allegra, L., Centanni, S., 2006. Anxiety and depression in COPD patients: The roles of gender and disease severity. Respir Med 100, 1767-1774.

Dodd, D.S., Yarom, J., Loring, S.H., Engel, L.A., 1988. O2 cost of inspiratory and expiratory resistive breathing in humans. J Appl Physiol 65, 2518-2523.

Doherty, M., Dimitriou, L., 1997. Comparison of lung volume in Greek swimmers, land based athletes, and sedentary controls using allometric scaling. Br J Sports Med 31, 337-341.

Downey, A.E., Chenoweth, L.M., Townsend, D.K., Ranum, J.D., Ferguson, C.S., Harms, C.A., 2007. Effects of inspiratory muscle training on exercise responses in normoxia and hypoxia. Respir Physiol Neurobiol 156, 137-146.

Drevets, W.C., Frank, E., Price, J.C., Kupfer, D.J., Holt, D., Greer, P.J., Huang, Y.Y., Gautier, C., Mathis, C., 1999. PET imaging of serotonin 1A receptor binding in depression. Biological Psychiatry 46, 1375-1387.

Edwards, A.M., Walker, R.E., 2009. Inspiratory muscle training and endurance: a central metabolic control perspective. Int J Sports Physiol Perform 4, 122-128.

Fairbarn, M.S., Coutts, K.C., Pardy, R.L., McKenzie, D.C., 1991. Improved respiratory muscle endurance of highly trained cyclists and the effects on maximal exercise performance. Int J Sports Med 12, 66-70.

Fernandes, L., Fonseca, J., Martins, S., Delgado, L., Pereira, A.C., Vaz, M., Branco, G., 2010. Association of anxiety with asthma: subjective and objective outcome measures. Psychosomatics 51, 39-46.

Freedman, R., Adler, L.E., Gerhardt, G.A., Waldo, M., Baker, N., Rose, G.M., Drebing, C., Nagamoto, H., Bickford-Wimer, P., Franks, R., 1987. Neurobiological studies of sensory gating in schizophrenia. Schizophr Bull 13, 669-678.

Fuller, D., Sullivan, J., Fregosi, R.F., 1996. Expiratory muscle endurance performance after exhaustive submaximal exercise. J Appl Physiol 80, 1495-1502.

Gandevia, S.C., Killian, K.J., Campbell, E.J., 1981. The effect of respiratory muscle fatigue on respiratory sensations. Clin Sci (Lond) 60, 463-466.

Gaudreau, J.D., Gagnon, P., 2005. Psychotogenic drugs and delirium pathogenesis: the central role of the thalamus. Med Hypotheses 64, 471-475.

Gething, A.D., Williams, M., Davies, B., 2004. Inspiratory resistive loading improves cycling capacity: a placebo controlled trial. Br J Sports Med 38, 730-736.

Goodwin, R.D., Pine, D.S., 2002. Respiratory disease and panic attacks among adults in the United States. Chest 122, 645-650.

Gosselink, R., Kovacs, L., Ketelaer, P., Carton, H., Decramer, M., 2000. Respiratory muscle weakness and respiratory muscle training in severely disabled multiple sclerosis patients. Arch Phys Med Rehabil 81, 747-751.

Graeff, F.G., Guimaraes, F.S., De Andrade, T.G., Deakin, J.F., 1996. Role of 5-HT in stress, anxiety, and depression. Pharmacol Biochem Behav 54, 129-141.

Graeff, F.G., Viana, M.B., Mora, P.O., 1997. Dual role of 5-HT in defense and anxiety. Neurosci Biobehav Rev 21, 791-799.

Griffiths, L.A., McConnell, A.K., 2007. The influence of inspiratory and expiratory muscle training upon rowing performance. Eur J Appl Physiol 99, 457-466.

Guidotti, A., Auta, J., Davis, J.M., Di-Giorgi-Gerevini, V., Dwivedi, Y., Grayson, D.R., Impagnatiello, F., Pandey, G., Pesold, C., Sharma, R., Uzunov, D., Costa, E., 2000. Decrease in reelin and glutamic acid decarboxylase67 (GAD67) expression in schizophrenia and bipolar disorder: a postmortem brain study. Arch Gen Psychiatry 57, 1061-1069.

Guz, A., 1997. Brain, breathing and breathlessness. Respir Physiol 109, 197-204.

Hakkinen, K., Komi, P.V., 1983. Electromyographic changes during strength training and detraining. Med Sci Sports Exerc 15, 455-460.

Harada, K., Yamaji, T., Matsuoka, N., 2008. Activation of the serotonin 5-HT(2C) receptor is involved in the enhanced anxiety in rats after single-prolonged stress. Pharmacol Biochem Behav 89, 11-16.

Harms, C.A., Wetter, T.J., St Croix, C.M., Pegelow, D.F., Dempsey, J.A., 2000. Effects of respiratory muscle work on exercise performance. J Appl Physiol 89, 131-138.

Harro, J., Vasar, E., 1991. Cholecystokinin-induced anxiety: how is it reflected in studies on exploratory behaviour? Neurosci Biobehav Rev 15, 473-477.

Harro, J., Vasar, E., Bradwejn, J., 1993. CCK in animal and human research on anxiety. Trends Pharmacol Sci 14, 244-249.

Harver, A., Mahler, D.A., Daubenspeck, J.A., 1989. Targeted inspiratory muscle training improves respiratory muscle function and reduces dyspnea in patients with chronic obstructive pulmonary disease. Ann Intern Med 111, 117-124.

Hasler, G., Gergen, P.J., Kleinbaum, D.G., Ajdacic, V., Gamma, A., Eich, D., Rossler, W., Angst, J., 2005. Asthma and panic in young adults: a 20-year prospective community study. Am J Respir Crit Care Med 171, 1224-1230.

Heijtz, R.D., Kolb, B., Forssberg, H., 2007. Motor inhibitory role of dopamine D1 receptors: implications for ADHD. Physiol Behav 92, 155-160.

Heisler, L.K., Chu, H.M., Brennan, T.J., Danao, J.A., Bajwa, P., Parsons, L.H., Tecott, L.H., 1998. Elevated anxiety and antidepressant-like responses in serotonin 5-HT1A receptor mutant mice. Proc Natl Acad Sci U S A 95, 15049-15054.

Heisler, L.K., Zhou, L., Bajwa, P., Hsu, J., Tecott, L.H., 2007. Serotonin 5-HT(2C) receptors regulate anxiety-like behavior. Genes Brain Behav 6, 491-496.

Henke, K.G., Sharratt, M., Pegelow, D., Dempsey, J.A., 1988. Regulation of end-expiratory lung volume during exercise. J Appl Physiol 64, 135-146.

Hensler, J.G., 2006. Serotonergic modulation of the limbic system. Neuroscience & Biobehavioral Reviews 30, 203-214.

Herrero, M.T., Barcia, C., Navarro, J.M., 2002. Functional anatomy of thalamus and basal ganglia. Childs Nerv Syst 18, 386-404.

Hertel, P., Nomikos, G.G., Iurlo, M., Svensson, T.H., 1996. Risperidone: regional effects in vivo on release and metabolism of dopamine and serotonin in the rat brain. Psychopharmacology (Berl) 124, 74-86.

Hill, J.M., 2000. Discharge of group IV phrenic afferent fibers increases during diaphragmatic fatigue. Brain Res 856, 240-244.

Hoffman-Ruddy, B., (2001). Expiratory Pressure Threshold Loading in High-Risk Performers, Communication Sciences and Disorders. University of Florida, Gainesville, FL.

Holm, P., Sattler, A., Fregosi, R.F., 2004. Endurance training of respiratory muscles improves cycling performance in fit young cyclists. BMC Physiol 4, 9.

Holmberg, H.C., Rosdahl, H., Svedenhag, J., 2007. Lung function, arterial saturation and oxygen uptake in elite cross country skiers: influence of exercise mode. Scand J Med Sci Sports 17, 437-444.

Holmer, I., 1972. Oxygen uptake during swimming in man. J Appl Physiol 33, 502-509.

Holmer, I., Lundin, A., Eriksson, B.O., 1974. Maximum oxygen uptake during swimming and running by elite swimmers. J Appl Physiol 36, 711-714.

Homma, I., Masaoka, Y., (1999). Nonchemical and behavioral effects on breathing, in: Altose, M.D., Kawakami, Y. (Eds.), Control of Breathing in Health and Disease. Marcel Dekker, New York, pp. 89-104.

Hong, S.K., Cerretelli, P., Cruz, J.C., Rahn, H., 1969. Mechanics of respiration during submersion in water. J Appl Physiol 27, 535-538.

Hoyer, D., Hannon, J.P., Martin, G.R., 2002. Molecular, pharmacological and functional diversity of 5-HT receptors. Pharmacology Biochemistry and Behavior 71, 533-554.

Hughes, T.R., Mao, M., Jones, A.R., Burchard, J., Marton, M.J., Shannon, K.W., Lefkowitz, S.M., Ziman, M., Schelter, J.M., Meyer, M.R., Kobayashi, S., Davis, C., Dai, H., He, Y.D., Stephaniants, S.B., Cavet, G., Walker, W.L., West, A., Coffey, E., Shoemaker, D.D., Stoughton, R., Blanchard, A.P., Friend, S.H., Linsley, P.S., 2001. Expression profiling using microarrays fabricated by an ink-jet oligonucleotide synthesizer. Nat Biotechnol 19, 342-347.

Iandelli, I., Aliverti, A., Kayser, B., Dellaca, R., Cala, S.J., Duranti, R., Kelly, S., Scano, G., Sliwinski, P., Yan, S., Macklem, P.T., Pedotti, A., 2002. Determinants of exercise performance in normal men with externally imposed expiratory flow limitation. J Appl Physiol 92, 1943-1952.

Jahn, O., Eckart, K., Brauns, O., Tezval, H., Spiess, J., 2002. The binding protein of corticotropin-releasing factor: ligand-binding site and subunit structure. Proc Natl Acad Sci U S A 99, 12055-12060.

Javanbakht, A., 2006. Sensory gating deficits, pattern completion, and disturbed fronto-limbic balance, a model for description of hallucinations and delusions in schizophrenia. Med Hypotheses 67, 1173-1184.

Johnson, B.D., Babcock, M.A., Suman, O.E., Dempsey, J.A., 1993. Exercise-induced diaphragmatic fatigue in healthy humans. J Physiol 460, 385-405.

Jones, B.J., Blackburn, T.P., 2002. The medical benefit of 5-HT research. Pharmacology Biochemistry and Behavior 71, 555-568.

Jones, E.G., Leavitt, R.Y., 1974. Retrograde axonal transport and the demonstration of non-specific projections to the cerebral cortex and striatum from thalamic intralaminar nuclei in the rat, cat and monkey. J Comp Neurol 154, 349-377.

Jones, N.L., Killian, K.J., 2000. Exercise limitation in health and disease. N Engl J Med 343, 632-641.

Karolyi, I.J., Burrows, H.L., Ramesh, T.M., Nakajima, M., Lesh, J.S., Seong, E., Camper, S.A., Seasholtz, A.F., 1999. Altered anxiety and weight gain in corticotropin-releasing hormone-binding protein-deficient mice. Proc Natl Acad Sci U S A 96, 11595-11600.

Kayser, B., Sliwinski, P., Yan, S., Tobiasz, M., Macklem, P.T., 1997. Respiratory effort sensation during exercise with induced expiratory-flow limitation in healthy humans. J Appl Physiol 83, 936-947.

Kearon, M.C., Summers, E., Jones, N.L., Campbell, E.J., Killian, K.J., 1991. Breathing during prolonged exercise in humans. J Physiol 442, 477-487.

Kellerman, B.A., Martin, A.D., Davenport, P.W., 2000. Inspiratory strengthening effect on resistive load detection and magnitude estimation. Med Sci Sports Exerc 32, 1859-1867.

Kennett, G.A., Dourish, C.T., Curzon, G., 1987. Antidepressant-like action of 5-HT1A agonists and conventional antidepressants in an animal model of depression. Eur J Pharmacol 134, 265-274.

Kilding, A.E., Brown, S., McConnell, A.K., 2010. Inspiratory muscle training improves 100 and 200 m swimming performance. Eur J Appl Physiol 108, 505-511.

Killian, K.J., Campbell, E.J., (1995). Dyspnea, in: Roussos, C. (Ed.), The Thorax, Part B: Applied Physiology. Marcel Dekker, New York.

Killian, K.J., Gandevia, S.C., (1996). Sense of Effort and Dyspnea, in: Adams, L., Guz, A. (Eds.), Respiratory Sensation. Marcel Dekker, New York, pp. 181-200.

Killian, K.J., Mahutte, C.K., Campbell, E.J., 1981. Magnitude scaling of externally added loads to breathing. Am Rev Respir Dis 123, 12-15.

Kim, J., Davenport, P., Sapienza, C., 2009. Effect of expiratory muscle strength training on elderly cough function. Arch Gerontol Geriatr 48, 361-366.

Kimble, M., Kaufman, M., 2004. Clinical correlates of neurological change in posttraumatic stress disorder: an overview of critical systems. Psychiatr Clin North Am 27, 49-65, viii.

Klak, K., Palucha, A., Branski, P., Sowa, M., Pilc, A., 2007. Combined administration of PHCCC, a positive allosteric modulator of mGlu4 receptors and ACPT-I, mGlu III receptor agonist evokes antidepressant-like effects in rats. Amino Acids 32, 169-172.

Kobayashi, T., Washiyama, K., Ikeda, K., 2004. Inhibition of G protein-activated inwardly rectifying K+ channels by various antidepressant drugs. Neuropsychopharmacology 29, 1841-1851.

Koehler, R.C., Bishop, B., 1979. Expiratory duration and abdominal muscle responses to elastic and resistive loading. J Appl Physiol 46, 730-737.

Koga, S., Shiojiri, T., Shibasaki, M., Kondo, N., Fukuba, Y., Barstow, T.J., 1999. Kinetics of oxygen uptake during supine and upright heavy exercise. J Appl Physiol 87, 253-260.

Konstantaki, M., Trowbridge, E.A., Swaine, I.L., 1998. The relationship between blood lactate and heart rate responses to swim bench exercise and women's competitive water polo. J Sports Sci 16, 251-256.

Krishnan, B.S., Zintel, T., McParland, C., Gallagher, C.G., 2000. Evolution of inspiratory and expiratory muscle pressures during endurance exercise. J Appl Physiol 88, 234-245.

Kroff, J., (2008). New Insights into Respiratory Muscle Function in an Athletic Population. Stellenbosch University.

Krout, K.E., Belzer, R.E., Loewy, A.D., 2002. Brainstem projections to midline and intralaminar thalamic nuclei of the rat. J Comp Neurol 448, 53-101.

Krout, K.E., Loewy, A.D., 2000a. Parabrachial nucleus projections to midline and intralaminar thalamic nuclei of the rat. J Comp Neurol 428, 475-494.

Krout, K.E., Loewy, A.D., 2000b. Periaqueductal gray matter projections to midline and intralaminar thalamic nuclei of the rat. J Comp Neurol 424, 111-141.

Krout, K.E., Loewy, A.D., Westby, G.W., Redgrave, P., 2001. Superior colliculus projections to midline and intralaminar thalamic nuclei of the rat. J Comp Neurol 431, 198-216.

Kunik, M.E., Roundy, K., Veazey, C., Souchek, J., Richardson, P., Wray, N.P., Stanley, M.A., 2005. Surprisingly high prevalence of anxiety and depression in chronic breathing disorders. Chest 127, 1205-1211.

Kyroussis, D., Mills, G.H., Polkey, M.I., Hamnegard, C.H., Koulouris, N., Green, M., Moxham, J., 1996. Abdominal muscle fatigue after maximal ventilation in humans. J Appl Physiol 81, 1477-1483.

Lieberman, J.A., Mailman, R.B., Duncan, G., Sikich, L., Chakos, M., Nichols, D.E., Kraus, J.E., 1998. Serotonergic basis of antipsychotic drug effects in schizophrenia. Biological Psychiatry 44, 1099-1117.

Lindh, A.M., Peyrebrune, M.C., Ingham, S.A., Bailey, D.M., Folland, J.P., 2008. Sodium bicarbonate improves swimming performance. Int J Sports Med 29, 519-523.

Lisboa, C., Villafranca, C., Leiva, A., Cruz, E., Pertuze, J., Borzone, G., 1997. Inspiratory muscle training in chronic airflow limitation: effect on exercise performance. Eur Respir J 10, 537-542.

Loke, J., Mahler, D.A., Virgulto, J.A., 1982. Respiratory muscle fatigue after marathon running. J Appl Physiol 52, 821-824.

Lomax, M.E., McConnell, A.K., 2003. Inspiratory muscle fatigue in swimmers after a single 200 m swim. J Sports Sci 21, 659-664.

Mador, M.J., Acevedo, F.A., 1991. Effect of respiratory muscle fatigue on subsequent exercise performance. J Appl Physiol 70, 2059-2065.

Mador, M.J., Magalang, U.J., Rodis, A., Kufel, T.J., 1993. Diaphragmatic fatigue after exercise in healthy human subjects. Am Rev Respir Dis 148, 1571-1575.

Magel, J.R., Faulkner, J.A., 1967. Maximum oxygen uptakes of college swimmers. J Appl Physiol 22, 929-933.

Maglischo, E.W., (2003). Physiological Responses to Exercise, Swimming Fastest: The Essential Reference on Technique, Training, and Program Design. Human Kinetics.

Manning, H.L., Schwartzstein, R.M., 1995. Pathophysiology of dyspnea. N Engl J Med 333, 1547-1553.

McConnell, A.K., Griffiths, L.A., 2010. Acute Cardiorespiratory Responses to Inspiratory Pressure Threshold Loading. Med Sci Sports Exerc.

McCormick, D.A., Bal, T., 1994. Sensory gating mechanisms of the thalamus. Curr Opin Neurobiol 4, 550-556.

McKay, E.E., Braund, R.W., Chalmers, R.J., Williams, C.S., 1983. Physical work capacity and lung function in competitive swimmers. Br J Sports Med 17, 27-33.

McKay, L.C., Evans, K.C., Frackowiak, R.S., Corfield, D.R., 2003. Neural correlates of voluntary breathing in humans. J Appl Physiol 95, 1170-1178.

Millan, M.J., 2000. Improving the treatment of schizophrenia: focus on serotonin (5-HT)(1A) receptors. J Pharmacol Exp Ther 295, 853-861.

Mitchell, J.H., 1990. J.B. Wolffe memorial lecture. Neural control of the circulation during exercise. Med Sci Sports Exerc 22, 141-154.

Mizuno, M., 1991. Human respiratory muscles: fibre morphology and capillary supply. Eur Respir J 4, 587-601.

Mizuno, M., Secher, N.H., 1989. Histochemical characteristics of human expiratory and inspiratory intercostal muscles. J Appl Physiol 67, 592-598.

Moritani, T., deVries, H.A., 1979. Neural factors versus hypertrophy in the time course of muscle strength gain. Am J Phys Med 58, 115-130.

Mota, S., Guell, R., Barreiro, E., Solanes, I., Ramirez-Sarmiento, A., Orozco-Levi, M., Casan, P., Gea, J., Sanchis, J., 2007. Clinical outcomes of expiratory muscle training in severe COPD patients. Respir Med 101, 516-524.

Moussas, G., Tselebis, A., Karkanias, A., Stamouli, D., Ilias, I., Bratis, D., Vassila-Demi, K., 2008. A comparative study of anxiety and depression in patients with bronchial asthma, chronic obstructive pulmonary disease and tuberculosis in a general hospital of chest diseases. Ann Gen Psychiatry 7, 7.

Nash, J.R., Sargent, P.A., Rabiner, E.A., Hood, S.D., Argyropoulos, S.V., Potokar, J.P., Grasby, P.M., Nutt, D.J., 2008. Serotonin 5-HT1A receptor binding in people with panic disorder: positron emission tomography study. Br J Psychiatry 193, 229-234.

Neumeister, A., Bain, E., Nugent, A.C., Carson, R.E., Bonne, O., Luckenbaugh, D.A., Eckelman, W., Herscovitch, P., Charney, D.S., Drevets, W.C., 2004. Reduced serotonin type 1A receptor binding in panic disorder. J Neurosci 24, 589-591.

Newman, J., 1995. Thalamic contributions to attention and consciousness. Conscious Cogn 4, 172-193.

Nikitin, A., Egorov, S., Daraselia, N., Mazo, I., 2003. Pathway studio--the analysis and navigation of molecular networks. Bioinformatics 19, 2155-2157.

O'Donnell, D.E., Banzett, R.B., Carrieri-Kohlman, V., Casaburi, R., Davenport, P.W., Gandevia, S.C., Gelb, A.F., Mahler, D.A., Webb, K.A., 2007. Pathophysiology of dyspnea in chronic obstructive pulmonary disease: a roundtable. Proc Am Thorac Soc 4, 145-168.

Omachi, T.A., Katz, P.P., Yelin, E.H., Gregorich, S.E., Iribarren, C., Blanc, P.D., Eisner, M.D., 2009. Depression and health-related quality of life in chronic obstructive pulmonary disease. Am J Med 122, 778 e779-715.

Ongur, D., Drevets, W.C., Price, J.L., 1998. Glial reduction in the subgenual prefrontal cortex in mood disorders. Proc Natl Acad Sci U S A 95, 13290-13295.

Paivinen, M.K., Keskinen, K.L., Tikkanen, H.O., 2010. Swimming and asthma: factors underlying respiratory symptoms in competitive swimmers. Clin Respir J 4, 97-103.

Pate, K.M., Hotchkiss, M., Bernhardt, V., Shahan, P., Vovk, A., Davenport, P.W., 2008. Tracheal obstruction elicited c-Fos expression in the somatosensory and affective central neural pathways. Am. J. Respir. Crit. Care Med. 177.

Pate, K.M., Scheuer, D.A., Davenport, P.W., 2010. Behavioral & physiological changes associated with chronic tracheal obstructions in conscious rats. FASEB J 24.

Paxinos, G., Watson, C., 1998. The Rat Brain in Stereotaxic Coordinates. Academic Press, New York.

Phillipson, E.A., 1974. Vagal control of breathing pattern independent of lung inflation in conscious dogs. J Appl Physiol 37, 183-189.

Pitts, T., Bolser, D., Rosenbek, J., Troche, M., Okun, M., Sapienza, C., 2008. Impact of Expiratory Muscle Strength Training on Voluntary Cough and Swallow Function in Parkinson Disease. Chest.

Polla, B., D'Antona, G., Bottinelli, R., Reggiani, C., 2004. Respiratory muscle fibres: specialisation and plasticity. Thorax 59, 808-817.

Potts, A.D., Charlton, J.E., Smith, H.M., 2002. Bilateral arm power imbalance in swim bench exercise to exhaustion. J Sports Sci 20, 975-979.

Psycharakis, S.G., 2010. A Longitudinal Analysis on the Validity and Reliability of ratings of Perceived Exertion for Elite Swimmers. J Strength Cond Res.

Ramboz, S., Oosting, R., Amara, D.A., Kung, H.F., Blier, P., Mendelsohn, M., Mann, J.J., Brunner, D., Hen, R., 1998. Serotonin receptor 1A knockout: an animal model of anxiety-related disorder. Proc Natl Acad Sci U S A 95, 14476-14481.

Ramcharan, E.J., Gnadt, J.W., Sherman, S.M., 2000. Burst and tonic firing in thalamic cells of unanesthetized, behaving monkeys. Vis Neurosci 17, 55-62.

Rao, E., Weiss, B., Fukami, M., Rump, A., Niesler, B., Mertz, A., Muroya, K., Binder, G., Kirsch, S., Winkelmann, M., Nordsiek, G., Heinrich, U., Breuning, M.H., Ranke, M.B., Rosenthal, A., Ogata, T., Rappold, G.A., 1997. Pseudoautosomal deletions encompassing a novel homeobox gene cause growth failure in idiopathic short stature and Turner syndrome. Nat Genet 16, 54-63.

Romer, L.M., Lovering, A.T., Haverkamp, H.C., Pegelow, D.F., Dempsey, J.A., 2006. Effect of inspiratory muscle work on peripheral fatigue of locomotor muscles in healthy humans. J Physiol 571, 425-439.

Romer, L.M., McConnell, A.K., Jones, D.A., 2002. Effects of inspiratory muscle training on time-trial performance in trained cyclists. J Sports Sci 20, 547-562.

Romer, L.M., Miller, J.D., Haverkamp, H.C., Pegelow, D.F., Dempsey, J.A., 2007. Inspiratory muscles do not limit maximal incremental exercise performance in healthy subjects. Respir Physiol Neurobiol 156, 353-361.

Rong, C., Bei, H., Yun, M., Yuzhu, W., Mingwu, Z., 2008. Lung function and cytokine levels in professional athletes. J Asthma 45, 343-348.

Rotzinger, S., Vaccarino, F.J., 2003. Cholecystokinin receptor subtypes: role in the modulation of anxiety-related and reward-related behaviours in animal models. J Psychiatry Neurosci 28, 171-181.

Rowland, T., Bougault, V., Walther, G., Nottin, S., Vinett, A., Obert, P., 2008. Cardiac responses to swim bench exercise in age-group swimmers and non-athletic children. J Sci Med Sport.

Saenz del Burgo, L., Cortes, R., Mengod, G., Zarate, J., Echevarria, E., Salles, J., 2008. Distribution and neurochemical characterization of neurons expressing GIRK channels in the rat brain. J Comp Neurol 510, 581-606.

Saito, N., Shirai, Y., 2002. Protein kinase C gamma (PKC gamma): function of neuron specific isotype. J Biochem 132, 683-687.

Sale, D.G., 1988. Neural adaptation to resistance training. Med Sci Sports Exerc 20, S135-145.

Saleem, A.F., Sapienza, C.M., Okun, M.S., 2005. Respiratory muscle strength training: treatment and response duration in a patient with early idiopathic Parkinson's disease. NeuroRehabilitation 20, 323-333.

Saltin, B., Calbet, J.A., 2006. Point: in health and in a normoxic environment, VO2 max is limited primarily by cardiac output and locomotor muscle blood flow. J Appl Physiol 100, 744-745.

Sapienza, C.M., Davenport, P.W., Martin, A.D., 2002. Expiratory muscle training increases pressure support in high school band students. J Voice 16, 495-501.

Sasaki, M., Kurosawa, H., Kohzuki, M., 2005. Effects of inspiratory and expiratory muscle training in normal subjects. J Jpn Phys Ther Assoc 8, 29-37.

Savitz, J., Lucki, I., Drevets, W.C., 2009. 5-HT(1A) receptor function in major depressive disorder. Prog Neurobiol 88, 17-31.

Schreiber, R., De Vry, J., 1993. 5-HT1A receptor ligands in animal models of anxiety, impulsivity and depression: multiple mechanisms of action? Prog Neuropsychopharmacol Biol Psychiatry 17, 87-104.

Seifert, L., Komar, J., Lepretre, P.M., Lemaitre, F., Chavallard, F., Alberty, M., Houel, N., Hausswirth, C., Chollet, D., Hellard, P., 2010. Swim Specialty Affects Energy Cost and Motor Organization. Int J Sports Med.

Sherman, S.M., 1996. Dual response modes in lateral geniculate neurons: mechanisms and functions. Vis Neurosci 13, 205-213.

Sherman, S.M., 2001. Thalamic relay functions. Prog Brain Res 134, 51-69.

Sherman, S.M., Guillery, R.W., 2002. The role of the thalamus in the flow of information to the cortex. Philos Trans R Soc Lond B Biol Sci 357, 1695-1708.

Shyu, B.C., Kiritsy-Roy, J.A., Morrow, T.J., Casey, K.L., 1992. Neurophysiological, pharmacological and behavioral evidence for medial thalamic mediation of cocaine-induced dopaminergic analgesia. Brain Res 572, 216-223.

Sieck, G.C., Prakash, Y.S., (1997). The diaphragm muscle, in: Miller, A.D., Bianchi, A.L., Bishop, B.P. (Eds.), Neural Control of the Respiratory Muscles. CRC, Boca Raton, FL, pp. 7-20.

Smeltzer, S.C., Lavietes, M.H., Cook, S.D., 1996. Expiratory training in multiple sclerosis. Arch Phys Med Rehabil 77, 909-912.

Smith, B.K., Martin, A.D., Vandenborne, K., Davenport, P.W., 2010. Respiratory muscle phenotype and cross-sectional area following repeated tracheal occlusion. Am J Respir Crit Care Med 181.

Soghomonian, J.J., Martin, D.L., 1998. Two isoforms of glutamate decarboxylase: why? Trends Pharmacol Sci 19, 500-505.

Sonetti, D.A., Wetter, T.J., Pegelow, D.F., Dempsey, J.A., 2001. Effects of respiratory muscle training versus placebo on endurance exercise performance. Respir Physiol 127, 185-199.

Sperlich, B., Fricke, H., de Marees, M., Linville, J.W., Mester, J., 2009. Does respiratory muscle training increase physical performance? Mil Med 174, 977-982.

St Clair Gibson, A., Lambert, E.V., Rauch, L.H., Tucker, R., Baden, D.A., Foster, C., Noakes, T.D., 2006. The role of information processing between the brain and peripheral physiological systems in pacing and perception of effort. Sports Med 36, 705-722.

Stuart, D.G., Collings, W.D., 1959. Comparison of vital capacity and maximum breathing capacity of athletes and non-athletes. J Appl Physiol 14, 507-509.

Suga, N., Xiao, Z., Ma, X., Ji, W., 2002. Plasticity and corticofugal modulation for hearing in adult animals. Neuron 36, 9-18.

Suzuki, S., Sato, M., Okubo, T., 1995. Expiratory muscle training and sensation of respiratory effort during exercise in normal subjects. Thorax 50, 366-370.

Suzuki, S., Suzuki, J., Okubo, T., 1991. Expiratory muscle fatigue in normal subjects. J Appl Physiol 70, 2632-2639.

Swadlow, H.A., Gusev, A.G., 2001. The impact of 'bursting' thalamic impulses at a neocortical synapse. Nat Neurosci 4, 402-408.

Swaine, I.L., Zanker, C.L., 1996. The reproducibility of cardiopulmonary responses to exercise using a swim bench. Int J Sports Med 17, 140-144.

Taylor, B.J., How, S.C., Romer, L.M., 2006. Exercise-induced abdominal muscle fatigue in healthy humans. J Appl Physiol 100, 1554-1562.

Taylor, B.J., Romer, L.M., 2008. Effect of expiratory muscle fatigue on exercise tolerance and locomotor muscle fatigue in healthy humans. J Appl Physiol 104, 1442-1451.

ten Brinke, A., Ouwerkerk, M.E., Zwinderman, A.H., Spinhoven, P., Bel, E.H., 2001. Psychopathology in patients with severe asthma is associated with increased health care utilization. Am J Respir Crit Care Med 163, 1093-1096.

Valenca, A.M., Falcao, R., Freire, R.C., Nascimento, I., Nascentes, R., Zin, W.A., Nardi, A.E., 2006. The relationship between the severity of asthma and comorbidities with anxiety and depressive disorders. Rev Bras Psiquiatr 28, 206-208.

Van Den Eede, F., Van Broeckhoven, C., Claes, S.J., 2005. Corticotropin-releasing factor-binding protein, stress and major depression. Ageing Res Rev 4, 213-239.

van Schaick, H.S., Smidt, M.P., Rovescalli, A.C., Luijten, M., van der Kleij, A.A., Asoh, S., Kozak, C.A., Nirenberg, M., Burbach, J.P., 1997. Homeobox gene Prx3 expression in rodent brain and extraneural tissues. Proc Natl Acad Sci U S A 94, 12993-12998.

Vandenbogaerde, T.J., Hopkins, W.G., 2010. Monitoring acute effects on athletic performance with mixed linear modeling. Med Sci Sports Exerc 42, 1339-1344.

Verges, S., Boutellier, U., Spengler, C.M., 2008a. Effect of respiratory muscle endurance training on respiratory sensations, respiratory control and exercise performance: a 15-year experience. Respir Physiol Neurobiol 161, 16-22.

Verges, S., Kruttli, U., Stahl, B., Frigg, R., Spengler, C.M., 2008b. Respiratory control, respiratory sensations and cycling endurance after respiratory muscle endurance training. Adv Exp Med Biol 605, 239-244.

Verges, S., Sager, Y., Erni, C., Spengler, C.M., 2007. Expiratory muscle fatigue impairs exercise performance. Eur J Appl Physiol 101, 225-232.

Verges, S., Schulz, C., Perret, C., Spengler, C.M., 2006. Impaired abdominal muscle contractility after high-intensity exhaustive exercise assessed by magnetic stimulation. Muscle Nerve 34, 423-430.

Vermeire, S.T., Audenaert, K.R., Dobbeleir, A.A., De Meester, R.H., De Vos, F.J., Peremans, K.Y., 2009. Evaluation of the brain 5-HT2A receptor binding index in dogs with anxiety disorders, measured with 123I-5I-R91150 and SPECT. J Nucl Med 50, 284-289.

Vertes, R.P., Linley, S.B., Hoover, W.B., 2010. Pattern of distribution of serotonergic fibers to the thalamus of the rat. Brain Struct Funct 215, 1-28.

Volianitis, S., McConnell, A.K., Koutedakis, Y., McNaughton, L., Backx, K., Jones, D.A., 2001. Inspiratory muscle training improves rowing performance. Med Sci Sports Exerc 33, 803-809.

Vovk, A., Pate, K.M., Davenport, P., (2006). Respiratory response to transient, reversible tracheal obstruction in rats, 2006 Neuroscience Meeting Planner. Society for Neuroscience, Atlanta, GA.

Wagner, P.D., 1996. A theoretical analysis of factors determining VO2 MAX at sea level and altitude. Respir Physiol 106, 329-343.

Wagner, P.D., 2006. Counterpoint: in health and in normoxic environment VO2max is limited primarily by cardiac output and locomotor muscle blood flow. J Appl Physiol 100, 745-747; discussion 747-748.

Weiner, P., Magadle, R., Beckerman, M., Weiner, M., Berar-Yanay, N., 2003a. Comparison of specific expiratory, inspiratory, and combined muscle training programs in COPD. Chest 124, 1357-1364.

Weiner, P., Magadle, R., Beckerman, M., Weiner, M., Berar-Yanay, N., 2003b. Specific expiratory muscle training in COPD. Chest 124, 468-473.

Weisstaub, N.V., Zhou, M., Lira, A., Lambe, E., Gonzalez-Maeso, J., Hornung, J.P., Sibille, E., Underwood, M., Itohara, S., Dauer, W.T., Ansorge, M.S., Morelli, E., Mann, J.J., Toth, M., Aghajanian, G., Sealfon, S.C., Hen, R., Gingrich, J.A., 2006. Cortical 5-HT2A receptor signaling modulates anxiety-like behaviors in mice. Science 313, 536-540.

Wells, G.D., Plyley, M., Thomas, S., Goodman, L., Duffin, J., 2005. Effects of concurrent inspiratory and expiratory muscle training on respiratory and exercise performance in competitive swimmers. Eur J Appl Physiol 94, 527-540.

Wylegala, J.A., Pendergast, D.R., Gosselin, L.E., Warkander, D.E., Lundgren, C.E., 2007. Respiratory muscle training improves swimming endurance in divers. Eur J Appl Physiol 99, 393-404.

Yates, J.S., Davenport, P.W., Reep, R.L., 1994. Thalamocortical projections activated by phrenic nerve afferents in the cat. Neurosci Lett 180, 114-118.

Young, K.A., Holcomb, L.A., Yazdani, U., Hicks, P.B., German, D.C., 2004. Elevated neuron number in the limbic thalamus in major depression. Am J Psychiatry 161, 1270-1277.

Zechman, F.W., Frazier, D.T., Lally, D.A., 1976. Respiratory volume-time relationships during resistive loading in the cat. J Appl Physiol 40, 177-183.

Zhang, W., Davenport, P.W., 2003. Activation of thalamic ventroposteriolateral neurons by phrenic nerve afferents in cats and rats. J Appl Physiol 94, 220-226.

BIOGRAPHICAL SKETCH

Vipa Bernhardt was born in Riyadh, Saudi Arabia and grew up in Bad Hersfeld, Germany, earning her Abitur from the Modellschule Obersberg in 2002. She graduated summa cum laude with a Bachelor of Science degree in Neurological Sciences and a Bachelor of Arts degree in Music Performance from the University of Florida in 2006.

Throughout her undergraduate years she received an athletic scholarship for being a member of the varsity swim team. Vipa is a five-time Southeastern Conference (SEC) champion and a 19-time All-American and still holds two University of Florida school records. In 2003 she received the Tracy Caulkins Outstanding Freshman Award and in 2006 she was named UF's most valuable swimmer. International competitions for her home country Germany included European Championships, World University Games, World Championships and the 2004 Summer Olympic Games. For her success in both her studies and as a swimmer, she was recognized as the SEC Women's Scholar Athlete for two consecutive years.

Vipa entered UF's Interdisciplinary Program in 2006 and, shortly after, joined the laboratory of Dr. Paul W. Davenport, where she could combine her interests in science and sports by studying the effects of respiratory muscle training in swimmers. She has accepted a post-doctoral research associate position at the National Aquatics and Sports Medicine Institute at Washington State University.